NTNU
Det skapende universitet

Analyse og modellering av dype energibrønner

Andreas B. Schwencke

NTNU

Norwegian University
of Science and Technology

Department of Energy
and Process Engineering

EPT-M-2013-99

MASTER THESIS

for

Stud.techn. Andreas Schwencke

Spring 2013

Analysis and modeling of deep energy wells

Analyse og modellering av dype energibrønner

Background and objective

Ground source heat pump (GSHP) systems usually utilize borehole heat exchangers (BHE) based on boreholes with a depth ranging between $100 - 300$ m depth as a source and sink for thermal energy. A number of wells drilled with a separation distance of a few meters and then connected in parallel can form the basis for a large installation. While the installation can be virtually invisible once it is constructed it still requires a certain space. To reduce the required surface area, the depth of the boreholes can be increased. Recently GSHP installations have been constructed based on deeper boreholes in southern Norway. In this thesis, operation data from one or more installations based on boreholes with a depth of approximately 500 m shall be collected and analyzed. The data will then form the boundaries for a numerical model that will be used to simulate the borehole heat exchangers, and also be used to verify the numerical simulations. The numerical model will then enable further studies and optimization of the system(s).

The following tasks are to be considered:

1. Evaluation of available methods with different degree of complexity for simulation of BHE. Limitations with respect to effects such as interaction between boreholes, length-wise temperature variations, ground water flow etc. shall be considered. This will form background and motivation for the choice of method applied in the modeling part of the thesis.

2. Collection of operational data from one or more BHE installations, to be decided in cooperation with the Department. The installation(s) shall be described and the instrumentation presented. The data shall be presented and discussed.

3. Setup of a numerical model to simulate the BHE(s). The numerical model can either be based on In-house software to simulate BHE or it can be based on other available numerical codes.

5. Perform a sensitivity and parametric study with the applied model in order to optimize the operation of the system(s). Specifications for the study will be made in cooperation with the Department.

6. Suggestions for further work shall be made.

- ” --

Within 14 days of receiving the written text on the master thesis, the candidate shall submit a research plan for his project to the department.

When the thesis is evaluated, emphasis is put on processing of the results, and that they are presented in tabular and/or graphic form in a clear manner, and that they are analyzed carefully.

The thesis should be formulated as a research report with summary both in English and Norwegian, conclusion, literature references, table of contents etc. During the preparation of the text, the candidate should make an effort to produce a well-structured and easily readable report. In order to ease the evaluation of the thesis, it is important that the cross-references are correct. In the making of the report, strong emphasis should be placed on both a thorough discussion of the results and an orderly presentation.

The candidate is requested to initiate and keep close contact with his/her academic supervisor(s) throughout the working period. The candidate must follow the rules and regulations of NTNU as well as passive directions given by the Department of Energy and Process Engineering.

Risk assessment of the candidate's work shall be carried out according to the department's procedures. The risk assessment must be documented and included as part of the final report. Events related to the candidate's work adversely affecting the health, safety or security, must be documented and included as part of the final report. If the documentation on risk assessment represents a large number of pages, the full version is to be submitted electronically to the supervisor and an excerpt is included in the report.

Pursuant to "Regulations concerning the supplementary provisions to the technology study program/Master of Science" at NTNU §20, the Department reserves the permission to utilize all the results and data for teaching and research purposes as well as in future publications.

The final report is to be submitted digitally in DAIM. An executive summary of the thesis including title, student's name, supervisor's name, year, department name, and NTNU's logo and name, shall be submitted to the department as a separate pdf file. Based on an agreement with the supervisor, the final report and other material and documents may be given to the supervisor in digital format.

☐ Work to be done in lab (Water power lab, Fluids engineering lab, Thermal engineering lab)

☐ Field work

Department of Energy and Process Engineering, 14. January 2013

_____   _____
Olav Bolland   Erling Næss
Department Head   Academic Supervisor

Preface

This master thesis was written spring 2013 as part of my master's degree in Mechanical Engineering at the Norwegian University of Science and Technology, department of Energy and Process Engineering.

I would like to thank Erling Næss, Randi Kalskin Ramstad and Henrik Holmberg for their help and guidance in the development of my master thesis.

Trondheim June 10, 2013

Andreas Biørnstad Schwencke

Abstract

In the Borehole Heat Exchangers (BHE)s installed at Skoger elementary school in Drammen, heat is extracted or injected from a fluid circulating inside a single u-pipe collector to the surrounding ground. The system consists of five 500 meter deep BHEs that are used as an energy source for the heat pump system. System operational data was used to predict the long time performance of the BHEs installed at Skoger by using a 2-dimensional and a 3-dimensional model developed in Comsol Multiphysics.

The 3D model was used to calculate the thermal resistance between the borehole wall and the fluid inside the collectors, the borehole resistance, for different heat extraction and injection rates and to evaluate the BHE performance for different fluid velocities. The borehole resistance was used as an input to the 2D model. The 2D model was developed to predict the long term performance since the 3D model was ineffective for long time simulation periods because of extensive computational time needed. However the 3D model provided the 2D model with input data for evaluation of different ground and system conditions, such as thermal interaction between the boreholes, ground conductivity and temperature gradient along the borehole, and their influence on the BHE long time performance.

The borehole resistance is shown to be dependent upon the fluid velocity inside the collectors, the thermal effects of the density gradient of the water surrounding the collector pipes, the amount of heat extracted or injected and whether heat is extracted or injected from the energy wells. A significant increase in borehole resistance for a constant heat extraction rate is found when the heat transfer effect of the natural convection flow is excluded and heat transfer is controlled by pure conduction. Including heat transfer effects of natural convection in BHE simulation models is therefore of great importance for short as well as long time simulation for groundwater filled boreholes. If the volumetric flow rate is changed while keeping a constant heat injection or extraction, a more even temperature profile between the up-and downward fluid flow is found. This enhances the BHE performance, but at the cost of higher pumping power.

The performance of a BHE system is to a large extent dependent on the yearly difference between energy extracted and injected to the energy wells and a precise determination of the site ground conductivity value. This is because low BHE heat injection rates and an overestimation of the ground conductivity may lead to poorer heat pump working conditions and in worst case system failure.

Sammendrag

I energibrønnene installert på Skoger barneskole i Drammen, blir varme trukket ut eller injisert fra fluidet som sirkulerer i én enkel u-rør kollektor til berget rundt. Systemet består av fem 500 meter dype energibrønner som brukes som energikilde for varmepumpesystemet. Driftsdata siden 2011 er brukt til å forutsi langtidsytelsen for energibrønnene som er installert på Skoger ved bruk av en 2-dimensjonal og en 3-dimensjonal modell utviklet i COMSOL Multiphysics.

3D-modellen ble brukt til å beregne borehullsmotstanden, som er den termiske motstanden mellom borehullsveggen og fluidet inne i kollektoren, for forskjellige varmeekstraksjon og injeksjonsrater, og til å evaluere ytelsen til energibrønnene ved forskjellige fluidhastigheter. 2D-modellen ble utviklet for å forutsi den langsiktige ytelsen til energibrønnene installert på Skoger, siden 3D-modellen var ineffektiv for langtids simuleringsperioder på grunn av relativt store krav til datamaskinens kapasitet. Borehullsmotstanden ble utregnet fra 3D modellen og brukt som en input for 2D-modellen ved evaluering av ulike berg- og systemtilstander slik som termisk interaksjon mellom borehullene, konduktivitet til berget og bergets temperaturgradient langs borehullet og deres innflytelse på energibrønnenes langtidsytelse.

Borehullsmotstanden for u-rør kollektoren installert på Skoger er vist å være avhengig av fluidhastigheten inne i kollektoren, tetthetsgradienten til vannet rundt kollektoren, mengden av varme trukket ut eller injiseret og hvorvidt varme blir trukket ut eller injisert til energibrønnene. En betydelig økning i borehullmotstand for en konstant varmeekstraksjonseffekt er funnet når varmeoverføringseffekten fra naturlig konveksjon er utelatt i beregningsmodellen. Å inkludere varmeoverføringseffektene fra naturlig konveksjon i beregningsmodeller er derfor av stor betydning for kort- og langtidssimulering for grunnvannsfylte borehull.

Hvis den volumetriske strømningshastigheten økes ved en konstant varmeinjeksjon- eller ekstraksjonseffekt, vil temperaturprofilene langs borehullets dybdeakse bli mer lineær for det oppad– og nedadstrømmende fluidet. Dette vil forbedre ytelsen til energibrønnene, men vil komme på bekostning av høyere pumpeeffekt.

Langtidsytelsen til et energibrønnsystem er i stor grad avhengig av den årlige energidifferansen mellom energi trukket ut og injisert fra energibrønnene samt en nøyaktig bestemmelse av bergets termiske konduktivitet. Dette er fordi lave energiinjeksjonsrater og en overvurdering av bergets konduktivitet i designprosessen av energibrønnsystemet vil kunne føre til dårligere arbeidsforhold for varmepumpen og i verste fall systemfeil.

Contents

List of figures

List of tables

Nomenclature

A	Aspect ratio	[-]
c	Specific heat capacity	[J/Kg·K]
Gr	Grashof number	[-]
Gr^*	Modified Grashof number	[-]
h	Convective heat transfer coefficient	[W/m^{2}K]
L	Borehole depth	[m]
$\dot{m}_f$	Fluid flow rate	[kg/s]
Nu	Nusselt number	[-]
Ra	Rayleigh number	[-]
Ra^*	Modified Rayleigh number	[-]
r	Radial distance	[m]
r_b	Borehole radius	[m]
r_{eq}	Equivalent radius	[m]
Re	Reynolds number	[-]
R_b	Borehole resistance	[m·K/W]
T_b	Borehole temperature	[°C]
T_{bhw}	Borehole wall temperature	[°C]
T_{cond}	Condensation temperature	[°C]
T_{evap}	Evaporation temperature	[°C]
$T_{f,mean}$	Average temperature between in and outgoing fluid temperature	[°C]
$T_{f,in}$	Inlet fluid temperature	[°C]

$T_{f,out}$	Outlet fluid temperature	[°C]
T_{pw}	Collector pipe wall temperature	[°C]
T_0	Initial ground temperature	[°C]
T_∞	Undisturbed ground temperature	[°C]
$\dot{V}$	Volumetric flow	[m^3/s]
q	Heat rate per meter	[W/m]
q_{pw}	Heat rate per meter at the collector pipe wall	[W/m]
$Q_{electric}$	Electric power input to the heat pump	[W]
$Q_{heat\ pump}$	Power delivered from heat pump	[W]
$Q_{energy\ wells}$	Power delivered from energy wells	[W]

Greek symbols

α	Thermal diffusivity	[m^2/s]
β	Volumetric thermal expansion coefficient	[1/K]
κ	Thermal conductivity	[W/m·K]
μ	Dynamic viscosity	[kg/ms]
ν	Kinematic viscosity	[m^2/s]
ρ	Density	[kg/m^3]
∇^2	Laplace operator	

Subscripts

f	Fluid	

in	Inlet
out	Outlet
pw	Pipe wall
bhw	Borehole wall

Abbreviations

BHE	Borehole Heat Exchanger
COP	Coefficient of Performance (Heat Pump)
EED	Earth Energy Designer Program
GLEHEPro	Ground Loop Heat Exchanger Program
GSHP	Ground Source Heat Pump
HP	Heat Pump
NGU	Geological Survey of Norway
TRT	Thermal Response Test
EG	Ethylene Glycol- water solution

1 Introduction

Increased global warming due to greenhouse gas emission is an issue discussed by politicians all over the world. Governmental plans of reducing the greenhouse gas emission promote building energy efficient buildings with renewable energy sources through subsidizes. Ground source heat pump (GSPH) systems are receiving increased interest because of their potential of reducing buildings primary electrical energy consumption and the thereby the greenhouse gas emission worldwide. Air is today's most common heat source for heat pumps, but using the ground as a heat source has expanded over the last decades. The easy energy access using air as a heat source and the comparatively relatively higher installation cost for GSHPs favors air as a heat source, but the drawbacks using air a heat source is that the energy efficiency decreases with increasing heating demand at cold winter days. The ground temperature is almost constant during the season and ground source heat pumps will therefore provide high energy efficiency even at low ambient temperatures. Thousands of GSHP installations are installed worldwide, and further acceptance for both standard depth and deeper boreholes will rely on development of accurate, reliable and fast simulation tools of long and short term simulation models. This will attribute to more reliable and effective system designs which will minimize the economical installation payback time and secure long time operation time.

GSHP systems are used to provide heating and cooling in both commercial and private buildings and use a heat pump with connection to a borehole heat exchanger (BHE). GSHP systems may use horizontal or vertical ground loop heat exchanger, but this thesis is limited to vertical heat exchanger. The vertical loop ground coupled systems requires less ground area than the horizontal systems, which makes them more applicable for commercial applications. For deep BHEs the ground temperatures can be seen as independent of the ambient temperature, which makes it possible to design system with effective heating and cooling. When cooling is demanded, usually in the summer and early autumn, the ground works as a heat sink, with excess energy from cooling/ventilation stored in the ground. In the winter when there is a heating demand, the ground is the system heat source.

1. INTRODUCTION
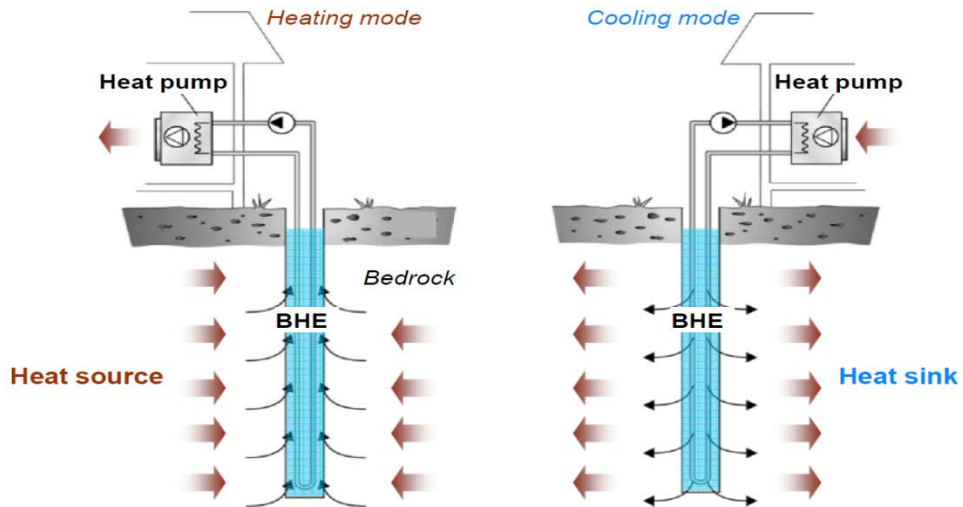
Figure 1-1 Heating and cooling mode, Stene (2012)

BHE systems may be installed with a single borehole, or with interconnected borehole networks, and together with the borehole depth the BHE system design is based on the building heating and cooling demand and the available ground area. For commercial use the depth of the boreholes usually vary from 60 meter to 300 meter, but in this thesis a system of five boreholes with an approximate depth of 500 meters is evaluated.

The GSHP systems typically consist of water-to-water and water-to-air heat pumps which are connected to a network of BHEs. In closed systems the heat carrier fluid is circulated in closed tubes. The most common single BHE is the u-pipe shown in Figure 1-2 where the heat carrier fluid is an antifreeze water solution. The gap between the u-pipe and the ground is typically filled with groundwater for or a grout mixture to ensure effective heat transfer from the ground to the heat carrier fluid. Groundwater filled boreholes are common in North European countries, and grout filled boreholes is commonly used in USA to prevent migration of contaminants from the antifreeze water solution inside the collector. Acuña (2013). In open systems the heat carrier fluid is in direct contact with the ground and higher thermodynamic performance than closed loop systems but it requires a certain ground water quality to avoid problems as corrosion, fouling and blockage in the heat exchanger between the groundwater and the refrigerant fluid in the heat pump.
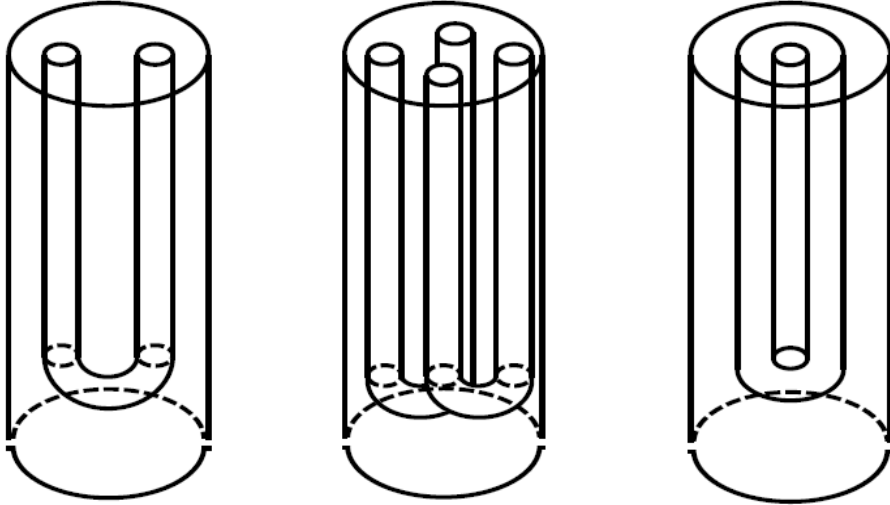
Figure 1-2 Three types of BHE geometries, single u-pipe, double u-pipe and annular tubes, He (2012)

The heat transfer in the BHE is dependent on the ground conditions such as the ground thermal conductivity, groundwater and fracture flow. Interaction with other boreholes might also influence the heat transferred from the ground to the heat carrier fluid.

Due to the change in building energy requirements the actual heat transfer in a BHE varies continuously. The supply and return temperatures of the heat carrier fluid will therefore fluctuate through a day. These variations influence the overall system performance and the heat pump coefficient of performance (COP) and to have a BHE simulation model that fast and effective can predict the fluctuations in the supply and return temperature on a short- as well as long time basis is essential. Specific ground properties like groundwater flow, determination of thermal conductivity and interactions with other boreholes should be considered and evaluated for each case to make the simulation as reliable as possible.

1.1 Problem illustration

Knowledge about the transient temperature distribution in the borehole, and effective heat transfer capacity of boreholes around 500 meters deep, is important to be able to design cost-and operation effective GSHP installations in the future. When designing and sizing deep BHEs, effects like ground water flow and interactions between boreholes may

influence the heat transfer in the borehole. Importance of such influences must be evaluated and taken into account when developing measurement and evaluation methods.

1.2 Objectives

This master thesis is aiming to develop a program that can be used for 500 meter deep boreholes, based on data collected from the GSHP system installed at Skoger elementary school in 2010. There are five boreholes, each at 500 meter and the collected data will form the boundaries for a numerical model that will be used to simulate the borehole heat exchangers. By changing inputs, the performance of the GSHP system will be analyzed and optimized.

1.3 Structure

- Literature review of different numerical models, with different degree of complexity
- Ground effects on BHE performance
- Describe installations at Skoger elementary school
- Set-up of a 3D numerical model
- Set-up of a 2D numerical model
- Use models to predict the performance of the system at Skoger school
- Analyze the performance of the BHE
- Parametric study

2 Literature review

2.1 Introduction

This chapter presents a literature review of different model developments of borehole heat exchanger. Literature review regarding model validations, applications and limitations will form a background for the choice of method applied in the modeling part of the thesis.

The lifetime of a borehole heat exchanger depends on avoidance of excessive heat loss in the borehole field, and the COP of the heat pump is directly influenced by the fluctuations of the supply and return temperature of the heat carrier fluid. This is reasons why it is important to have models that effectively estimate the return and supply temperature for short as well as long term periods.

2.1.1 Application of BHE

Applications for BHE models are design of BHE which includes e.g. sizing the borehole depth and determine the number and spacing of boreholes, evaluation of overall performance by integrating the models with heat transfer models for buildings and HVAC systems and interpretation of in-situ ground thermal conductivity test data with analytical models.

So far the modeling of a BHE has been done using a long-time steady state temperature response, which involves many simplification assumptions. In real GSHP systems a frequency of varying heat load results in a transient temperature response in the borehole for short as well as long time intervals. With higher heat load frequency a short time step simulation model will be more precise than a long step simulation model.

The heat response of the BHE is dependent on the heat transfer inside the borehole and thermal circumstances around the BHE. Inside the borehole the thermal resistance and thermal mass describes the heat transfer. The thermal resistance of the borehole is dependent whether the borehole is filled with grouting or groundwater. This resistance is pure conductive in grouting filled boreholes, and for groundwater filled boreholes the resistance is also based on natural convection. Groundwater around the borehole and

thermal interference with adjacent boreholes influences the heat flow from and to the borehole.

2.2 Analytical models

A number of variations of two analytical methods, infinite line source- and cylindrical source model, are being used to dimensioning BHEs and evaluating thermal response tests. A lack of accuracy for short time periods are due to several simplification assumptions that are necessary to make according to type of material and BHE geometry. The line and cylindrical source method can produce results for either a constant pipe surface temperature or a constant heat transfer rate to or from the surrounding ground. Combined approaches of analytical and numerical are also used to simulate thermal behavior of BHEs. With analytical models it is possible to approximate parameters by minimizing the difference between the experiment data by systematically varying the ground thermal conductivity and the borehole resistance and the model by adjusting the model output. Today the cylindrical source model is used in America, and in Europe the infinite line source model is the most commonly used model.

2.2.1 Infinite Length Line Source Method

An analytical model based on the line source model proposed to design BHEs, was presented by Ingersoll et al. (1954). The model simplifies the borehole to an infinite long line source, and the heat transfer along the borehole length and heat transferred through the upper and bottom part of the borehole is neglected. The heat transfer in the ground is dependent on time and dominated by radial conductive heat transfer along the borehole axis. Another model simplification is constant ground formation and perfect contact between the heat source and the surrounding ground. The line source model includes a heat capacity effect in the borehole equal to the surrounding ground material, which makes it react different than the cylindrical source model for short simulation time. Ingersoll and Plass (1948) approach is defined

$$T(r,t) - T_0 = \frac{q}{4\pi\kappa} \int_y^\infty \frac{e^{-u}}{u} du = \frac{q}{4\pi\kappa} F(y) \qquad (2\text{-}1)$$

where

$$y = \frac{r}{2\sqrt{\alpha t}} \tag{2-2}$$

for $y < 0.2$, $F(y)$ yields:

$$F(y) = 2.303 \log_{10}\frac{1}{y} + \frac{y^2}{2} - \frac{y^4}{8} - 0.2886 \tag{2-3}$$

For $y > 0.2$, $F(y)$ is tabulated in Ingersoll and Plass (1948).

The most commonly used approach to the infinite line source was developed by Carlslaw and Jaeger (1947)

$$T(r,t) - T_0 = \frac{q}{4\pi\kappa}\int_w^\infty \frac{e^{-u}}{u}du = \frac{q}{4\pi\kappa}E_1(w) \tag{2-4}$$

where

$$w = \frac{r^2}{4\alpha t} \tag{2-5}$$

And E_1 is approximated to

$$E_1(w) = w - \ln(w) - \gamma - \frac{w^2}{2(2!)} + \frac{w^3}{3(3!)} + \cdots + \frac{(-1)^{n+1}w^n}{n(n!)} \approx \ln(w) - \gamma \tag{2-6}$$

With Euler constant $\gamma = 0.5772157$ and error less than 10% for a time, $t > \frac{5r_b{}^2}{\alpha}$

Assuming steady state inside the borehole, a borehole thermal resistance can represent the relationship between the mean fluid temperature inside the collector and the borehole wall temperature is given by equation (2-8) from Gehlin (2002)

$$T_{f,mean} = T(r = r_b, t) + qR_b = q(R_b + \frac{1}{4\pi\kappa}[\ln\left(\frac{1}{w}\right) - \gamma]) + T_0 \tag{2-7}$$

Where

$$T_{f,mean} = \frac{T_{f,in} + T_{f,out}}{2} \tag{2-8}$$

2.2.2   Cylindrical Source Method

The infinite line source model is a simplified variation of the cylindrical source model. The analytical cylindrical source solution has, like the infinite line source model, a base which has been refined over the years. Carlslaw and Jaeger (1947) developed the cylindrical source solution, and it has been applied by presenting the heat exchanger pipes as one coaxial pipe, and approximating the BHE as an infinite cylinder surrounded by homogenous medium with constant properties. It gives an exact solution for constant heat transfer between the ground and the buried infinite cylinder, with assuming the heat transfer process as pure conduction and perfect contact between the infinite cylinder and the ground. The cylindrical source model represents the heat flow process from the circulating fluid to the borehole wall as a thermal resistance, and like the infinite line source theory the models neglects heat transfer in axial borehole direction and the thermal short circuiting effects between the u-pipe pipes. The cylindrical source model approach makes it possible to implement the specific borehole geometry and heat capacities of fluid, and borehole filling. Disadvantages connected to the model are that it is not accurate for short time simulations and it relies on estimates of the ground's volumetric specific heat and the ground's thermal conductivity. Assuming constant heat flux along the temperature difference between the ground temperature at a radial distance r from the cylinder source at time t and the initial temperature T_0 borehole is based on the one-dimensional heat equation in radial direction the cylindrical solution developed by Carlslaw and Jaeger (1947) and can be expressed as

$$T(r, t) - T_0 = \frac{q}{k} \, G(\tau, p) \tag{2-9}$$

where

$$\tau = \frac{\alpha t}{r^2} \tag{2-10}$$

$$p = \frac{r}{r_b} \tag{2-11}$$

r_b is the borehole wall radius

$$G(\tau, p) = \frac{1}{\pi^2} \int\limits_0^\infty \frac{e^{-\tau\beta^2} - 1}{J_1^2(\beta) + Y_1^2(\beta)} [J_0(p\beta)Y_1(\beta) - J_1(\beta)Y_0(p\beta)] \frac{1}{\beta^2} \, d\beta \qquad (2\text{-}12)$$

In the above equation the J_0 and J_1 are Bessel functions of the first kind, and Y_0 and Y_1 are Bessel functions of the second kind. $G(z, p)$ is function of time and distance from the borehole center.

2.3   Numerical Models

Numerical models are based on finite element, finite volume or finite difference methods. These methods can be designed to take ground and BHE properties like BHE geometry, varying heat transfer rates, downward and upward fluid flow thermal short circuiting effects, pipe and wall contact resistances, ground water flow and interaction with other boreholes into consideration. The accuracy of the numerical models is therefore higher than the analytical models which make them more appropriate for theoretical analysis. Numerical models have a higher flexibility than analytical because they are well suited for situations with variable heat injection, but according to the complexity of the numerical model, extensive computational time might be required compared to the analytical models and are therefore not suited to be incorporated directly into building energy simulation software.

2.3.1   Two dimensional numerical Models

2.3.2   Hybrid Models

2.3.3   Long time step g-function

An alternative to the numerical models are hybrid models. A hybrid model presented by Eskilson (1987) is able to be implemented in both design and simulation software. Although the analytical models do not need extensive computational time, they are less suited for simulations of a BHE system that have time varying heat transfer rates and interact with other boreholes. Eskilson (1987) developed combined analytical and numerical methods for BHEs thermal storage applications. Eskilson's model was developed to provide for the ground response to heat extraction or injection over long time periods, based on a dimensionless temperature response factor called g-function, for determining the

temperature response of a BHE at the borehole wall. A two dimensional radial-axial finite difference method for a single borehole calculates the temperature response to a single step heat pulse, and an intricate superposition technique then determines the temperature response to the given BHE array using the temperature distribution obtained of a single borehole. These temperature responses are then normalized to the g-function. A response to any heat input can then be calculated with heat injection devolved to a series of step functions, and each unit step can be superimposed to calculate the overall response. The g-function denotes the step response function with a time dependent borehole resistance

$$T_{bw} - T_{\infty} = \sum_i \frac{\Delta q_i}{2\pi \kappa} g\left(\frac{t - t_i}{t_s}, \frac{r_b}{H}\right) \tag{2-13}$$

Where

$$t_s = \frac{H^2}{9\alpha} \tag{2-14}$$

Here H is the borehole depth, r_b is the borehole radius and the change in heat extraction at time t_i is Δq_i.

The borehole is simplified as a cylinder with a finite diameter and length, and represents the relationship between the fluid and the borehole wall temperature by a thermal resistance. The model will therefore not be able to provide short time response since the numerical model does not include the thermal capacities and conductivities of the different material inside the borehole. The approach is therefore called the long time step g-function and is valid for time greater than a couple of hours ($t > \frac{5r_b^2}{\kappa}$) to several years. The g-function for different BHE configurations and geometries has to be pre-computed in order to imply them into building energy simulation software such as EED, TRANSYS, Energy Plus and GLEHEPRO.

2.3.4   Short time-step g-function

It is necessary to have a less time consuming simulation model with ability to operate at short time scales when incorporating simulation models in whole-energy design and analysis program. Solving the partial differential heat conduction equation by applying the finite volume method to a two dimensional radial axial coordinate system, Yavuzturk (1999) extended the g-function to account for effects of the grouting material and apply

for short time steps. Resistance of the grout and pipe due to conduction inside the bore-hole and the fluid flow convection resistance, which is accounted for through an effective pipe wall resistance combining convection and conduction were modeled by simulating only half of the borehole with a polar grid, using the symmetry of the borehole. Figure 2-1 shows a representation of the borehole simulated and illustrates how the u-pipe is represented using the pie sector approximation.
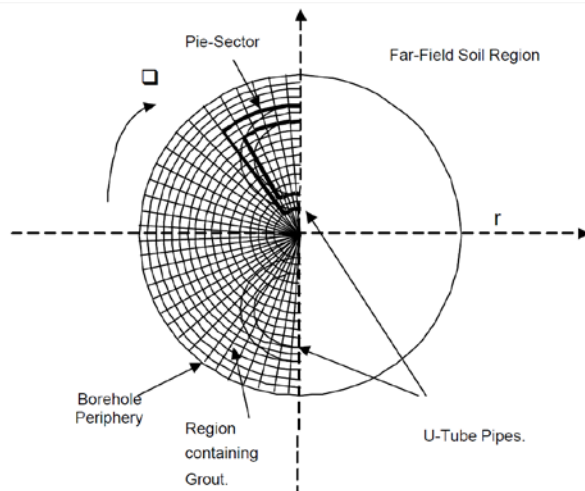
Figure 2-1 2D fully discretized model with pie-sector mesh, Yavuzturk (1999)

Along with the simplification that three dimensional effects at the end of the u-pipe and at the ground surface are neglected, in-homogeneities in the ground are neglected. The fluid transfer inside the pipes was approximated with a constant heat flux boundary con-dition at the pipe wall. The biggest model disadvantage together with constant heat flux boundary is that the thermal mass of the fluid is neglected as the dynamic of the fluid transport along the borehole depth is not accounted for.

2.3.5   Three dimensional numerical models

Two dimensional numerical models can be used to calculate the dynamic response of grout material, pipes and rock, and they have been developed to distinguish between different grouting and pipe properties and geometries, by including the effects of the flu-ids thermal mass. Such two dimensional models are not able to calculate variation of fluid temperature inside the collector along the borehole axis, and must therefore make simpli-fications about the fluid temperature and the belonging boundary conditions. Averaging

the inlet and the outlet fluid temperature as an approximation to the real fluid temperature, or equal one of the pipe legs to the inlet fluid temperature and the other to the outlet temperature is commonly used simplifications for two dimensional models. To avoid such simplification assumptions three dimensional models have been developed to study the heat transfer in a BHE more carefully and they are useful for detailed study of a BHE. Three dimensional models might include effects of fluid flow variation along the BHE, fluid and borehole temperature variations along the borehole depth, different layers of rock, thermal dispersivity, different boundary conditions at the surface, initial vertical temperature gradients and heat transfer below the BHE.

2.3.6   Thermal Resistance and Capacity Models

In order to be able to simulate heat transfer in an efficient way with minimum computational effort and without reducing the accuracy of the models, pseudo three dimensional numerical models are developed. Discretized three dimensional models are therefore developed to evaluate three dimensional effects of heat transport in and outside the borehole, transient fluid transport inside the collectors and thermal short-circuiting with reduced computational time.

Discretizing the material and geometry inside and outside the borehole of complex BHE geometries has been widely used in the recent development of BHE simulation models. The discretized models are shown to be an accurate and effective method to explicitly simulate a transient BHE heat response. Both 2D and 3D models has lately been developed, and the 2D representation is shown to be more efficient in computation, but heat transfer processes are more accurate represented by the 3D models.

A Capacity Resistance Model (CaRM) was developed by De Carli et al. (2009) to simulate the thermal behavior of vertical ground heat exchangers, and uses the electrical analogy with lumped capacities and thermal resistances to solve the transient heat transfer. This model allows considering fluid flow inside the collector pipes, for u-pipe, double u-pipe or coaxial borehole geometries. Assuming that the heat transfer is dominated in the radial direction and neglecting the heat flux in the vertical direction, the heat transfer of the ground is seen to be one a dimensional heat conduction problem. With the borehole and the ground divided into (m) overlapped slices in the vertical direction and for each

slice the ground surrounding the borehole divided into annular subregions (n) in the radial directions, shown in Figure 2-2, each of them with different thermophysical properties. The temperature within any annular subregion is therefore only dependent on time and radial direction.
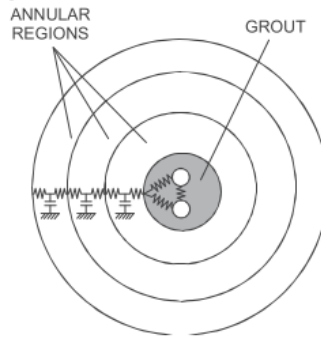
Figure 2-2 Modeling of the annular regions, Carli et al. (2009)

In CaRM the control volume approach is used to discretize the heat conduction differential equation, where the heat conduction equation is

$$\frac{\partial T}{\partial t} = \alpha \nabla^2 T \qquad\qquad 2\text{-}15$$

Figure 2-3 shows the modeling of the surrounding ground along the borehole depth.
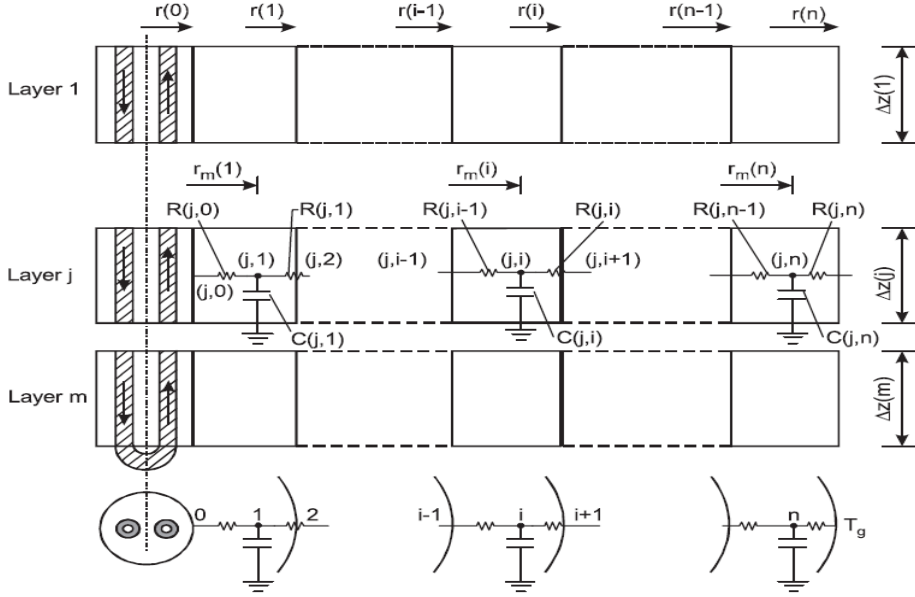
Figure 2-3 Modeling of the surrounding ground, De Carli et al. (2009)

Neglecting temperature gradients within the solid, the ground heat conduction for each slice can be written

$$\frac{T_{(j,i-1)} - T_{(j,i)}}{R_{(j,i-1)}} + \frac{T_{(j,i+1)} - T_{(j,i)}}{R_{(j,i)}} = C_{(j,i)} \frac{T_{(j,i-1)} - T_{-\Delta\tau\,(j,i-1)}}{\Delta t} \tag{2-16}$$

with $T_{(j,n)} = T_{\infty}$ is the boundary condition and T_{∞} is the undisturbed ground temperature and $T_{-\Delta\tau}$ is the mean temperature at previous step. The thermal resistance between two adjacent annular regions is

$$R_{(j,i)} = \frac{1}{2\pi L \kappa} \frac{\sqrt{r_{(i)}^2 - r_{(i-1)}^2/2}}{\sqrt{r_{(i-1)}^2 - r_{(i-2)}^2/2}} \tag{2-17}$$

Where r is the radial distance, j is the number of slice in the vertical direction and i is the number of the annular region in the radial direction.

Neglecting the heat storage capacity of the solid, the thermal flux from surface 1 to surface 2 at temperatures T_1 and T_2 can be represented

$$q = \frac{T_1 - T_2}{R_{1,2}} \tag{2-18}$$

The thermal heat capacity is calculated by the following equation

$$C_{(j,i)} = \rho c_p \pi (r_{(i)}^2 - r_{(i-1)}^2) \Delta z \tag{2-19}$$

where Δz is the length of the slice in the vertical direction.

Different borehole geometries can be represented by the resistance of the borehole which is an input in for the model. The specific resistances of a BHE need to be calculated from another finite element method. When neglecting the fluid thermal capacity, the fluid temperature can be calculated by

$$\dot{m}_f \, c_{pf} \left(T_{f,in(j)} - T_{f,out(j)} \right) = 2\pi \, r_i \, h \, \Delta z (T_{f(j)} - T_{p(j)}) \tag{2-20}$$

where $T_{f(j)}$ is the mean temperature of the fluid inside the specific cell, and $T_{p(j)}$ is the mean cell internal surface temperature. The error by taking $T_{f(j)}$ equal to the outlet temperature of the specific cell is said to be limited as the cell is small and the inlet and outlet temperature is usually small.

The CaRM model by De Carli et al. (2009) makes it possible to evaluate the ground temperature at different depth and radial distances from the borehole and the fluid temperature profile. A cylindrical symmetry around the borehole is assumed and only conduction is considered for the ground, and the heat transfer between the lowest part of BHE and the ground underneath its end is not considered. This model is not suited for short time step simulations because the fluid thermal capacity is neglected and only the thermal resistance is used to account for the resistance of the borehole filling, the fluid convection heat transfer, of the pipe walls and the heat transfer between the pipes.

Zarrella et al. (2011) presented an improvement of the CaRM model which considers the borehole thermal capacitance, both for the borehole filling and the heat carrier fluid inside the collector. The model was analyzed for a double u-pipe collector, where an extra thermal node is implemented in the BHE. Figure 2-4 shows the borehole divided in two zones the core and the shell. Heat transfer for short time steps can be calculated by adding the thermal capacities to the specific zones.
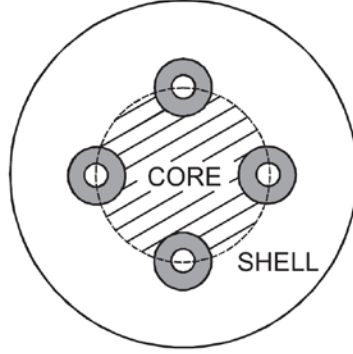
Figure 2-4 Principle of two different capacity zones, Zarrella et al. (2011)

Equation (2-20) including the thermal capacity, and by considering the rate of variation of the fluid internal energy can be written

$$\dot{m}_f\, c_{pf}\big(T_{f,in(j)} - T_{f,out(j)}\big) - 2\pi\, r_i\, h\, \Delta z(T_{f(j)} - T_{p(j)}) = \rho_f c_f \pi r_{(p)}^2 \Delta z \frac{T_{f(j)} - T_{f-\Delta t\,(j)}}{\Delta\tau} \qquad (2\text{-}21)$$

The heat transfer rate due to the variations of fluid temperature along the borehole depth and the heat carrier fluid capacity can be rather important to the short time heat transfer effects. It can be calculated by

$$q = \rho_f\, c_f\, \pi\, r_{p,i}^2\, L\, \frac{T_f - T_{f-\Delta t}}{L/v_f} \qquad (2\text{-}22)$$

Where v_f is the fluid velocity, L is the length of the pipe and L/v_f is the circulation time of the fluid inside the collector.

Another three-dimensional numerical simulation model was developed by Bauer et al. (2011). Two models were developed including the thermal capacity of the fluid inside the collector tubes and the grout, which makes the models able to consider the heat and mass transfer inside the borehole. To reduce the number of elements representing the borehole only half of the borehole was considered and for one of the models a simplified resistance and capacity model (TRCM) was used to describe the borehole geometry. This was shown to not decrease the accuracy of the steady state computation, but it affected the transient capabilities. The second model discretized a 2D model of the borehole showed in Figure 2-5.
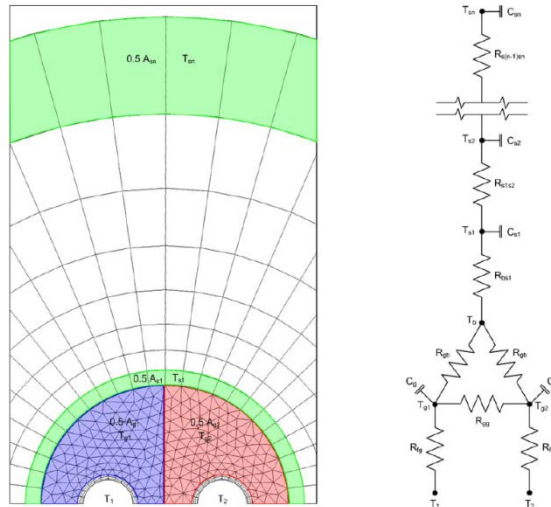
Figure 2-5 Fully discretized horizontal 2D finite element method and corresponding TRCM model, from left to right, Bauer et al. (2011)

This model can deal with the internal resistance between the downward and upward fluid flow and the resistance between the fluid and the borehole wall. The soil is simplified as one dimension and Figure 2-6 shows how the layers are connected, but groundwater flow is not considered.
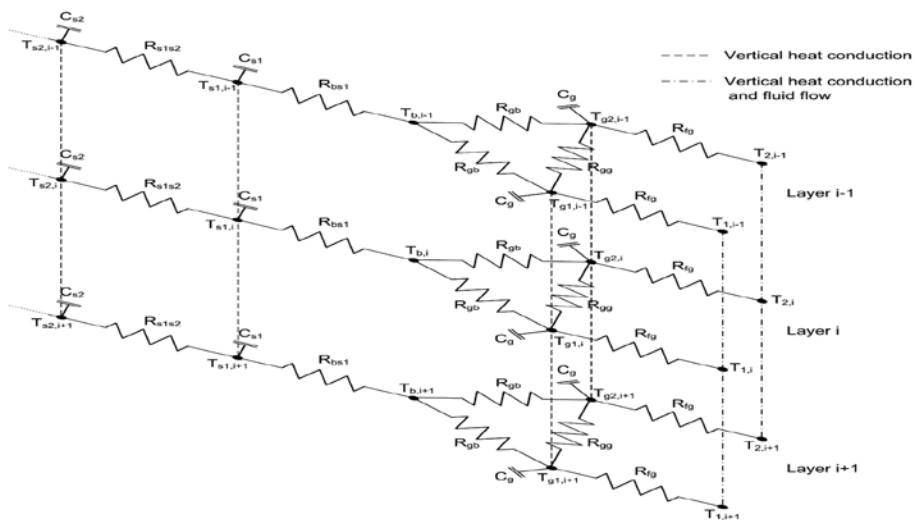
Figure 2-6 Connection of 2D horizontal models to a 3D model, Bauer et al. (2011)

2.3.7 Discretized Three-Dimensional Models

Al-Khoury and Bonnier (2006) and Al-Khoury et al. (2005) developed a transient and steady state model, with purpose of reducing the required number of finite elements necessary to describe the heat flow in a BHE. The model is able to simulate transient and steady state for both single and double u-pipes including groundwater flow. This is done by using a one dimensional finite element method to simulate the heat transfer in the u-pipes and the grout, which implies a temperature variation along the borehole depth, and a three dimensional finite element method to solve the partial differential equation of heat and convection to simulate groundwater flow in a porous medium in contact with a borehole. These two models were coupled, using the temperature at the boundary conditions of the model that describes the heat flow inside the borehole as a boundary condition for the three dimensional model describing the soil surrounding the BHE and by energy conservation equations for the components within the BHE given by equation (2-23).

$$ c\rho \frac{\partial T}{\partial t} = \kappa \frac{\partial^2 T}{\partial x^2} + \kappa \frac{\partial^2 T}{\partial y^2} + \kappa \frac{\partial^2 T}{\partial z^2} - c_w \rho_w \left(q_{w,x} \frac{\partial T}{\partial x} + q_{w,y} \frac{\partial T}{\partial y} + q_{w,z} \frac{\partial T}{\partial z} \right) + Q \qquad (2\text{-}23) $$

Were $q_{w,x}$ is the groundwater flow in x-direction, T is the ground temperature and Q is a heat source (W/m^3)

Figure 2-7 shows how the borehole with its components are represented by a one dimensional model
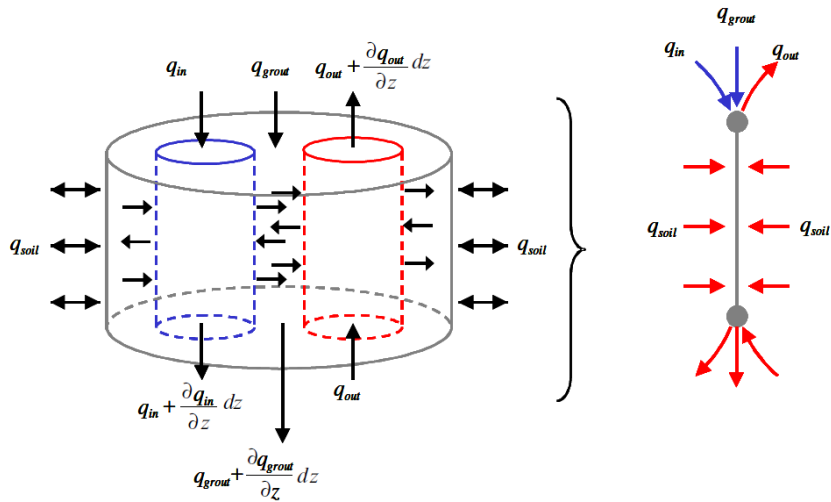
Figure 2-7 1D representation of the heat flow within the borehole, Al-Khoury et al. (2005)

Using only one element to represent the pipe flow and the conduction in the grouting material instead of a three dimensional full discretization reduces the discretization and size of the mesh significantly. The disadvantage of one dimensional representation of the heat flow is that the thermal mass of the pipes are neglected, and the grout temperature is assumed to be uniform which makes the model less accurate for transient computations. Figure 2-8 shows resistance between the different components within the borehole.
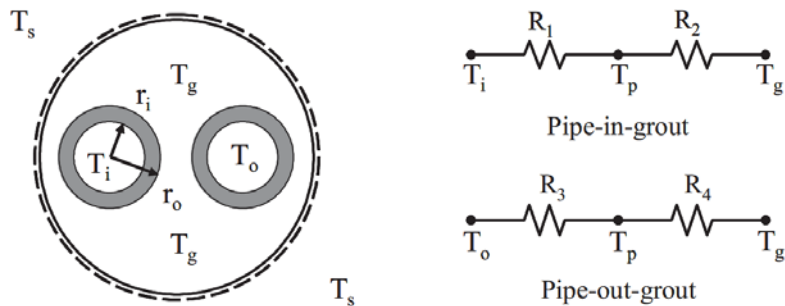
Figure 2-8 Pipe and grout heat flow resistance, Al-Khoury et al. (2005)

Diersch et al. (2010) extended the model developed by Al-Khoury and Bonnier (2006) by improving the relationship for the resistances inside the BHE, dividing the grout into

different zones depending on the number of pipes, and reducing the mesh dependency for elements around the borehole. The pipe to grout resistance was based on an improved thermal resistance and capacity model (TRCM) using one capacity point for each pipe in the BHE. This makes it possible to model the heat transfer inside the borehole more accurate than only using a single capacity point for the grout, because the thermal capacity of each zone of the gout can be taken into account. The model can also deal with double u-pipe, coaxial pipes with centered and annular inlet. Figure 2-9 shows a representation of the thermal resistances and thermal capacities with the borehole divided in two parts for borehole with a single u-pipe.
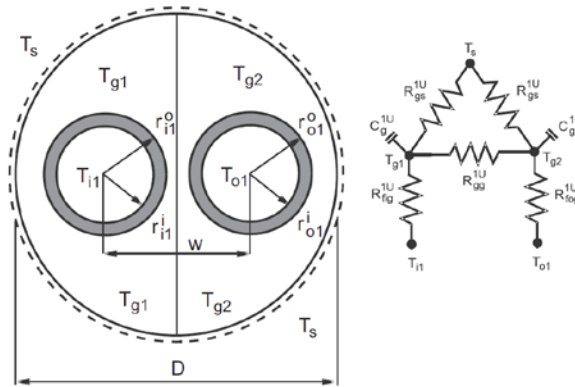
Figure 2-9 TRCM with two capacity points, Diersch et al. (2010)

The model developed by Diersch et al. (2010) links the local problem, which is the thermal process inside the borehole to the soil, that is considered as the global problem, by a thermal transfer relationship. They are formulated in the same way as Al-Khoury and Bonnier (2006) model, but an improved non-sequential coupling strategy for the BHE and the porous medium discretization is implemented. The model showed good agreement for both long- and short term solutions when the results were compared to a fully discretized three-dimensional model.

2.4   Fully Discretized Three-Dimensional Numerical models

A number of numerical models with different aspects of the borehole geometry and ground conditions by implementing different boundary conditions and approximations have been developed to evaluate the three dimensional heat transfer effect in a BHE, and to highlight the limitations and improve the accuracy of 2D models. Finite volume, finite

difference and finite element programs requires extensive computational time, and to reduce the computational time it is necessary to reduce the number of elements representing the borehole without decreasing the accuracy of the model. With higher complexity comes longer simulation time and the computational time ratio between a two dimensional model and a three dimensional model may lay in the range of 1/36, which makes the fully discretized models impractical for engineering purposes. Three dimensional fully discretized models make it possible to implement ground and borehole conditions without any assumptions to make the model as realistic as possible. Combined with power increase of computers through the next decades it may be possible in the future to implement fully discretized models to simulation programs without the demand of extensive computational time. He (2012).

2.5   Ground Effects

2.5.1   Groundwater influence

Gehlin and Hellström (2003) developed a 2D dimensional numerical model to investigate the effects of groundwater flow on the borehole wall temperature compared to pure conduction in the ground. Three different groundwater flow approaches were based on the same two dimensional numerical models with the same representation of the borehole and the surroundings. The models were made with an equivalent radius model representing a single u-pipe water filled borehole, shown in Figure 2-10, where the thermal capacity water was taken into account, but the vertical heat flow is neglected as the model only considers two dimensions.
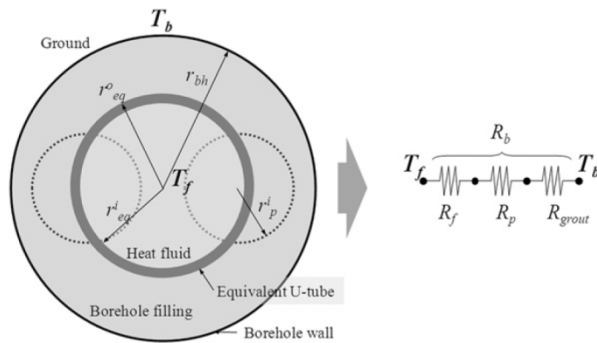
Figure 2-10 Equivalent radius model, Choi et al. (2012)

Developing three different ground water flow scenarios and compare them to each other and a pure conduction case was done, to explain and evaluate high ground thermal conductivity estimations from field observations from thermal response tests. Homogenous groundwater flow around a borehole surrounded by a porous media, homogenous groundwater flow in a porous media near the borehole and groundwater flow in a fracture near the borehole was simulated by Gehlin and Hellström (2003), and shown in Figure 2-11.
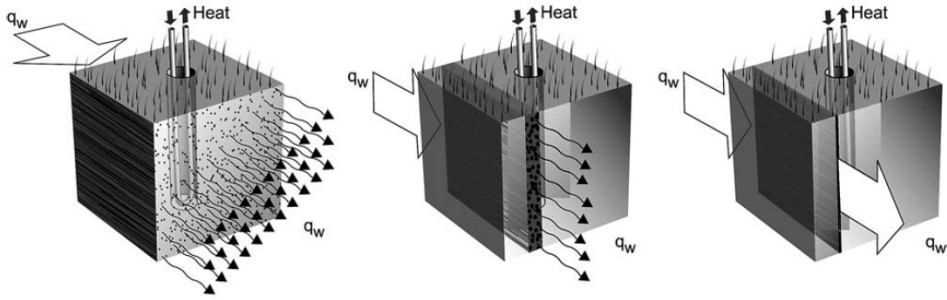
Figure 2-11 Groundwater flow situations simulated, Gehlin and Hellström (2003)

For the first case Darcy's law, which describes the fluid flow through a porous medium, was applied to the conductivity equation to make a conductive-convective transient equation for the heat flow rate. The incoming groundwater has the same temperature as the undisturbed ground, and flow only in one direction which is used for all three models. The two dimensional transient conductive-convective equation for the ground groundwater flow can be expresses as

$$c\rho \frac{\partial T}{\partial t} = \kappa \frac{\partial^2 T}{\partial x^2} + \kappa \frac{\partial^2 T}{\partial y^2} - c_w \rho_w q_w \frac{\partial T}{\partial x} \qquad (2\text{-}24)$$

Which is the heat conduction equation with an added term to account for convective heat flow due to convective groundwater flow q_w. The subscript w stands for groundwater, and T is the temperature in the ground.

For the porous zone with homogenous groundwater flow near the borehole both conductive and convective heat transfer occurs, but only conductive heat transfer is assumed for the impermeable ground. Heat capacity of the porous zone is the same as for water and the incoming groundwater.

The last model considers groundwater flow in a fracture surrounded by impermeable ground.

Groundwater flow is showed to have an influence on the heat transfer in the borehole but the flow structure is dependent on the ground conditions. For hard rock the groundwater flows through fractures in the ground, and an assumption of a homogenous porous ground may therefore include some errors. Gehlin and Hellström (2003) showed that the thermal influence of groundwater flow, after 100 hours from initial conditions, is highly dependent on the fluid flow velocity, and correlated to the specific groundwater flow model. The

effect of the porous and the fracture flow decreases as the distance from the borehole increases, but even at distances up to half a meter the porous zone and the fractured flow show an effective thermal conductivity that were 10% higher than for pure conduction case with a groundwater flow velocity of 10^{-6} m/s at distances of 0.6 meter and 0,75meter from the borehole, respectively.

2.5.2 Borehole arrays, with pure conduction

When the seasonal thermal loads are unbalanced, and groundwater flow in the ground is not present or the effects are negligible, a system design with sufficient distance between the boreholes and a low enough thermal load per unit BHE length is crucial for an effective long term BHE field performance. A risk of system collapse after a few decades is possible if these two parameters are not designed carefully. Lazzari et al. (2010) evaluated the mean fluid drop for different borehole arrays, heating loads and thermal ground conductivity by developing a two-dimensional numerical model and neglecting ground water flow. The objective was to look at the long time BHE performance of a double u-pipe. The time periodic heat loads was simulated with summer and winter operation or just winter operation, where the BHEs operates as heat source in the winter and heat sink in the summer.
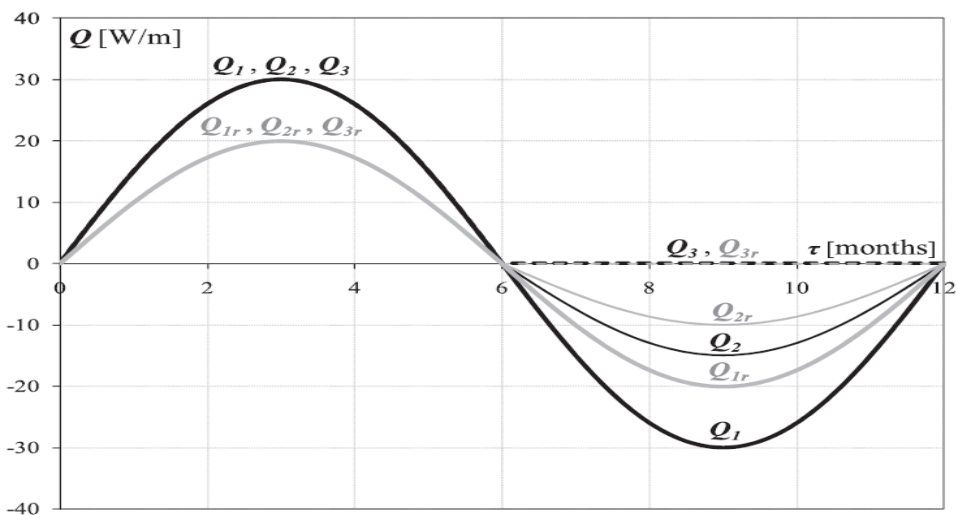
Figure 2-12 Heating amplitudes, Lazzari et al. (2010)

Figure 2-12 shows the heating periods with maximum heating amplitudes of 30 and 20 W/m. Since the model is a two-dimensional model Lazzari et al. (2010) assumed the tem-

perature distribution along the vertical direction to have a negligible influence of the long time performance. Q_1 denotes the heating load for a BHE working both in the winter and the summer, Q_3 represents only winter operation. Both Q_1 and Q_3 have a maximum heating amplitude of 30 W/m and Q_r represents a maximum heating amplitude of 20 W/m. With ground thermal conductivity equal to 2.8 [W/m·K] Figure 2-13 shows that the yearly maximum $T_{f,mean}=(T_{f,in}+T_{f,out})/2$ difference of the working fluid inside the collectors is about 17,5°C for Q_1 and 9.5°C for Q_3 for a double u-pipe with initial ground temperature $T_0=14$°C equal to the initial $T_{f,mean}$.
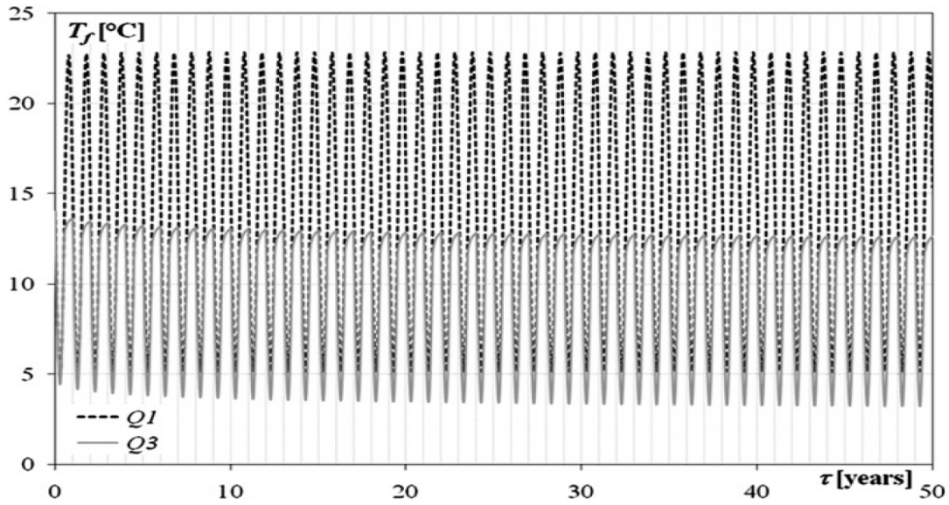
Figure 2-13 $T_{f,mean}$ for $T_{f,mean}$ and $T_{f,mean}$, Lazzari et al. (2010)

Through a period of 50 years the mean value of $T_{f,mean}$ for Q_1 is almost the same as the undisturbed ground temperature which is set to 14°C, but for the heating load Q_3 the minimum mean temperature decreases during the first years, then remains almost constant. Combinations between different borehole arrays and heating loads are evaluated by plotting the minimum $T_{f,mean}$ in Figure 2-14, Figure 2-15 and Figure 2-16.
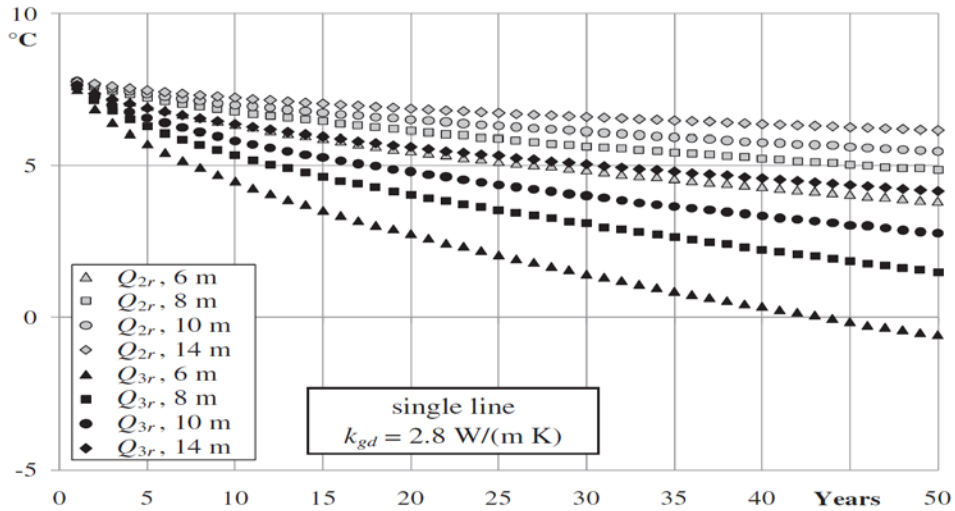
Figure 2-14 Minimum $T_{f,mean}$ for κ=2.8 W/mK and reduced heat loads, Lazzari et al. (2010)
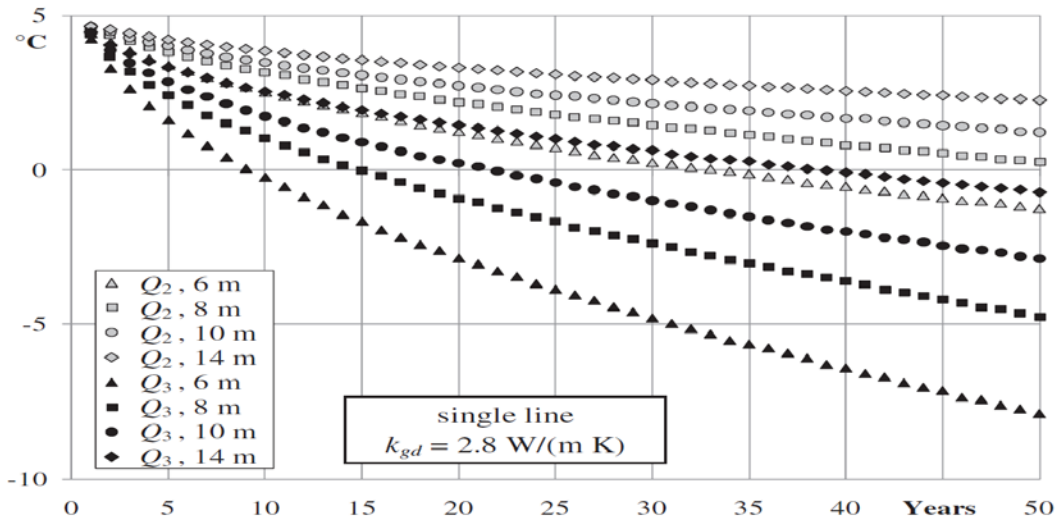
Figure 2-15 Minimum $T_{f,,mean}$ for κ=2.8 W/mK with reduced heat recovery, Lazzari et al. (2010)

Figure 2-14 and Figure 2-15 shows the minimum $T_{f,mean}$ for a single line of infinite BHEs simulated over 50 years with different BHE spacing with a maximum heating load equal to 30 W/m and 20 W/m, respectively. The black dots represent only winter operation and the white dots represents winter operation and heating compensation during the summer. The reduced thermal loads $Q_{1,r}$ $Q_{2,r}$ and $Q_{3,r}$ have the same time evolution of

26

$T_{f,mean}$ as the heating loads of 30 W/m, but the amplitude oscillations are smaller. This explains the difference of the minimum $T_{f,mean}$ after the first year of operation.

The interesting parameter is the temperature drop of the minimum $T_{f,mean}$ where a small drop results in an effective long term performance of the BHE. To secure a long term effective BHE performance Lazzari et al. (2010) considered the distance between adjacent BHEs to acceptable as long as the minimum $T_{f,mean}$ of the working fluid remains above -5°C. All of the different heat loads in Figure 2-14 have a $T_{f,mean}$ above -5°C, the single line BHE array will therefore have an effective long term performance. With heating loads equal to Q_3, Figure 2-15 shows that the distance between the BHEs should be 8 meters or more to have a sustainability production with a single line array of BHEs.

Lazzari et al. (2010) also did a study to evaluate the minimum $T_{f,mean}$ when the thermal conductivity in the ground was set to 1.4 W/mK. Figure 2-16 shows that for a maximum heat load of 30 W/m and maximum recharge rate of 20 W/m, the distance between the adjacent boreholes should be 14 meter or more to keep the minimum $T_{f,mean}$ over -5°C after 50 years of operation. If the thermal conductivity of the ground is overestimated in the design process, the efficiency of the system could be significantly reduced if the boreholes are drilled too close to each other. To be able to have precise values for the thermal conductivity in the ground is therefore crucial if the available distances between the boreholes are limited. For a total borehole depth of 2000 meter or more, Ramstad (2012) recommends to perform an in-situ thermal response test is to get a precise value of the local ground thermal conductivity and borehole resistance.
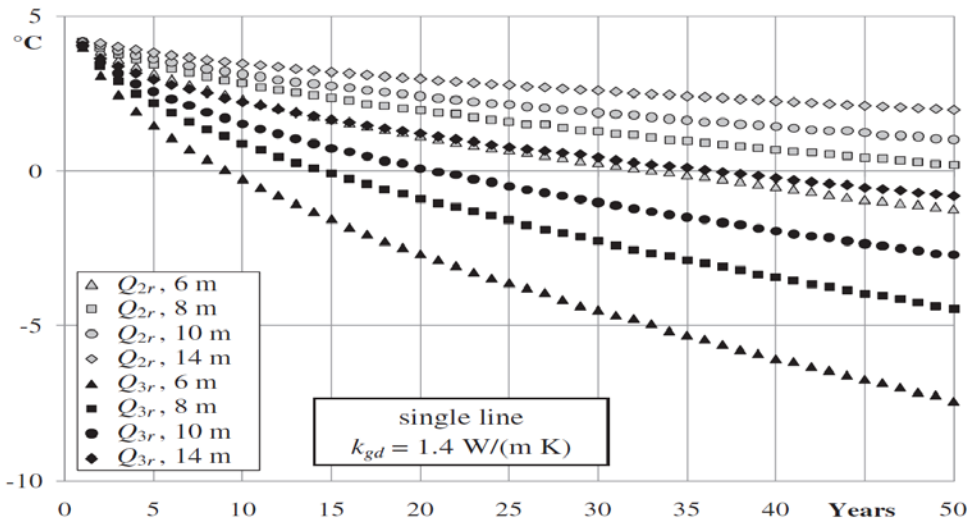
Figure 2-16 Minimum $T_{f,mean}$ for κ=1.4 W/mK with reduced heat recovery, Lazzari et al. (2010)

27

2.5.3   Borehole arrays, including groundwater flow

Influence of groundwater flow rate and direction on a single borehole and borehole arrays has been evaluated through different studies. Choi et al. (2012) developed a two dimensional numerical model to evaluate the influence of groundwater flow on L-shaped, Iine shaped and rectangular borehole arrays with 10 meter spacing between the boreholes and nine boreholes for each array. By varying the groundwater flow rates and the attack angel on the arrays, they showed that heat transfer efficiency of the BHE depends on both the BHE array and the groundwater flow rate. The model developed by Choi et al. (2012) was a two dimensional transient model were the heat transfer inside the borehole was calculated with a steady state thermal resistance, and the u-pipe approximated by an equivalent radius model. Since main objective of the simulation was to investigate the long term behavior, this was assumed to be valid approximations. The temperature of the fluid flow inside the collector was approximated to be an average of the inlet and outlet temperature. The heat transfer rate of surrounding ground was expressed by the conductive-convective two-dimensional model with steady state Darcy flow. Since the GSHP systems in northern Europe are mainly used for heating operation, no heat reloading was considered which can be transferable to e.g. schools. The energy load was considered heaviest in the winter months, and zero in the period between June and August as shown in Figure 2-17.
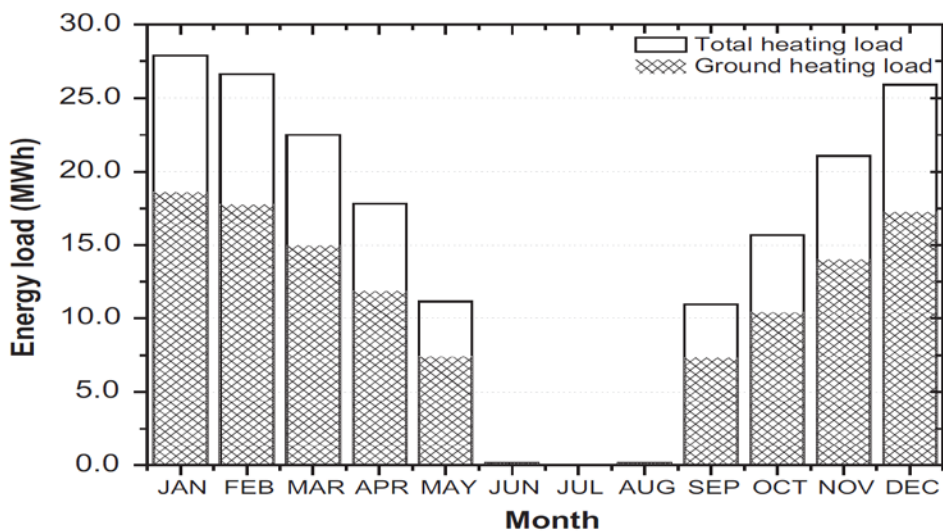
Figure 2-17 Energy load, Choi et al. (2012)

Initial ground temperature was set to 9°C. Choi et al. (2012) plotted the different arrays with groundwater flow rate and the maximum temperature difference between the initial mean fluid temperature and minimum mean fluid temperature for a simulation period of

15 years. Figure 2-18 shows the influence of groundwater flow direction and flow rate on the maximum mean fluid temperature difference, were θ=0° represents a groundwater flow normal to the line array.
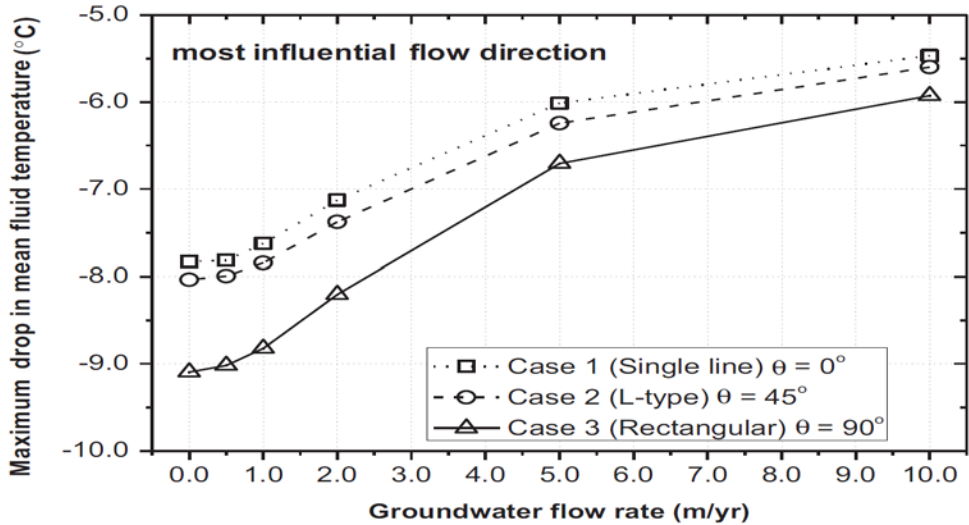
Figure 2-18 Groundwater flow influence on different borehole arrays after 15 years of operation, Choi et al. (2012)

A small temperature drop for the maximum drop in mean fluid temperature means more stable long term performance of the heat pump, and reduced uncertainties regarding fluid freezing of surrounding water and permafrost of the surrounding ground. Figure 2-18 show that regardless of the array type, low rates of groundwater flow does not influence the heat transfer around the borehole compared to pure conduction, and that the rectangular array has the largest mean fluid temperature drop at all groundwater flow rates. The rectangular array was more influenced by the groundwater flow than of the direction, and had a larger maximum mean temperature difference compared to L-array and line array due to the high interaction between the boreholes. The direction of the groundwater flow influenced the I-array the most, with a reduction of 13% in maximum mean temperature difference compared to groundwater flow parallel to the I-array. This shows that designing GSHP systems groundwater flow rate and direction should be considered when designing borehole arrays, and according to Choi et al. (2012) up to 10% of installation and operation cost can then be saved.

2.5.4 Models used for evaluation of Thermal Response tests

Line source and cylindrical source model used for evaluation of TRT only considers conductive heat transfer. The effective thermal conductivity and the thermal resistance in the borehole are the only parameters that include all the heat transport effect relevant to the BHE and the ground heat transfer processes, fully discretized three dimensional models are developed to evaluate these approximations.

Signorelli et al. (2006) evaluated the effect of the borehole length by comparing line source model with a three dimensional numerical model with constant heating power throughout the simulation, a constant heat flow at the bottom of the BHE and a constant surface temperature was used to simulate a realistic vertical geothermal gradient. Borehole depths ranging from 40 to 400 meters was considered, and Figure 2-19 shows that the line source estimation error increases with borehole depth.
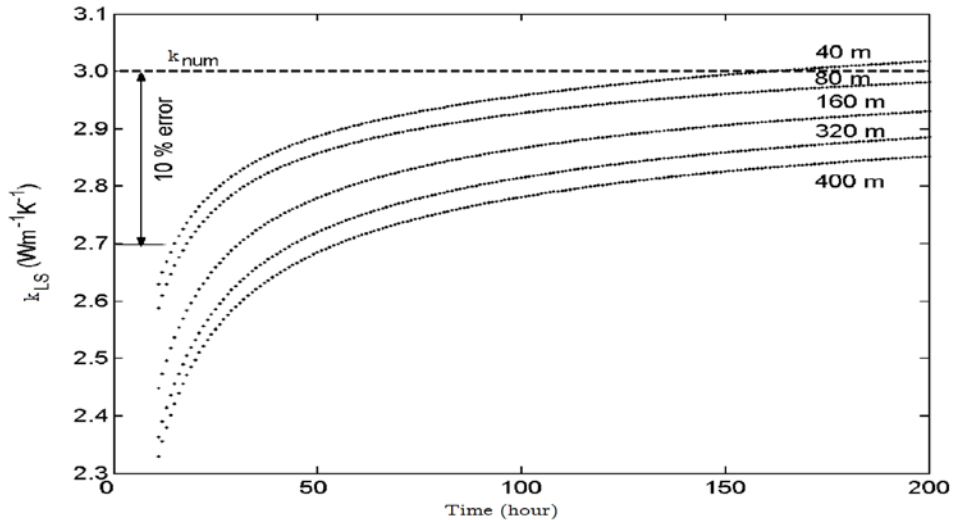
Figure 2-19 Ground conductivity and line source estimation error, Signorelli et al. (2006)

κ is the thermal conductivity of the surrounding ground, were and k_{num} is the actual thermal conductivity of the simulated case, k_{LS} is the thermal conductivity based on the line source model. k_{LS} is calculated from the temperature changes generated from the numerical model assuming a constant k_{num} equal to 3 W/m·K. Short-circuiting between the up and down streaming fluid inside the collector is neglected by the line source model, and because it only assumes radial temperature field it does not take into account the effects of the vertical geothermal temperature gradient. Signorelli et al. (2006) explained the underestimation of k_{LS} for borehole depths of 160, 320 and 400 meters, with the increased effects of the temperature difference between the up and down streaming fluid

inside the collector and the vertical geothermal temperature gradient with borehole depth. The maximum error allowed for a thermal response test is 10% after a certain time, since factors such as borehole length, unstable data, and boundary conditions could affect the error in computed thermal conductivities. Figure 2-9 shows that even for borehole depth of 400 meters the error of the computed thermal conductivities by the line source model, the error is less than 10% compared to the actual ground conductivities.

The model developed by Signorelli et al. (2006) was designed with grouting around the collector pipes, which means that the influence of the heat transfer effects of natural convection of groundwater filled boreholes is not evaluated.

2.5.5 Models that includes natural convection inside the borehole

During operation of boreholes filled with groundwater, the heat extraction or injection will induce a temperature gradient in the borehole. This leads to a density gradient in the groundwater, which results in a convective heat flow. For groundwater filled boreholes the natural convection will affect the heat transfer between the ground and the working fluid, reducing the thermal resistance compared to stagnant water. The convective flow of the groundwater depends on the temperature gradient between the borehole wall and the collector wall, and it will therefore depend on the ground temperature, the amount of heat injected or extracted and whether heat is injected or extracted. A thermal response test where heat is injected into the borehole might therefore result in a different borehole resistance than a borehole heat exchanger in operation which extracts heat. Figure 2-20 shows a velocity profile of water between borehole wall and pipe wall induced by a temperature gradient between the pipe wall and the borehole wall.
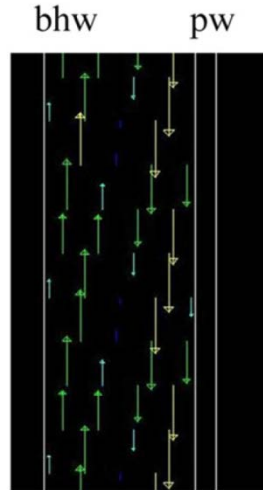
Figure 2-20 Velocity profile of natural convection induced flow, Gustafsson and Westerlund (2011)

A multi-injection rate thermal response test was performed by Gustafsson and Wester-lund (2009) with no influence from regional groundwater flow. Results showed that a larger heat injection results in a decrease in the borehole thermal resistance. The large heat injection triggers more convective heat transfer, thus lowering the resistance in the borehole. The test also showed that the length of the collector did not influence the natural convection in the borehole. Without any influence from groundwater flow the thermal resistance decreased from 0.12 to 0.065 mK/W with an increase of heat injected from 21 W/m to 83 W/m, due to an increase in the convective flow in the borehole. This results supports that higher flow velocities of the borehole water due to the larger density differences in the borehole water enhances the heat transfer in the borehole.

The thermal effects of natural convection are highly dependent on the given geometry and orientation. A simplification of the borehole geometry is often used to make it possible to have a numerical solution. Studies on the heat transfer effects of natural convection have been done with a numerical model, approximating a BHE u-pipe geometry to an equivalent radius geometry with constant heat flux or constant temperature at the inner wall and constant temperature at the outer wall as boundary conditions.

Since the natural convection influence on the borehole resistance is dependent on the relationship between the changes in water density in the radial direction several Nusselt number relationships have been developed, with possibilities of varying the boundary conditions by implementing a Rayleigh number, the radius ratio and the aspect ratio. The Nusselt number can be used to investigate the heat flow increase due to convective heat transfer compared to stagnant water with only conductive heat transfer, but there

are none published Nusselt number correlations for BHE u-pipe geometry applications. Approximating the u-pipe geometry to an equivalent radius model is therefore necessary to be able to use Nusselt number correlations for natural convection induced heat transfer.

The Nusselt number is the ratio of convective to conductive heat transfer across the boundary

$$Nu = \frac{R_{b\ conduction}}{R_{b\ convection}} \qquad (2\text{-}25)$$

and

$$R_{b\ convection} = \frac{R_{b\ conduction}}{Nu} \qquad (2\text{-}26)$$

With Nusselt relations given in equation (2-25) and (2-26) an effective thermal conductivity can be derived, when $R_{b\ conduction}$ and Nu is known. By implementing an effective thermal conductivity a water filled borehole can be simulated with the effects of an approximated natural convection inside the borehole.

Gustafsson and Westerlund (2011) made a 3D model to study the effects of convection and phase change in a water filled borehole. The model was made with an equivalent diameter approximating a u-pipe collector with a specified thickness and a fluid inlet at the bottom and outlet at the top. The height of the model was only one meter, so it practically has the same restrictions as a two-dimensional model. In the model the fluid enter the inlet with a fluid flow velocity at 1 m/s and the fluid inlet temperature varied, starting at 15°C and decreasing linearly with 0.67°C per simulated hour. The undisturbed ground temperature was 6°C during the simulation. With the heat flow in the pipe wall calculated numerically, the borehole resistance was calculated by

$$R_b = \frac{T_{bhw} - (T_{f,in} + T_{f,out})/2}{q_{pw}} \qquad (2\text{-}27)$$
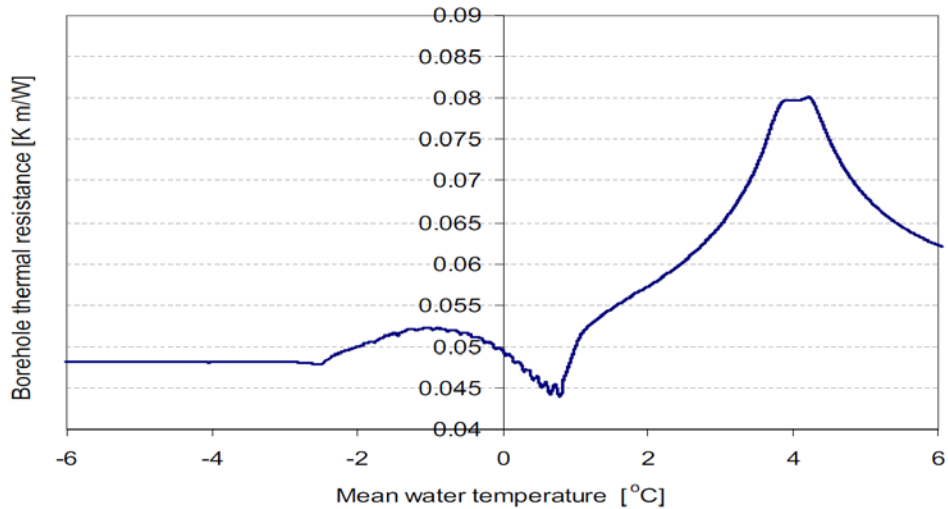
Figure 2-21 Borehole resistance with change in mean water temperature, Gustafsson and Westerlund (2011)

Figure 2-21 show how the borehole thermal resistance varies with mean water temperature which is the mean value of the collector pipe temperature and the borehole wall temperature. As the inlet temperature decreases the borehole resistance peaks at temperatures around 4°C because the water has its highest desist around 4°C as shown in Figure 2-22. When the mean water temperature in the borehole is around 4°C the convective flow is almost negligible, and the borehole resistance is close to the stagnant water case. Figure 2.19 shows that the borehole resistance has a large variation for positive mean water temperatures inside the borehole, and it is constant for a mean water temperature lower than -2°C because the water inside the borehole is frozen. Ice has a thermal conductivity approximately three times higher than for the stagnant water case which results in a lower borehole resistance for meant temperatures around -2°C than 4°C. Since the temperature is given as a mean water temperature, the ice forming before the mean water temperatures reaches 0°C.
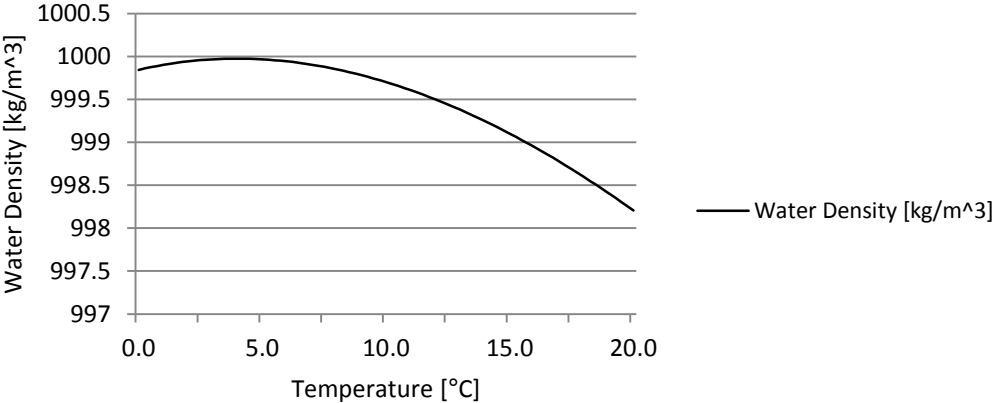
Figure 2-22 Change in water density with change in temperature

2.6   Summary

This chapter consists of a literature review looking at different BHE simulation models and the thermal influence of different borehole arrays with and without groundwater flow, of a vertical temperature gradient along the borehole depth and the influence of natural convection inside the borehole. Since the complexity of the models increases with number of dimensions and ground and borehole effects included in the model, the most complex models is most time consuming. The models presented in this chapter are divided into three categories, analytical models, two-dimensional numerical models, thermal resistance and capacity models.

The analytical models are used for BHE design and in-situ TRT evaluation because of its simplicity and speed. The models have been developed making simplifying assumptions for the borehole and the ground. Because the analytical models do not take the thermal capacity and the correct borehole geometry into account, the models is not applicable to short time simulations and design simulation tasks and interaction between boreholes on a long timescales.

Eskilson (1987) g-function model combined analytical and numerical solutions and used thermal resistance inside the borehole to combine the fluid inside the collectors and borehole wall temperature. Only long term heat flux response for ranges of borehole arrays could be simulated since the model does not include thermal heat capacity for the fluid or the grouting.

Yavuzturk (1999) developed a two-dimensional numerical model for short timescales. The material inside the borehole was discretized to include the thermal mass of the pipes and grout. Two-dimensional models like the model developed by Yavuzturk (1999), describes the heat transfer accurately for short as well as long timescales because they are able to represent the different borehole geometries and thermal mass of grout, pipe and fluid inside the borehole. Compared to three-dimensional models some simplifications have to be done, such as ground temperature and fluid temperature variations along the borehole depth cannot be represented explicitly.

Three-dimensional models can give a more accurate representation of a BHE. They are able to avoid simplifications made with two-dimensional models, such as fluid temperature variations along the borehole depth, initial vertical ground temperature gradients, season dependent surface temperature and different layers of rock. The thermal resistance and capacity models and the finite element models developed by Al-Khoury and Bonnier (2006) and extended by Diersch et al. (2010) coupled a heat transfer model within the

borehole with the heat transfer model of the surrounding ground using the borehole wall temperatures, and solving the different models simultaneously. This method reduces the mesh and thereby reduces the required simulation time which makes the models more practical for simulation purposes.
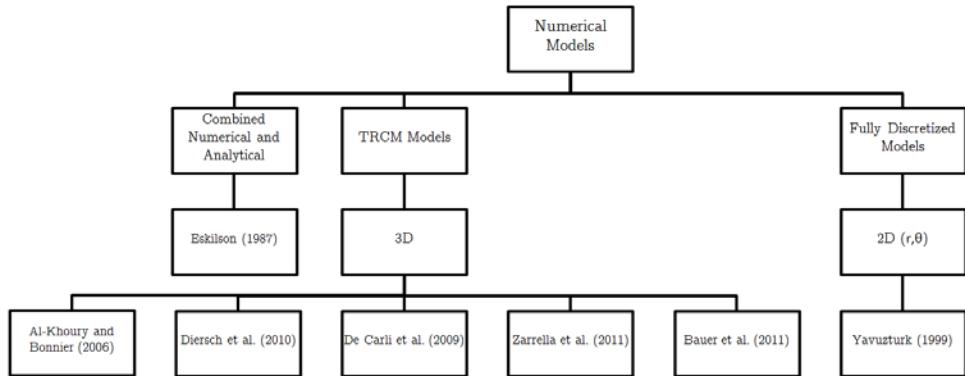
Figure 2-23 Numerical model overview

Figure 2-23 shows an overview over the different models for BHE simulation presented in chapter 2.3. Whether a numerical model is able to describe a specific problem are dependent on the ground conditions, the BHE-depth, type of backfilling and type of BHE array. Conditions that are shown to influence the heat transfer in the borehole are the initial vertical ground temperature gradient, natural convection inside the borehole for water filled boreholes, groundwater flow and the type of borehole array. Knowledge about the ground conditions is therefore important to be able to design a BHE with effective long term performance

.

3 System Description

In cooperation with the manager engineer of Drammen municipality, an arrangement was made to get access of operational data from Skoger elementary school located south of Drammen city center. The school was renovated in 2010 and operational data was logged from end of August 2011. Data that had been logged in Drammen municipality's data base was heat delivered from the heat pump installed, outside temperature, amount of energy recovered from heat recovery batteries and solar panels. Some important data was not recorded from the first day of operation such as out and in going temperatures from the energy wells and heat pump power input. Temperatures in and out from the five energy wells that are used as an energy source for the installed heat pump were started recorded 07.03.2013. In the middle of April an energy measurer was installed where the five energy wells were connected. This measurer was special ordered to be able to measure the volume flow of the fluid inside the collector tubes. A device that measures the heat pump power input was installed April 29, which should have been done when the school was renovated in 2010 to be able to see the COP variation during the system operating time. Since the heat delivered from the heat pump was logged from the system start, and the COP is unknown, a yearly variation of the heat pump COP is necessary to predict to be able to calculate the heat load of the energy wells.

This is complicated since the school heating demand increases and the outlet temperature from the energy wells are lower in the winter. The COP variations with different evaporation and condensation temperatures were predicted in chapter 3.3.

Five energy wells along with a gas boiler were installed to provide Skoger elementary school with sufficient room heating and heated water supply. The school was renovated in 2010 and a new sports hall was built the same year. With a total area of 5273m^2 the room heating and heated water supply was designed to be covered by heat delivered from the heat pump and a gas boiler, 150 kW and 450 kW respectively. With two years running time the gas boiler has not been used and the highest possible temperature for ventilation heat exchangers and heated water supply are therefore restricted by the heat pump set point of 55.8°C.

The ventilation system consists of, a Carrier 30RW-300 heat pump which uses five energy wells with a total length of 2500 meters as energy source. The delivered heat from the

heat pump enters an accumulation tank which distributes heated water to air ventilation, floor heating, radiators and water heating. The energy wells are charged by waste heat from room heating in late spring, summer and early autumn.

Figure 3-1 shows a print screen of the flow sheet of the temperatures in and out of the energy wells and heat pump, as well as the power of the heat recovery batteries taken January 1. 2013. It was unfortunately not possible to get access to the flow sheet. Therefore only a few print screens were made in the period between January and June.
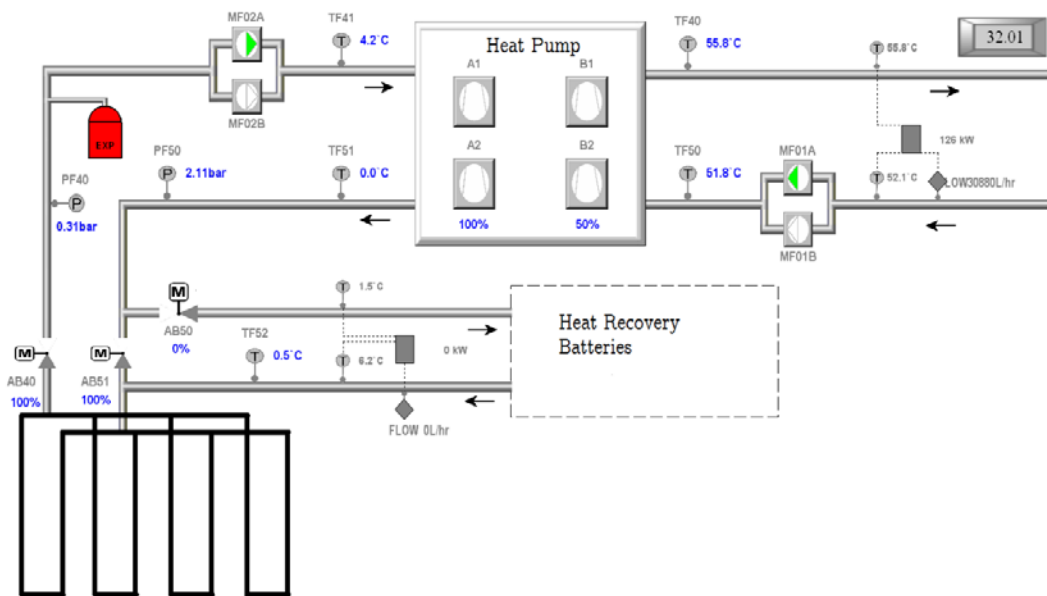
Figure 3-1 Print screen of the flow sheet 16.01.2013

3.1   System parts

3.1.1   Boreholes

The heat pump uses five 500 meters deep BHE located in the school yard to extract heat. The BHEs is oriented in a straight line with approximately 20 meter distance between the boreholes. The collector is a single u-pipe and has an outer diameter of 0.05 meter, inner diameter of 0.044meter and the borehole has a diameter of 0.14 meter shown in Figure 3-2. Tests done before the boreholes were drilled showed that the depth to solid rock was around 40 meters, and this makes it more efficient to drill fewer but deeper boreholes since clay has a lower thermal conductivity than granite granodiorite which is

the type of rock found in the Skoger region. Values from Ramstad (2012) shows that clay has up to 3 to 5 times more expensive drilling cost per meter than rock drilling.
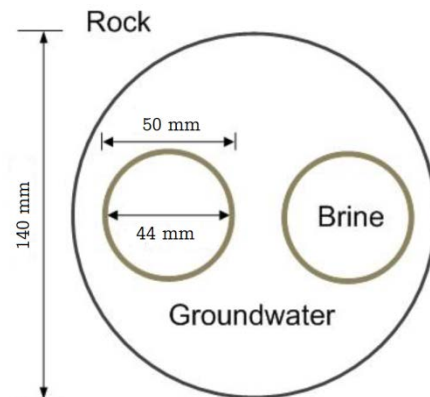
Figure 3-2 Borehole and u-pipe geometry

3.1.2   Working fluid

Brineol MEG 10 with 30%w/v is used as a working fluid. This is an ethylene glycol solution with a freezing point of -16.6°C. Thermal properties for ethylene glycol-water solution changes with temperature and 30%w/v is equivalent to 33%w/w. The thermal properties of the ethylene glycol solution, shown in Figure 3-3, Figure 3-4 and Figure 3-5 are based on data from vannglycol.excel(Erling Næss, personal conversation).
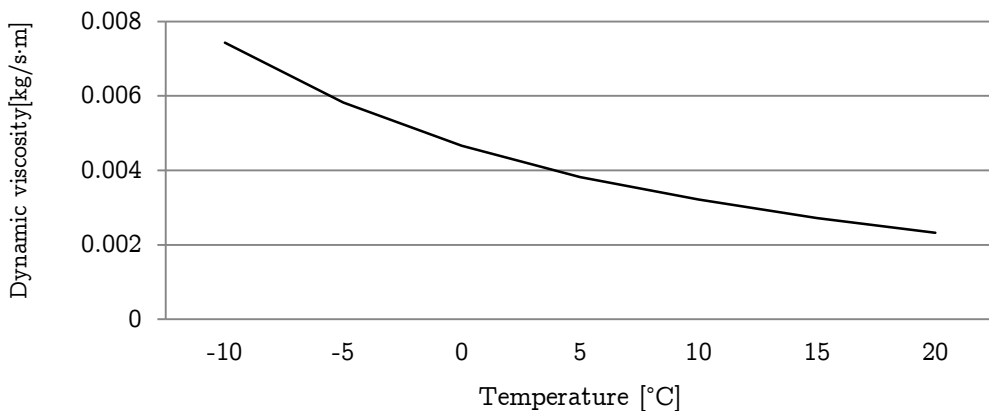
Figure 3-3 Dynamic viscosity of ethylene glycol-water solution (33%w/w)
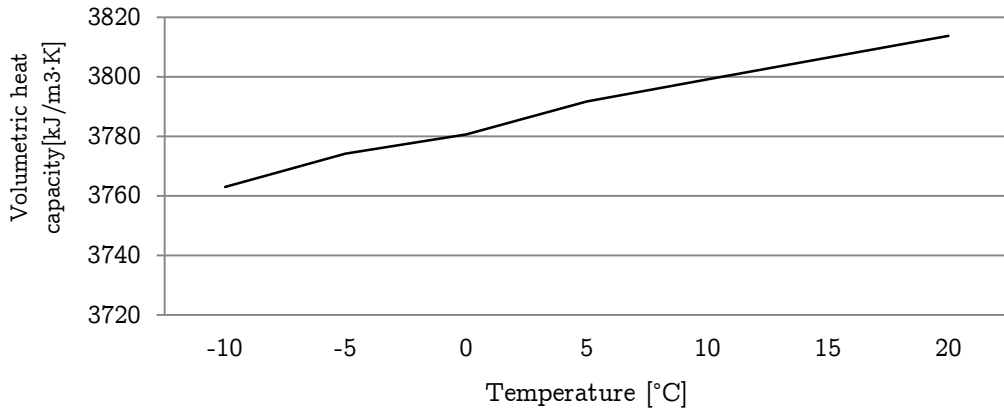
Figure 3-4 Volumetric heat capacity of ethylene glycol-water solution (33%w/w)
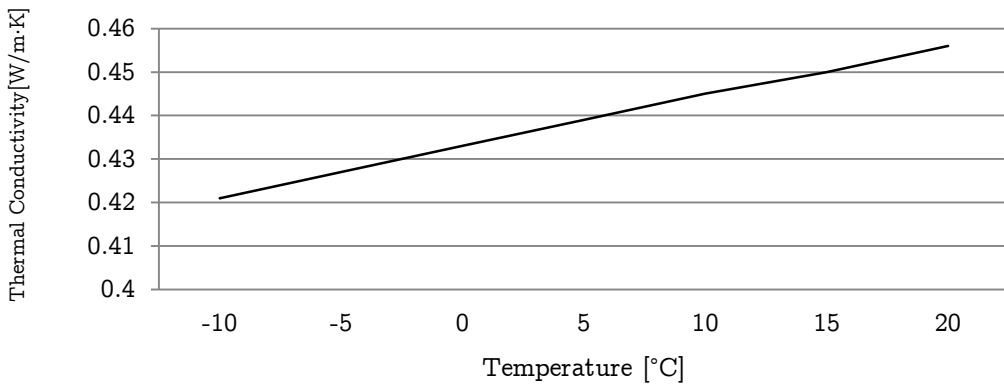
Figure 3-5 Thermal conductivity of ethylene glycol-water solution (33%w/w)

3.1.3 Heat pump

The heat pump installed is a Carrier 30RW-300 which uses heat from five 500 meter deep boreholes as energy source. Carrier 30RW-300 is a scroll compressor water-cooled liquid chiller, designed to operate efficient as a water chiller at moderate temperatures. At high evaporation temperatures it can operate relatively efficient as long as the condensation temperature is moderate. Incoming temperature from the wells has from February to March varied between 4°C and 9°C and return temperature to the wells varies with the

41

school heat demand, but it normally is 1°C to 4°C lower than the heat pump incoming temperature. The heat pump has a set point of 55.8°C and the return flow is volume flow regulated and the temperature to the heat pump lies around 52°C. Carrier 30RW-300 consists of four hermetic scroll compressors orientated in two circuits with two compressors in each circuit. The refrigeration fluid used is R407C.

R407C is a synthetic HFC and it is used as the working fluid in Carrier 30RW-300. The thermophysical properties for R407C are listed in Table 1

Table 1 R407C properties, Stene (2012)

R407C	
Molecular weight	86.2
Critical temp. t_c[°C]	86.0
$p_{saturated}$, 0°C [bar]	5.7
t_c,25bar [°C]	60
ρ_{liquid},0°C [kg/m^3]	1237
ρ_{vapour},0°C [kg/m^3]	20
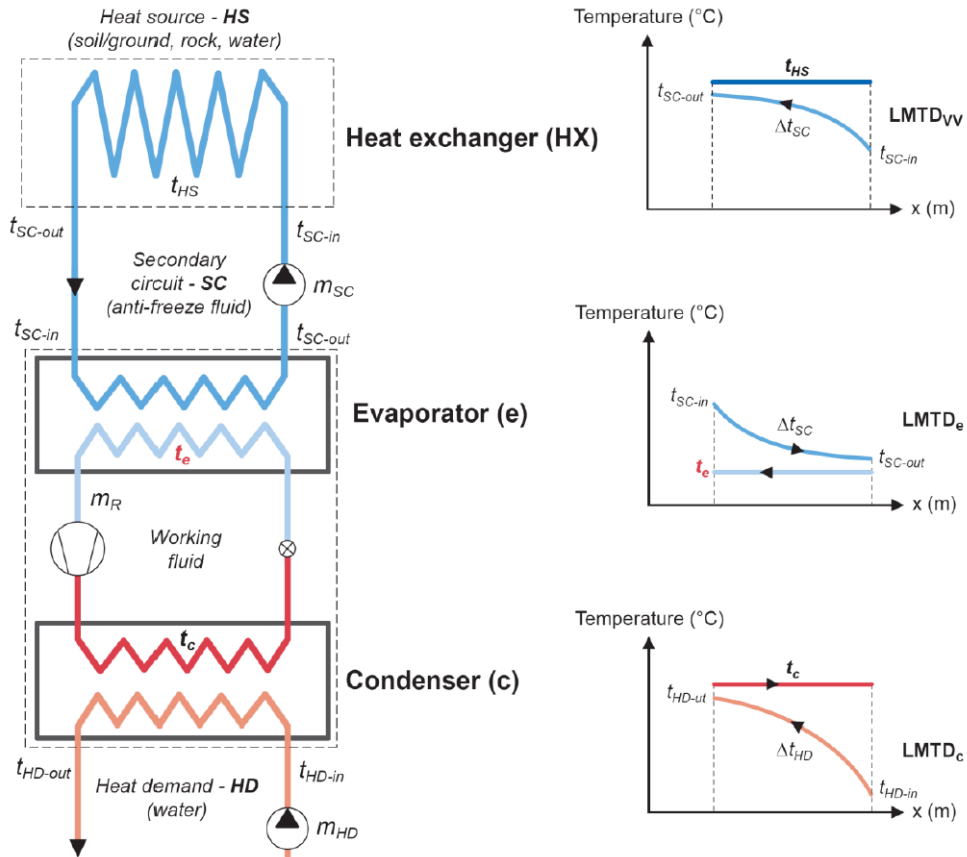
Figure 3-6 Principle design of the thermal connection between the BHE and heat pump, Stene (2012)

Figure 3-6 shows principle design of the energy balance in the heat exchangers when the ground is used as an energy source for the heat pump.

3.1.4   Gas boiler

A gas boiler with a capacity of 450 kW is installed to cover the peak loads and heat the water in the accumulation tank from 55 to 80°C. The chief engineer of Drammen municipality could inform that the heat pump has covered all of the heat demand at Skoger elementary school since the renovation, and that the gas has not yet been used.

3.1.5   Accumulation tank

The heat pump delivers water at 55.8°C to the accumulation tank that is used as a reservoir for hot water. This secures a stable heat delivery to the air ventilation, floor, radiators, a 2500m^2 sport hall and hot water and makes sure of stable operation conditions for

the heat pump. Since the gas boiler is only used to cover peak loads when the heat pump effect is insufficient, the highest temperature in the accumulation tank is 55.8°C. For hot water supply, a secondary water flow is heat exchanged with water inside the accumulation tank and drawn off at temperatures lower than 55.8°C depending on the heat exchanger efficiency. The heat pump is series connected to the accumulation tank, which means that only the accumulation tank is responsible for direct heat distribution to the school.

3.1.6 Heated water

The need for hot water in the school is limited, and it is mainly used to provide hot water to the showers. The school has three hot water tanks connected in series that receive hot water from the accumulation tank, and it stores hot water at 55.8°C. A temperature around 50°C is high enough for shower and hand wash water, but a problem with growth of legionella bacteria inside the hot water tanks might occur at these temperatures. Legionella bacteria in high concentrations could lead to a serious respiratory infection, and from Zijdemans (2012), the official recommendation to avoid growth of legionella bacteria is to keep the water inside the hot water tank higher than 70°C to ensure that the water in the lowest part of the hot water tank stays above 60°C. This is because legionella bacteria become inactivated at temperatures around 55°C-60°C.

Three hot water tanks are connected in series, which is more energy efficient than parallel connection when the water is heated by an extern heating source which in this case is the accumulation tank, and there is no heating element inside the hot water tank. Because of the high trough-flow for series connected hot water tanks, a significant reduction of humus accumulation in the bottom of the hot water tank is secured. Zijdemans (2012).

3.1.7 Radiators and floor heating

Radiators and floor heating are used in addition to ventilation heating, but since the school is primarily based on air ventilation, floor and radiator heating are in smaller scale than the air ventilation heating. Both radiators and floor heating has an incoming temperature from the accumulation tank close to 55°C and a return temperature of 40°C.

3.1.8 Solar panels

Solar panel with a total area of 27m^2 was installed to heat water inside the accumulation tank. Delivered energy from the solar panel is highly season dependent, and it produces only energy from early March to late October with an energy delivery peak in the middle of the summer. Since the solar panel have the highest efficiency when the school energy

demand is at its lowest, the energy collected from the sun helps relive heat pump work during the summer and is an indirect energy source for charging of the energy wells.

3.1.9 Air ventilation

Heating of air to ventilation systems stands for approximately 50% of the school total energy demand. Also here the accumulation tank provides heat distribution at temperatures close to 55°C and the return temperatures depends on the energy demand.

3.1.10 Charging of energy wells

The energy wells are recharged with heat given off from the air exiting the air ventilation system. Heat given off from the air exiting the air ventilation is heat exchanged with air entering the air ventilation. After the heat exchange with air entering the air ventilation, the excess energy from the air exiting the air ventilation is heat exchanged in heat recovery batteries with the ethylene glycol-water solution entering the energy wells. The recharge capacity increases with high temperature of the air entering the air ventilation system, and will therefore have the highest recharge capacity when the outside air temperature is high. The school energy demand increases with decreasing outside air temperature and the heat recovery batteries recharge capacity is at the lowest in the winter months, shown in Figure 3-7.
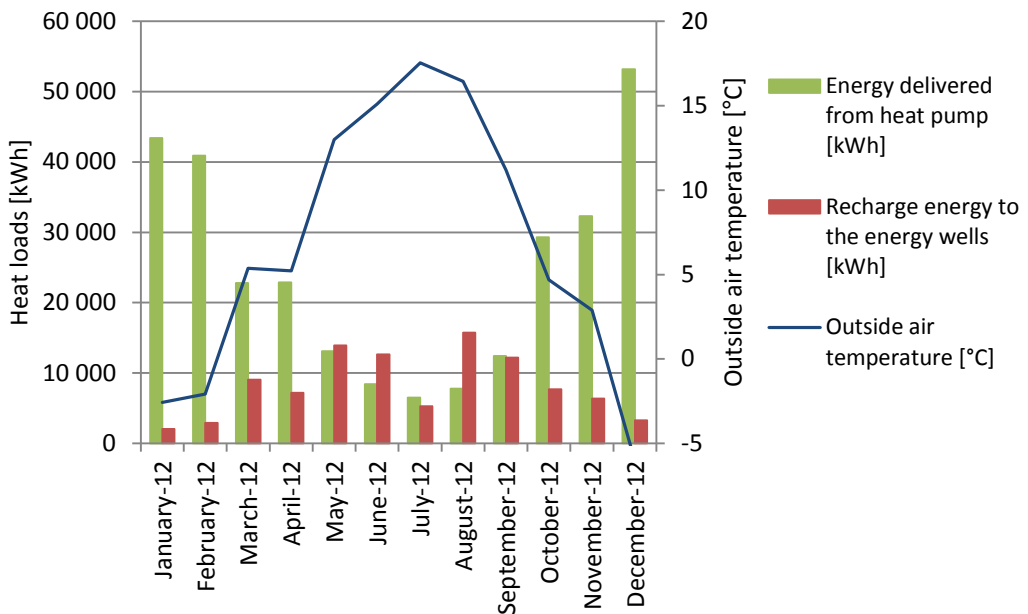
Figure 3-7 Heat delivered from heat pump and energy from recovery batteries in 2012

3. SYSTEM DESCRIPTION

At Skoger elementary school the cooling demand is limited since the school is closed from middle of June to middle of August. In May, June and August the thermal recharge of the energy wells peaks because the outside air temperature is high and a large amount of the exiting air from the air ventilation is heat exchanged with the ethylene glycol- water solution entering the energy wells return water through the heat recovery batteries. Since the air ventilation system operates with low energy consumption in June, the energy recharge of the energy wells is limited during this month.

Although the energy recharged to the energy wells only makes up a small part of the total energy extracted, an extended effective operational time is likely to presume.

The system description is based on a proposed system drawing from the entrepreneur, and conversations with the chief engineer of Drammen municipality. Set points in Figure 3-8 are not the system operating set points.
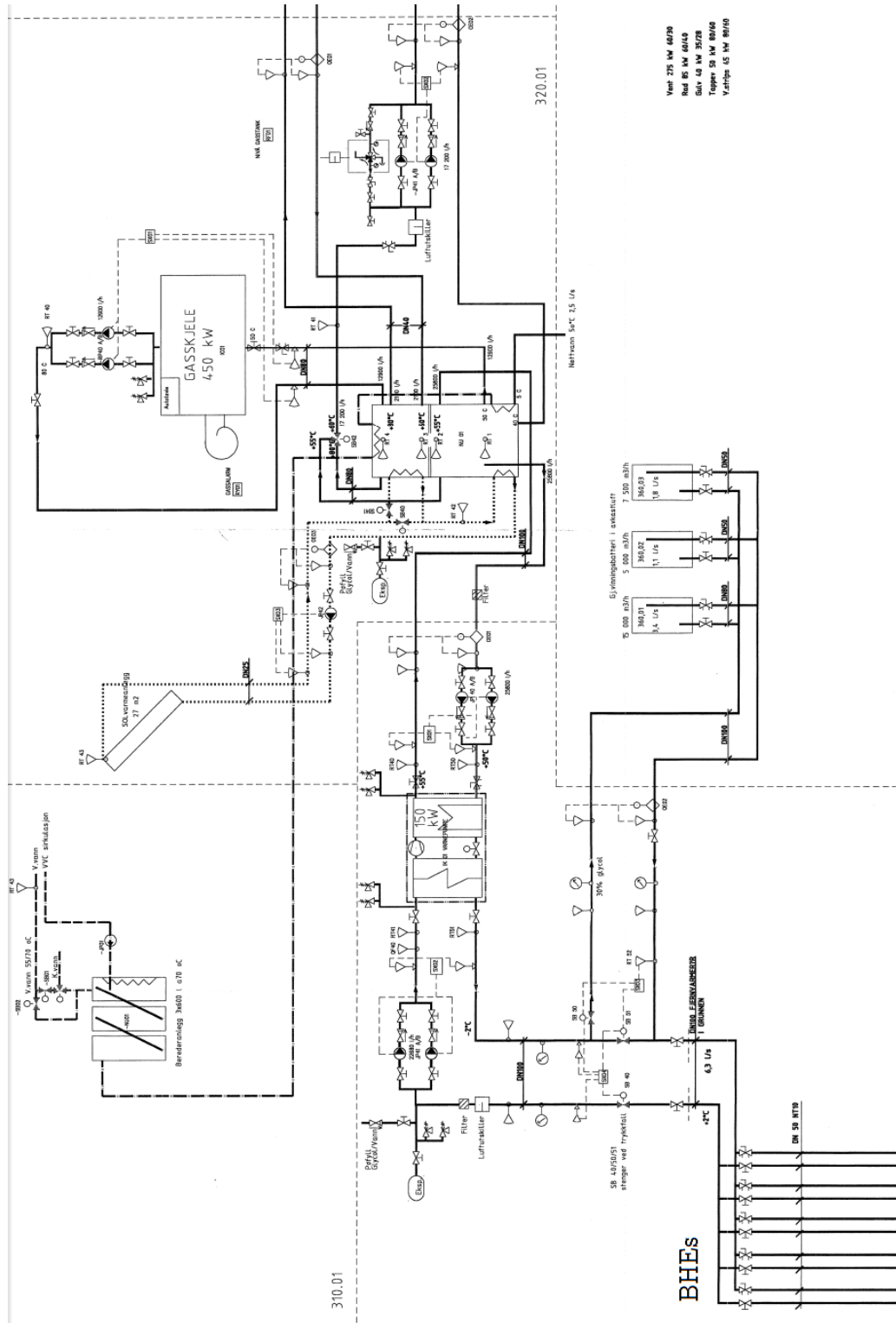
Figure 3-8 System drawing for heating of Skoger elementary school

3. SYSTEM DESCRIPTION

The drawing of the air ventilation system is excluded in the Figure 3-8, since this is not important for in this thesis.

3.2 Details of the borehole field and its elements

Table 2 Borehole field specifications

Element	Specification
Borehole	
Borehole depth	500 meter
Number of boreholes	5
Effective borehole depth	500
Borehole diameter	140 mm
Borehole filling material	Groundwater
Surrounding ground type	Bedrock
Ground conductivity	3.3 [W/mK]
Heat exchanger	
Type	Single u-pipe
Material	Polyethylene
Pipe outer diameter	50 mm
Pipe thickness	3 mm
Thermal conductivity	0.42 [W/mK]
Shank spacing	Not controlled
Circulating fluid	
Type	Ethylene Glycol (33%w/w)
Thermal conductivity	See Figure 3-5
Freezing point	-16.6° C
Volumetric heat capacity	See Figure 3-4
Total volumetric flow	0.004 m^3/s
Volumetric flow per BHE	0.0008 m^3/s

3.3 COP calculation

A precise COP of the heat pump installed at Skoger elementary school only is possible to calculate after 29.03.2013 when the device that measures the heat pump input power was installed. A number assumptions has to be made in order to estimate the heat pump COP installed at Skoger elementary school before measurer device was installed. Operational data accessible from Skoger elementary school is shown in Figure 3-9.
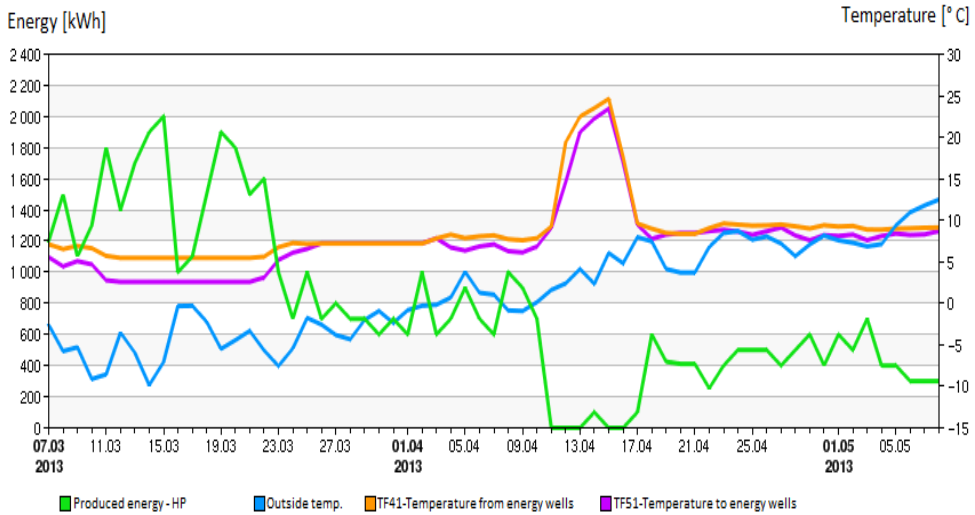
Figure 3-9 Operational data available from Skoger elementary school since March 7. 2013

Figure 3-9 is based on daily average data. The temperature peak around April 13 is caused by shut down of the system because of installation of a volumetric flow measurer of the ethylene glycol-water solution. Temperatures of 24°C is reached because the temperature measurer are located inside the control room, and during the volumetric measurer installation the temperature measured is equal to the control room temperature. In the period March 23 and April 5, the temperature measurer jumped out and did not record. A daily averaged COP is possible to calculate from these data to give an indication of the COP when the inlet temperature from the energy wells varies from 7°C to 9°C. Between April 2 and April 11 the heat recovery batteries recharged the energy wells, and the temperature measured out from the energy wells are therefore higher than it would have been without the recharge. A total average COP is calculated based on daily average COP excluding the three periods mentioned above. The COP is calculated with ethylene glycol- water solution properties at 5°C and the difference between the inlet and outlet temperature of the energy wells and power delivered from the heat pump. By knowing the volume flow it is possible to calculate the COP from the equation (3-1), (3-2) and (3-3).

$$Q_{\text{energy wells}} = \dot{V} \cdot cp \cdot \rho \cdot \Delta T \qquad (3\text{-}1)$$

$$Q_{\text{electic}} = Q_{\text{Heat pump}} - Q_{\text{energy wells}} \qquad (3\text{-}2)$$

$$COP = \frac{Q_{\text{Heat pump}}}{Q_{\text{electic}}} \qquad\qquad (3\text{-}3)$$

Based on data from Figure 3-9, and using equation (3-1), (3-2) and (3-3), a total average COP is calculated from a COP based on daily average values. The error might be high, but it is the most precise COP available with the present operational data collected from the Skoger elementary school database. The COP calculated was 2.7. Since the yearly operational data available is limited or unavailable another way to predict the COP is needed to relate the models in chapter 4 to the GSHP system in Drammen.

After talking to a Norwegian supplier of Carrier heat pumps, program access to Ecat2 and Coolselector was possible. Ecat2 is software developed by Carrier based on test data from Eurovent. The output from Ecat2 is therefore used as a reference value for the calculation of the COP.

Because of high test cost, only full load operation was tested and part load operation is therefore not possible to simulate in Ecat2(reference: personal conversation with supplier of Carrier heat pumps). Full load operation means that all four compressors in operation at the same time. Ecat2 input data for a Carrier 30RW-300 heat pump is shown in Table 3.

Table 3 Ecat2 software

Input data	Constant input data
Input data restrictions	
Minimum entering temperature, Cold side HP	0°C
Maximum leaving temperature, Hot side HP	50°C
Input data	
Evaporator	
Leaving temperature	
Entering temperature	
Fouling factor heat exchanger	0.04403m^{2}K/W
Brine type and %w/v	Ethylene Glycol 30%w/v
Condenser	
Leaving temperature	
Entering temperature	
Fouling factor heat exchanger	0.04403m^{2}K/W
Heat exchanger fluid type	Water

3. SYSTEM DESCRIPTION

The Coolselector software was downloaded from www.danfoss.com and calculates COP based on compressor power input and an idealized heat pump cycle with only one compressor. The Coolselector software is based on a compressor delivered from Danfoss. From the Norwegian Carrier supplier compressor component list, the specifications and properties for the compressor delivered with Carrier 30RW-300 equals to the compressor SZ320 delivered by Danfoss. Approximating these two compressors have more or less the same performance efficiency, the performance of the compressors installed in the heat Carrier 30RW-300 heat pump can be calculated.

Table 4 Coolselector software

Input data	Constant input data
Input data restrictions	
Minimum evaporation temperature	-5°C
Maximum condensation temperature	60°C
Heating or cooling	Heating
Compressor model	SZ320-6(50Hz)
Refrigerant	R407C
Evaporating temperature	
Condensing temperature	
Evaporator superheat	10K
Total superheat	10K
Sub cooling	1K

A COP was calculated combining Ecat2, Coolselector and values from Figure 3-1 by assuming that the volume flow has been constant since the first day of the system operation. A common ΔT in heat exchanger design lies between 2-5K, depending on the type and size of the heat exchanger. Since Ecat2 and Coolselector not have the same input criteria's, a minimum ΔT between the Coolselector evaporation and condensation temperature and Ecat2's entering temperature and leaving temperature, respectively, was both set to 5K, as shown in Figure 3-10, to be able to compare the software solutions.
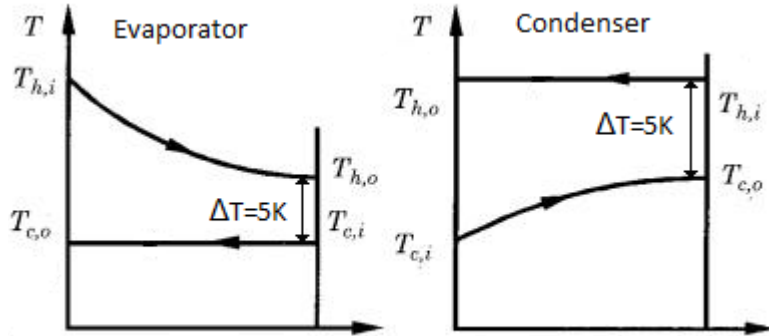
Figure 3-10 ΔT for evaporation and condensation

The Coolselector software is unable to calculate the COP for a set point of 55.8°C and evaporator temperature lower than -5°C, because this exceeds the design set points. And Ecat2 is not able to calculate the COP for higher set points than 50°C. An extrapolation of the COP was necessary to make in order to predict the COP for the Carrier 30RW-300 heat pump installed at Skoger.

The COP for the conditions in Figure 3-1 was used as a reference for the extrapolation of Coolselector and Ecat2 simulation values at T_{evap}=-5°C and T_{cond}=60°C.

The maximum temperature Ecat2 software can solve for is T_{evap}=-5°C and T_{cond}= 55°C, with a ΔT of 5K. Coolselector have a T_{evap} minimum of -5°C with a T_{cond} of 60°C. Since the refrigeration fluid R407C has an operating temperature of 60°C at 25bar, it is assumed that the condensation temperature is held constant at T_{cond}=60°C for the system in Drammen. This means that the chosen ΔT only is 4.2K for the condensate heat exchanger simulated in Coolselector. ΔT for the system in Drammen is unknown, and will vary with changes in T_{evap} and mass flow rate of R407C. ΔT=5K is set as an possible average ΔT to be able to compare the software's and later give an estimation of the heat pump COP installed in Drammen.

Carrier 30RW-300 consists of 4 compressor and Figure 3-1 shows how the system working with 3 compressors running, one compressor circuit running at 100% and the other at 50%. This values in Figure 3-1 is used as a reference for the Ecat2 and Coolselector software for T_{evap}=-5°C and T_{cond}=60°C.

Values used to calculate the COP from Figure 3-1 are listed in Table 5.

3. SYSTEM DESCRIPTION

Table 5 Values from Figure 3-1 Print screen of the flow sheet 16.01.2013

Parameters	Value
Energy wells	
Cold side	
T_{out}-TF41	4.2°C
T_{in}-TF51	0°C
ΔT	4.2K
$\dot{V}$	0.004[m³/s]
$cp \cdot \rho(2.5°C)$	3785[kJ/m³K]
Hot side	
T_{out}-TF40	55.8°C
T_{in}-TF50	51.8°C
ΔT	4K
$\dot{V}$	0.0086[m³/s]
$cp \cdot \rho(52.5°C)$	4129[kJ/m³K]

Using equation (3-1), (3-2) and (3-3) and values from Table 5 a COP was calculated to 1.81 with 3 compressors running.

To evaluate a COP at T_{evap}=-5°C and T_{cond}=60°C an extrapolation of Ecat2 values based on values from Table 5 and values from Coolselector. Since Ecat2 only calculates a COP when all four compressors are running. To make this extrapolation an assumption that the ratio of the losses between running 1 and 2, 2 and 3 and 3 and 4 etc. compressors are the same for each T_{evap} and T_{cond} is calculated.

Table 6 Condensation temperatures for T_{evap}=-5°C

Condensation temperature	COP Coolselector	COP Ecat2	η,4 Compressors	η,3 Compressors
35°C	4.62	3.83	0.83	0.87
40°C	4.07	3.27	0.80	0.85
45°C	3.58	2.77	0.77	0.83
50°C	3.15	2.33	0.74	0.80
55°C	2.77	1.95	0.70	0.78
60°C	2.44	1.6	0.66	0.74

Values in Table 6 shows estimated COP for T_{evap}=-5°C and T_{cond}=60°C for Ecat2 based on COP from Coolselector and Table 5. Values for the correction factor(η) compressors

are the COP from Ecat2 divided by COP_Coolselector. The correction factor for 4 compressors running is

$$\eta, 4\,\text{Compressors} = \frac{\text{COP\_Ecat2}}{\text{COP\_Coolselector}} \tag{3-4}$$

This calculation has been done for 1, 2, 3 and 4 compressors running and T_{evap}=-5°C, 0°C and 5°C covering the ethylene glycol-water solution temperatures recorded from the system in Drammen.

3.3.1 COP discussion

Figure 3-11 shows the COP for T_{evap}=-5°C
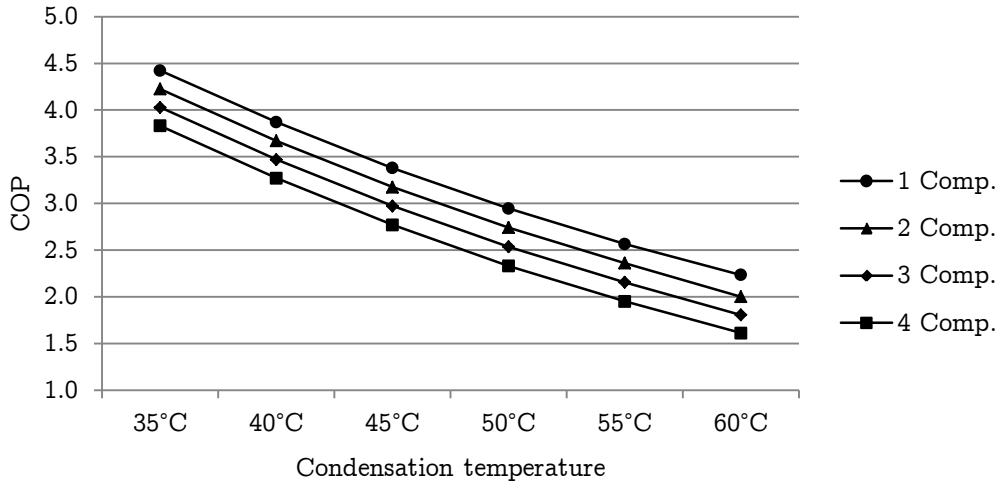
Figure 3-11 COP variations with change in T_{cond} for T_{evap}=-5°C

Figure 3-12 shows the COP for T_{evap}=0°C
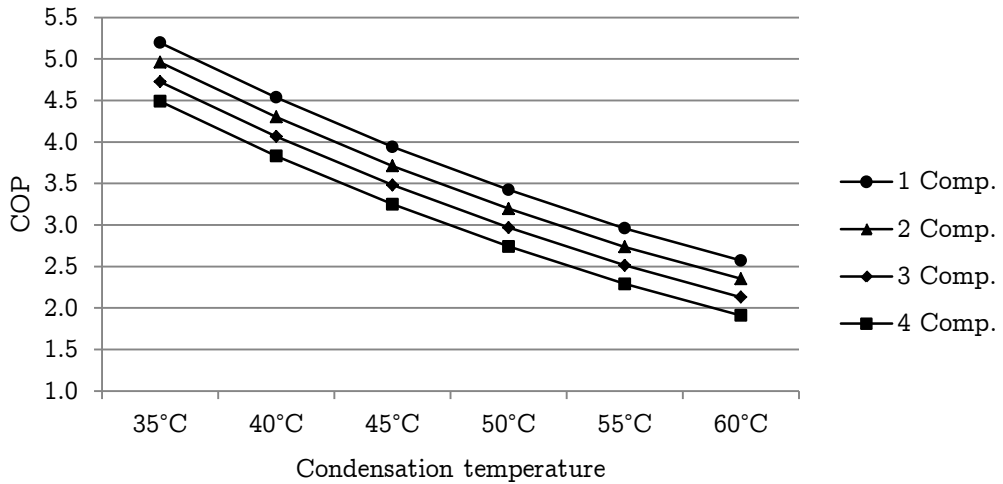
Figure 3-12 COP variations with change in T_{cond} for T_{evap}=0°C

Figure 3-13shows the COP for $T_{evap}=5°C$
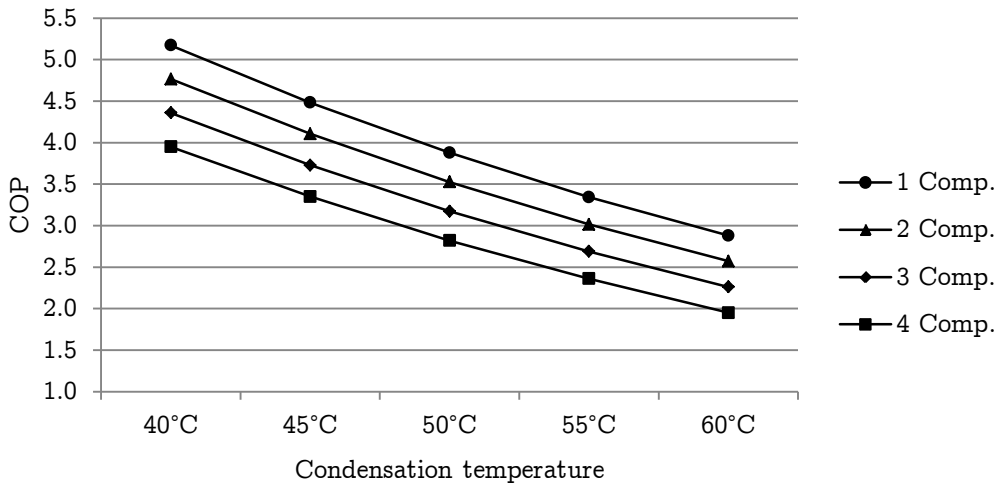
Figure 3-13 COP variations with change in T_{cond} for $T_{evap}=5°C$

Figure 3-11, Figure 3-12 and Figure 3-13 shows the COP variations with change in T_{cond}. For $T_{evap}=5°C$ a condensation temperature of 35 was not possible to simulate in Ecat2 because the set temperatures did not correspond to the Carrier heat pump operation limits. As expected a decrease in COP is observed with increased T_{cond} which is also showed in Figure 3-11, Figure 3-12 and Figure 3-13.
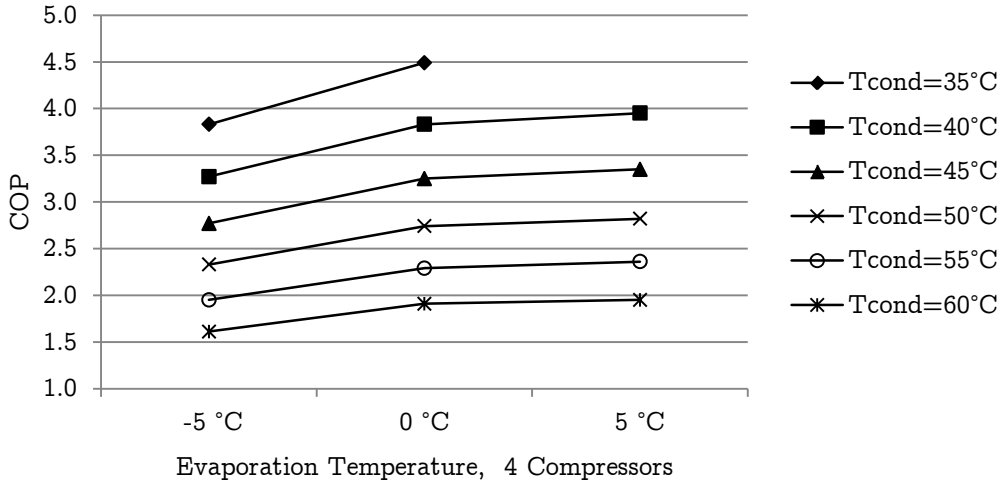
Figure 3-14 COP variations with change T_{evap} for 4 compressors in operation
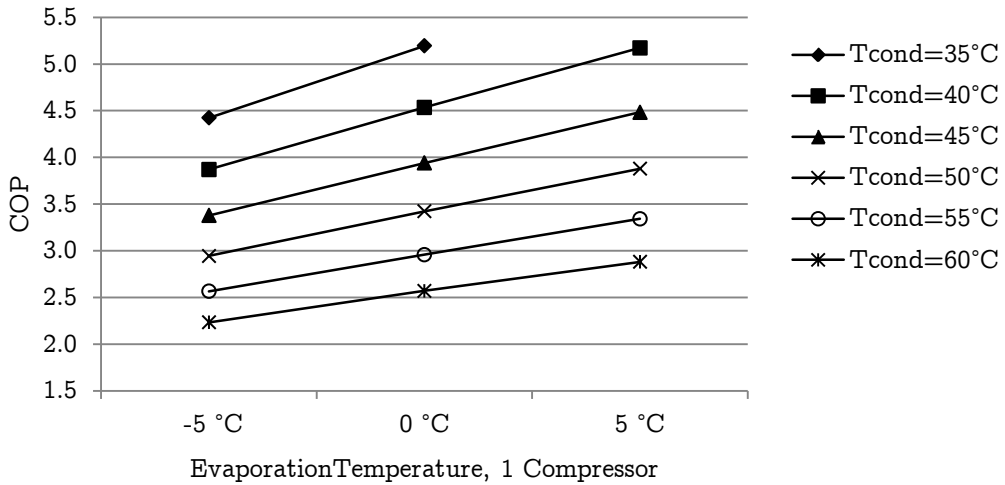
Figure 3-15 COP variations with change T_{evap} for 1 compressor in operation

From Figure 3-15 a linear correlation between the evaporation temperature and the COP is found for all condensation temperatures when one compressor is in operation. Figure 3-14 shows that the COP flattens out for T_{evap} larger than 0°C when 4 compressors are in operation at the same time. This means that a more effective operation of the heat pump will demand relatively high outgoing temperatures from the energy wells. It should be mentioned that the heat pump installed at Skoger elementary school is not very well suited for the set points that the school heating system demands. To keep the COP over 2.5 for T_{evap} larger or equal to 0°C, a maximum condensation temperature of 50°C should

be used. This is 10°C lower than the present condensation temperature the heat pump is working with. If the heat pump is not replaced with a more effective heat pump, the heating system should be redesigned to work at a lower set point. If the accumulation tank holds 45°C instead of 55.8°C the COP is dramatically increased, but a side effect is that the hot water have to be heated from electricity or other heat sources, because of high possibility of high legionella bacteria concentration at temperatures below 55°C inside the hot water tanks.

The hermetic scroll compressors installed in the Carrier 30RW-300 causes the low COP because of high leakage and heat losses for the operating pressure ratios for $T_{cond} = 60°C$. The heat pump is originally designed to operate as a water-cooler and the compressors are therefore not designed for high pressure ratios. Since the compressor exceeds their design pressure ratio, the efficiency is drastically decreased. To improve the heat pump performance, compressors designed for higher pressure ratios should replace the present compressors if the heat pump set point remains at 55.8°C, but this will not be further discussed in this thesis.

The average COP calculated in chapter 3.3 from the Skoger elementary school database in the period April 7 to May 7 was calculated to 2.7. Outgoing temperature from the energy wells lies around 8-10 degrees during the period, resulting in high COP values compared to February COP values from Figure 3-1. In the end of March only one compressor was in operation, while in beginning of April two compressors were working. Since the losses increases with the number of compressors working, the extrapolation of COP for the set point of 55.8°C which from Figure 3-15 gives a COP of 2.9 with one compressor running with $T_{evap}=5°C$ and $T_{cond}=60°C$. This shows good agreement to the average COP calculated in 3.3.

To be able to use the data with delivered heat from the heat pump, a COP has to be estimated. This will give the yearly variations of extracted heat from the energy wells. Because of high uncertainties around the COP the estimated energy extracted from the boreholes may carry an error exceeding the errors from assumptions made in the 2D model and the 3D model when studying the long term performance of the BHE installed at Skoger elementary school.

Assuming the heat pump switches between using three and four compressors during the winter season, and using one or two compressors during the summer season, the yearly average COP can be divided into two sections. Since correct COP data is only able from May 7, an estimation of the COP during the winter season is based on values taken from figures in chapter 3.3.1. The COP is shown to be dependent on the evaporation tempera-

ture and an average $T_{evap}=0°C$ from November to March is assumed since the ground temperature is lower during the winter month than the summer months. With $T_{cond}=60°C$ and assuming that the heat pump operates at equal amount of time at three and four compressors an average COP for $T_{evap}=0°C$ and $T_{cond}=60°C$ is proposed and shown in Table 7. This COP is used to calculate the heat extracted from the energy wells from November to March.

Table 7 Average COP1, March-November

COP, 3 compressors	COP, 4 compressors	Average COP, March-November
2.25	1.91	2.1

Assuming $T_{evap}=5°C$ because the ground temperature is higher during the summer month due to heat injection from the heat recovery batteries. With a constant $T_{cond}=60°C$ during the months from April to October and assuming that the heat pump operates at equal amount of time at one and two compressors an average COP is calculated from the values in chapter 3.3.1. The COP used to calculate the variations in heat extracted from April to October is shown in Table 8.

Table 8 Average COP1, April-October

COP, 1 compressor	COP, 2 compressors	Average COP, April-October
2.9	2.5	2.7

The COP is used to calculate the energy wells heat loads. Since the energy wells heat extraction and injection load is based on an average COP for the summer and winter months, at least 10% error should be accounted for due to fluctuations in the T_{evap} and the school heating demand.

3.3.2   Compressor heating capacity

The power inputs to the compressors are only dependent on the condensation temperature, but the heat pump heating capacity will vary with change in T_{evap} and T_{cond} because of the COP dependence of T_{evap}, shown in Figure 3-15.

Figure 3-16 shows the input power for different condensation temperatures.
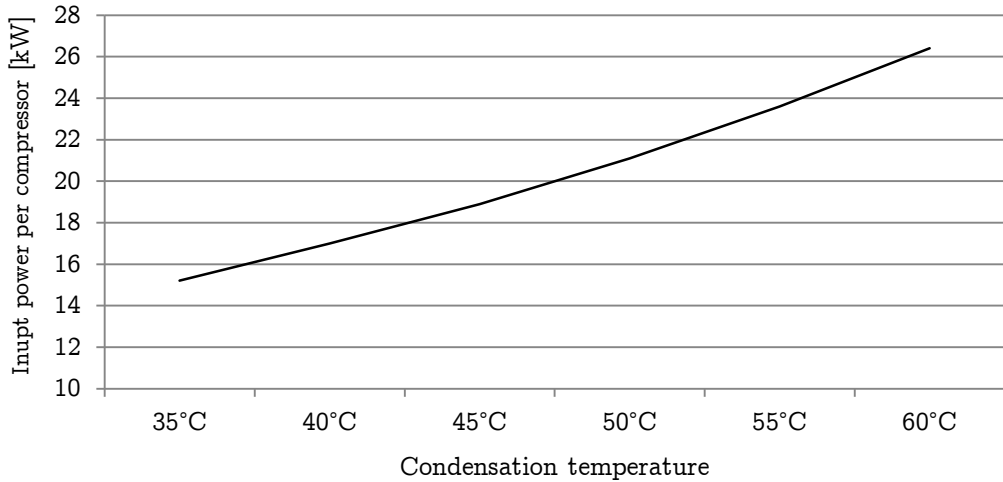
Figure 3-16 Input power per compressor

Due to increase in ratio of the condensation pressure to the evaporation pressure when increasing the condensation temperature, the input power per compressor is increased.

Figure 3-17 shows the heat pump maximum heating capacities for different evaporation and condensation temperatures. Values are obtained from Coolselector software and consistency is showed when comparing the values to Ecat2.
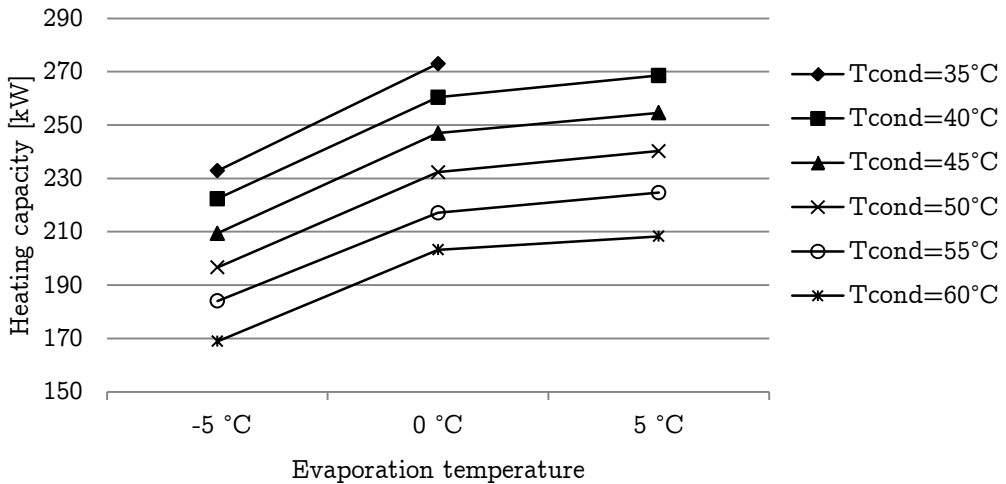
Figure 3-17 Heat pump maximum heating capacity

3.3.3   COP effects

Figures from chapter 3.3.1 shows that decreasing the operating set point of the heat pump, the COP will increase drastically. Changing the condensation temperature from 60°C to 50°C, and assuming and average T_{evap}=0°C from November to March, and that the heat pump operates at equal amount of time at three and four compressors. An average COP for T_{evap}=0°C and T_{cond}=50°C from November to March is shown in Table 9 and based on data from figures in chapter 3.3.1.

Table 9 Average COP2, November-March

COP, 3 compressors	COP, 4 compressors	Average COP November-March
3	2.7	2.85

Assuming T_{evap}=5°C and T_{cond}=50°C from April to October and that the heat pump operates at equal amount of time at one and two compressors. An average COP is based on values from chapter 3.3.1. The COP used to calculate the variations in heat extracted from April to October is shown in in Table 10.

Table 10 Average COP2, April-October

COP, 1 compressor	COP, 2 compressors	Average COP April-October
3.9	3.5	3.7

COP for T_{cond}=60°C is from now on referred to as COP 1, and COP for T_{cond}=50°C is from now on referred to as COP 2, showed in Table 11 and Table 12.

Table 11 Average COP1

COP 1	
Average COP, April-October	Average COP, November-March
2.7	2.1

Table 12 Average COP2

COP 2	
Average COP, April-October	Average COP, November-March
3.7	2.85

Table 13 Energy savings [kWh] November-February

Month	Heat delivered from HP [kWh]	Energy input COP1 [kWh]	Energy input COP2 [kWh]	Savings [kWh]
January	43400	20667	15228	5439
February	40900	19476	14350	5126
November	32300	15381	11333	4048
December	53200	25333	18666	6666
Total	169800	80857	59577	21280

Table 14 Energy savings [kWh] March-October

Month	Heat delivered from HP [kWh]	Energy input COP1 [kWh]	Energy input COP2 [kWh]	Savings [kWh]
March	22800	8444	6162	2282
April	22900	8481	6189	2292
May	13100	4852	3541	1311
June	8400	3111	2270	841
July	6500	2407	1757	650
August	7800	2889	2108	781
September	12400	4593	3351	1242
October	29300	10852	7919	2933
Total	123200	45629	33299	12330

Table 15 Total savings

Heat delivered from HP [kWh]	Energy input COP1 [kWh]	Energy input COP2 [kWh]	Total Savings
293000	126487	92876	33610

By reducing the condensation temperature the heat pump has better working conditions, and the COP is increased. For the schools energy consumption in 2012, the energy savings from reducing the heat pump condensation temperature from 60°C to 50°C is shown in Table 13 and Table 14. Table 15 shows the total possible savings for 2012. A reduction of energy input of 27% by improving the COP from COP1 to COP2 can be earned for a 2012 heat demand. With electricity cost of 1NOK/kWh, a yearly saving of almost 34000NOK is possible if the heat pump operation conditions are improved by lowering the condensation temperature from 60° to 50°C.

The heat pump set point is controlled by the schools hot water supply temperature, because the hot water tanks do not have electricity heating. By lowering the set point, the temperature delivered from the heat pump will not be sufficiently high to avoid problems like legionella bacteria. If the condensation temperature is put down to 50°C, installation of an electric heating element inside the hot water tanks to raise the hot water temperature to temperatures around 60°C. The initial installation cost and the yearly cost this will bring are not studied in this thesis.

3.4 Ground Thermal Conductivity Estimation

Estimation of the ground thermal conductivity is of importance in design and simulation tasks for BHEs. There are two commonly used methods to estimate the ground thermal conductivity. The first one consists of an estimation based on geological data of the site, and in Norway published data of the ground conductivity can be used from the Geological Survey of Norway. This is a quick and rough estimate, and since the value of the ground conductivity is given as a range, an average value can be used, but this makes the margin for over or under estimation large and the borehole array size and performance may be uncertain, Conservative estimation will be to use the lowest value, which increases the possibility for over sizing the BHE system.

The second ground thermal conductivity estimation technique is to perform a thermal response test (TRT). This is certainly more accurate than to base the ground conductivity value on values published from the Geological Survey of Norway, but much more expensive and it requires TRT equipment. Usually a controlled heat source continuously injects a constant amount of heat to the circulating fluid, and Gehlin (2002) proposed to use for an operation period of at least 50 hours. Inlet and outlet temperatures are recorded and analytical models presented in chapter 0 are used to estimate the thermal ground thermal conductivity. This gives a local estimation of the ground conductivity. A TRT test should be done for large BHE systems to secure high BHE performance and minimize the initial cost.
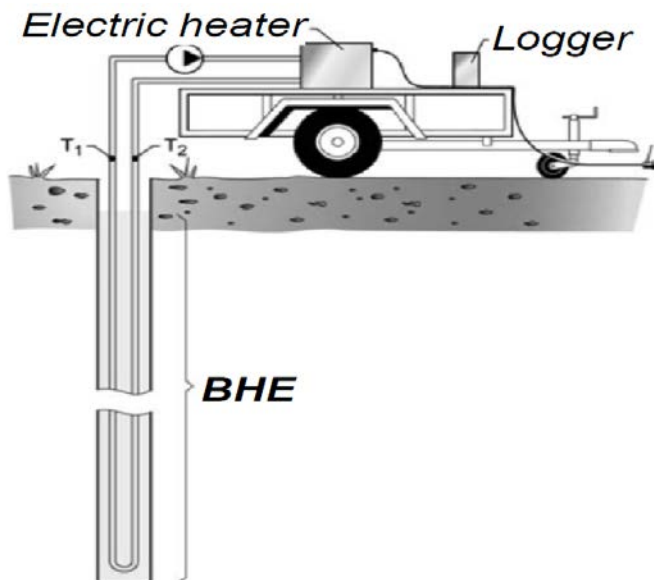
Figure 3-18 Set up of a thermal response test, Gehlin (2002)

To relate the model to the specific system at Skoger elementary school, it is necessary to use the same ground thermal conductivity. Chapter 2.5.2 shows that a lower ground thermal conductivity will result in a lower $T_{f,mean}$ over the operation years. An underestimation of the ground thermal conductivity may lead to a non-optimized GSHP system because the designer may compensate with deeper boreholes, and the operation cost will also be higher due to extra pumping power needed to circulate the fluid inside the collectors.

Since a TRT was not done before installing the BHEs at Skoger elementary school, the ground thermal conductivity used in the models developed to simulate the thermal response of the BHE system, had to be based on ground thermal conductivity values published by the Geological Survey of Norway.

From Geological Survey of Norway's (NGU) homepage the bedrock at Skoger elementary school was found.
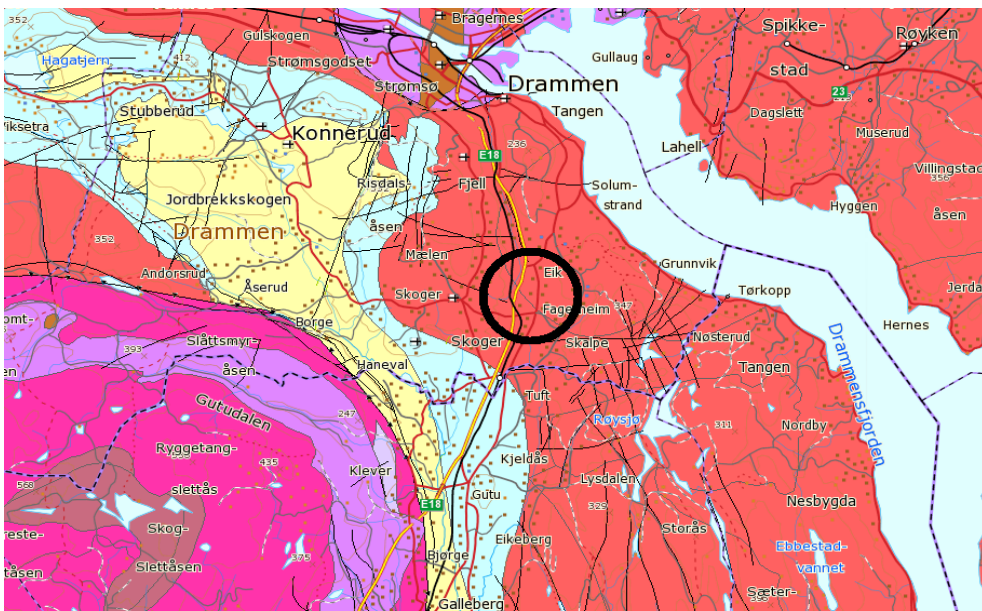
Figure 3-19 Mapped rock types in the region of Drammen (www.geo.ngu.no/kart/berggrunn)

The black ring represents the location of Skoger elementary school. The bedrock that surrounds Skoger elementary school is granite granodiorite. This type of ground is typical for the Drammen region and is also called Drammen's granite.

Ramstad et al. (2008) did a study of thermal conductivity of the rock types present in the Oslo region has been done and plotted in a box diagram Figure 3-20. The thermal conductivity of the rock types have been measured in a laboratory.
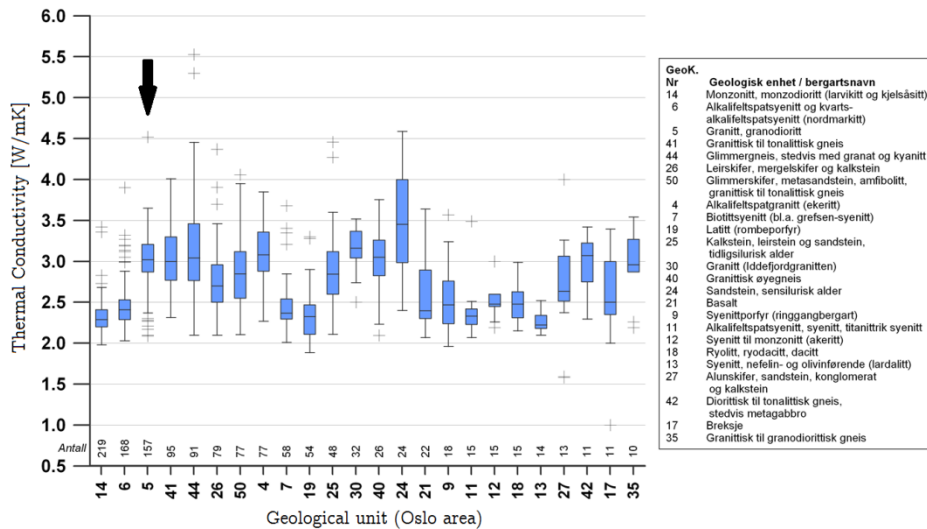
Figure 3-20 Thermal conductivity from laboratory tests, Ramstad et al. (2008)

Figure 3-20 shows the thermal conductivity of different rock types which has been found in the Oslo region. The black arrow in Figure 3-20 points out geological unit 5, which is the Drammen's granite at Skoger elementary school, and has a median value of 3.0 [W/m·K].

Because the laboratory samples are not saturated with water, and water has a higher thermal conductivity than air, is it naturally that the rock samples saturated with water has a higher thermal conductivity. Midttømme et al. (2000) suggested to add 10% to the dry rock thermal conductivity measured in the laboratory, to get values that are more similar to the real thermal conductivity field values. This means that the thermal conductivity of the Drammen's granite should be 3.3 [W/m·K]. This value is used in the models in chapter 4 and is set to be constant along the borehole depth.

3.5 Ground temperature gradient

An approximation for a vertical temperature gradient can be calculated by knowing the thermal conductivity of the ground and the heat flow from the earth interior. The heat

flow in Norway typically varies between 50 and 70 mW/m^2 even at depth of several hundred meters.

Pascal et al. (2010) determined heat flow based on measurements of thermal gradients at 15 different sites in Norway. The sites consist of 15 wells in the Oslo region, mid-Norway, Nordland and Finnmark exceeding 800 meter. Values in Figure 3-21 are based on these sites and 64.4mW/m^2 are shown for Southern Norway which includes the region around Drammen.
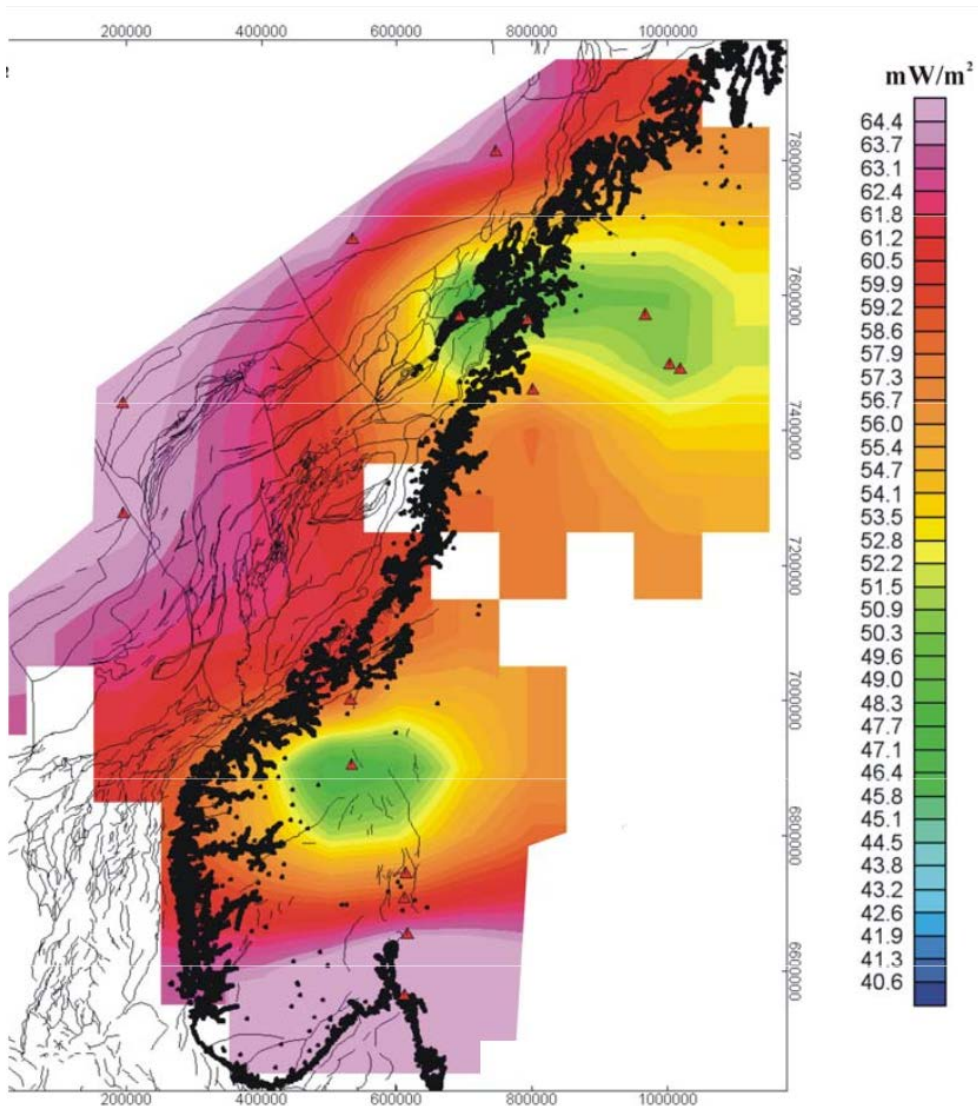
Figure 3-21 Modern heat flow map of Norway, Pascal et al. (2010)

A vertical temperature gradient can be calculated from equation (3-5) and (3-6).

$$q^{"} = -\kappa \cdot \frac{\Delta T}{L} \qquad\qquad (3\text{-}5)$$

$$T(L) - T_{surface} = \frac{q^{"} \cdot L}{\kappa} \qquad\qquad (3\text{-}6)$$

Table 16 Ground conditions used to calculate ground thermal gradient

$q^{"}$	0.0644 [W/m^2]
κ	3.3 [W/mK]
L	500 [m]

Computing equation (3-6) with values from

Table 16, $T(L) - T_{surface} = 9.8K$ and gives a temperature gradient of 1.95K/100meter. Data collected from Norwegian Meteorological Institute showed that the mean annual temperature since 1973 at Marienlyst in Drammen was 6°C. Marienlyst lays just 10 kilometers north of Skoger elementary school and are therefore a good approximation for the mean annual temperature and number of days where the ground is covered by snow. Marienlyst has since 1973 105.5 days/year covering the ground with snow. A way to calculate the mean annual surface temperature is given by Kjellsson (2009), where surface temperature is given by the mean annual temperature+1,5K/100 days with snow on the ground. This gives and the mean annual surface temperature of 6+1.58=7.58°C at Marienlyst. The temperature at 500 meter depth is calculated to be 7.58°C+9.8°C=17.38°C. The surface temperature changes during the year and this influences the temperature profile for the 20 first meters of the borehole. The calculated temperature gradient represents the real temperature conditions for the first 20 meters by a yearly average temperature gradient, but it becomes more precise at depths lower 20 meter where the influence of the surface temperature is almost insignificant.

3.6   Energy load since September 2011
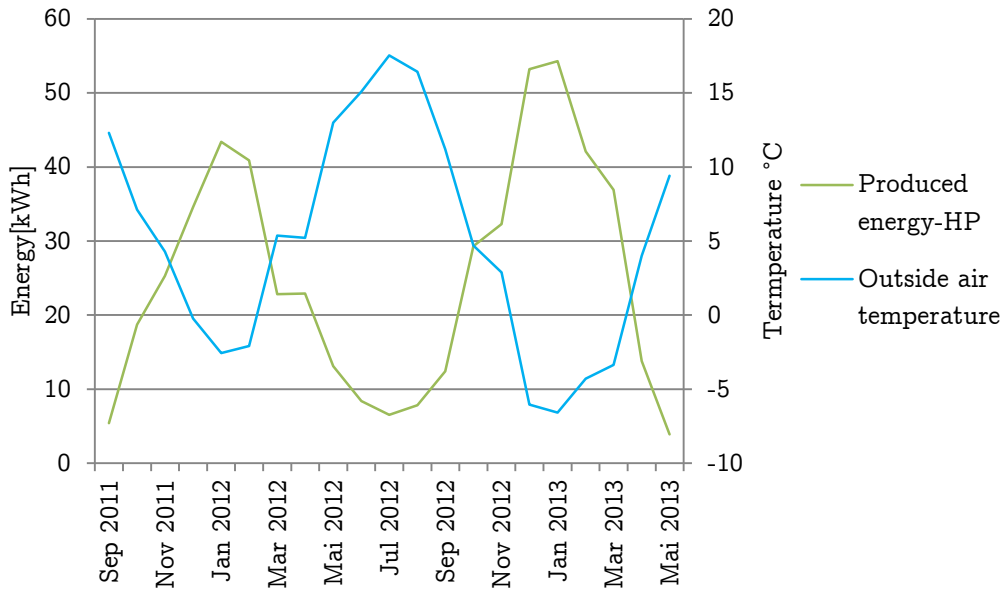
Figure 3-22 Energy delivered from the heat pump and outside air temperature

Figure 3-22 shows the produced energy from the heat pump and the outside air tempera-ture since the renovation of Skoger elementary school was done. An extrapolation of the energy delivered from the heat pump is used in the simulations done in chapter 4. The extrapolation for 10 years is based on the heat delivered from the heat pump in year 2011 followed by heat loads from year 2012 and is showed in Figure 3-23.
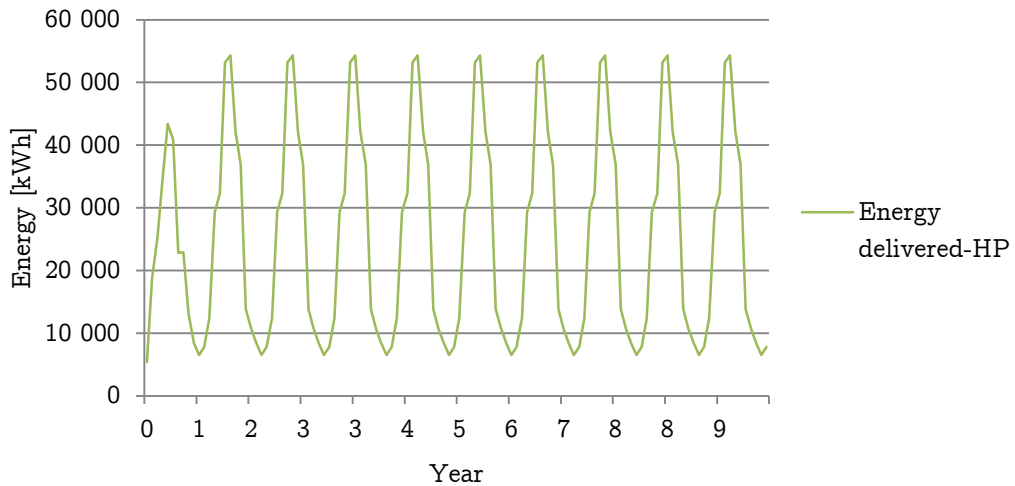
Figure 3-23 Extrapolated heat delivered from heat pump

3.6.1 Energy charged by heat recovery batteries

The energy wells are recharged as mentioned in chapter 3.1.10. This means that the heat recovery also has to be extrapolated to be able to simulate the heat load taken from the ground for longer periods than the system has been in operation. Figure 3-24 shows how the heat recovery and the heat delivered from the heat pump are correlated in the extrapolation from September 2011 to February 2013. Recharge energy values are only taken up to February 2013, because installation of measurement equipment for the energy wells has influenced the heat recovery batteries after February 2013. The extrapolation period of 10 years for recharge energy and heat delivered from the heat pump is shown in Figure 3-24.
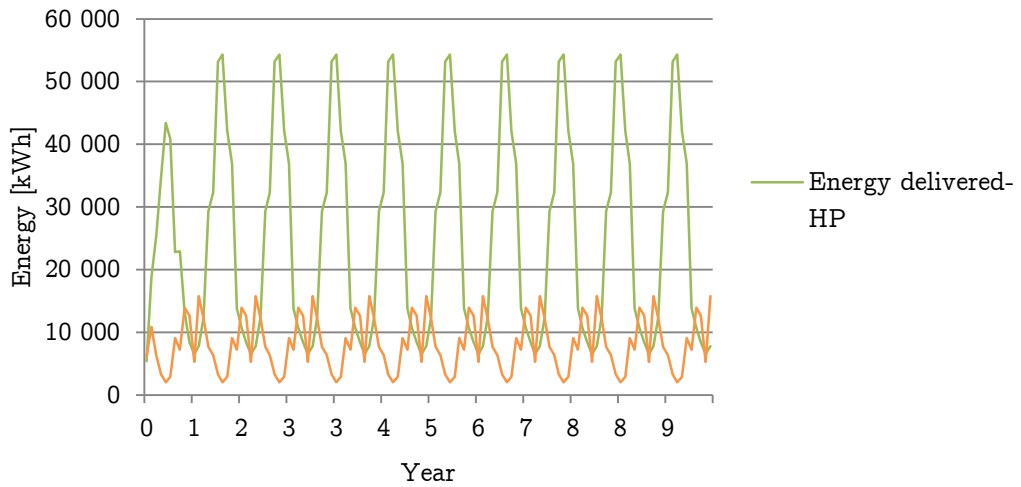
Figure 3-24 Heat recovery and the heat delivered from the heat pump
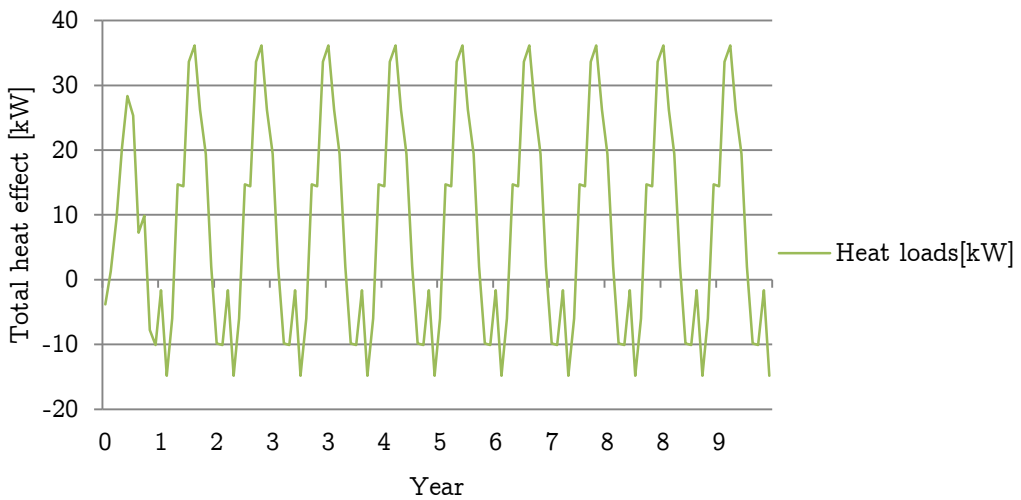
Figure 3-25 Heat effects from energy wells for extrapolation period of 10 years

The total heat load including heat from recovery batteries are drawn in Figure 3-25 for COPs equal to 2.1 and 2.7 for winter and summer months, respectively.
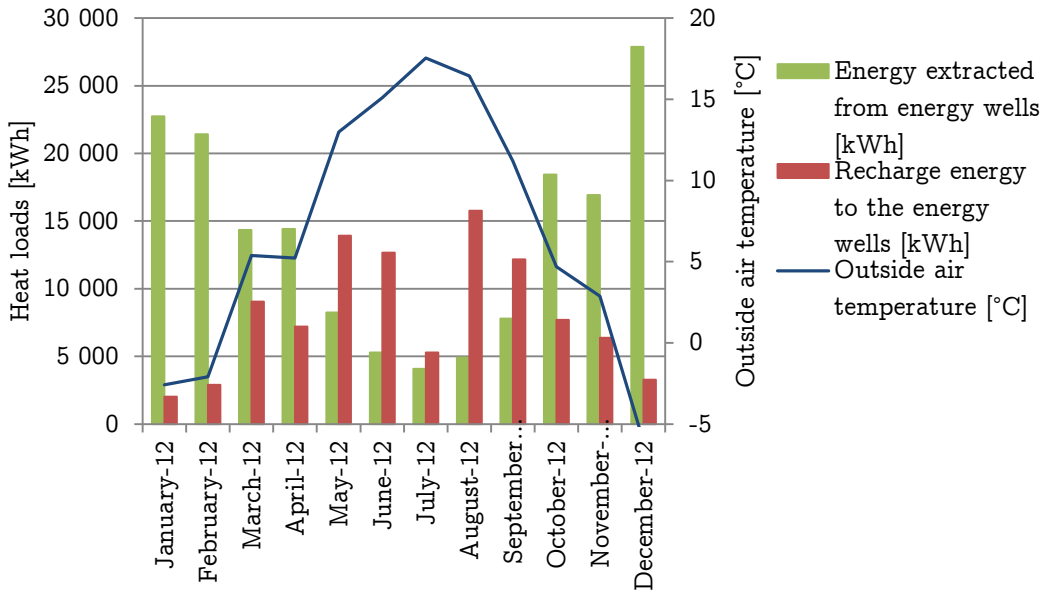
Figure 3-26 Energy extracted and injected from the energy wells in 2012 with COP equal to 2.1 and 2.7 for winter and summer month, respectively
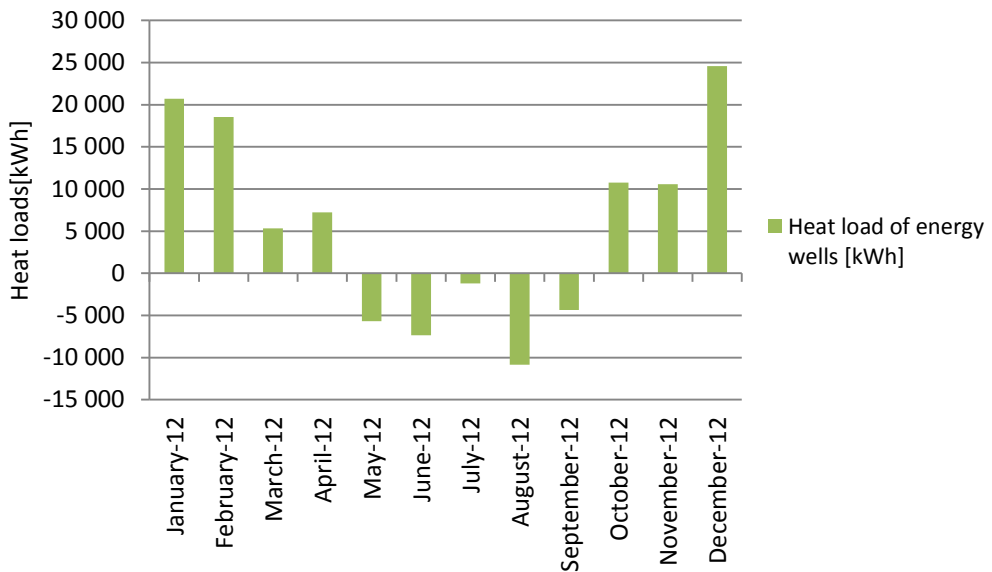
Figure 3-27 Energy wells monthly heat loads from 2012 with COP equal to 2.1 and 2.7 for winter and summer month, respectively

Figure 3-27 presents the average monthly energy load of the energy wells for year 2012 and shows that the heat recovery decreases from June to July because the air ventilation system energy demand is at its lowest during the summer vacation which reduces the energy well heat recovery amount.

Table 17 Heat pump energy input 2012, with COP1 and COP2

2012	COP1	COP2
Energy delivered form heat pump [kWh]	293000	293000
Energy extracted from energy wells [kWh]	166513	166513
Energy injection to energy wells [kWh]	108200	108200
Energy heat pump input [kWh]	126487	92876

Table 17 shows the total energy usage for Skoger elementary school for 2012 with energy loads extracted from the ground calculated with COP1.

The heat extracted from the energy wells are approximately 1.5 times higher than the energy injected to the energy wells, and the energy recharge effect on the long term performance of a BHE of will be shown later in this thesis.

4 Model Development

Based on the literature review of different BHE simulation models and ground effect, a two-dimensional model for a line array of five BHEs and a three-dimensional model for a single BHE are developed. The 3D model was developed using least possible BHE-geometry and ground simplifications to be able to evaluate the system at Skoger in an accurate way. Since the boreholes at Skoger are groundwater filled, implementing a natural convection heat transfer relation into the model is therefore important. Since it is easy to define a customized thermal conductivity to the materials used in the Comsol Multiphysics, developing a 3D model in Comsol was chosen. It is possible to implement natural convection relation into the TRCM models represented in chapter 2.3.6, but how this could be done will not be discussed in this thesis.

The intention is to study the thermal interaction between adjacent boreholes with a varying heat load similar to the energy demand of Skoger elementary school. Only a single u-pipe geometry will be studied because that is the type of collector installed in the borehole at Skoger elementary school in Drammen.

4.1 Finite Element method

Comsol Multiphysics uses the conservation laws for the momentum, mass and energy expressed in partial differential equations together with initial and boundary conditions, to solve the desirable problems. The equations are solved using stabilized finite element method, and different time-dependent solver algorithms for the time dependent problems.

To evaluate a mathematical model of a process in numerical simulations of a physical problem, it is necessary to employ a numerical method and a computer. The finite element method is often used and it is a powerful method to solve physical processes.

Finite elements are the subdomains which the domain of the problem are divided into. All of the finite elements in the domain are called the finite element mesh. This mesh can consist of different shapes. Physical quantities at selective points, or nodes, are developed as the physical process is approximated by functions, which could be linear or polynomi-

al, over each finite element. The element equations are assembled by balance of interelement forces and assuming the solution is continuous at the interelement boundaries. This makes it possible to get accurate representation of the solution within each element and for complex geometries.

The solution is often represented as a linear combination in terms of the nodal values u_j of u at the nodes. From Reddy (1993) the approximate solution u to a differential equation is at the form

$$u = \sum_{j=1}^{n} u_j \psi_j + \sum_{j=1}^{m} c_j \phi_j \qquad (4\text{-}1)$$

Where ψ_j is the interpolation functions, c_j are the node less coefficients, and ϕ_j are the associated approximation functions and n is the number of line segments

Number of nodes depends on the geometry of the element, the degree of the polynomial approximation and the integral form of the equations.

The error connected to the finite element method consists of three sources. These sources are due to the approximation of the domain, approximation of the solution and the error due to numerical computation. The error can be reduced by generating a finer finite element mesh, and reduce the time step in the numerical computation. By doing this the computational running time will increase, so it is important to weight the error compared to the running time.

Equation (4-2), (4-3) and (4-4) shows the heat differential equation in cylindrical coordinates for 3, 2 and 1 dimensions, respectively with Kreyszig (2006) as reference.

The heat differential equation in cylindrical coordinates for three dimensions:

$$\frac{\rho c_p}{\kappa} \frac{\partial T}{\partial t} = \frac{\partial^2 T}{\partial r^2} + \frac{1}{r} \frac{\partial T}{\partial r} + \frac{1}{r^2} \frac{\partial T}{\partial \theta} + \frac{1}{r^2} \frac{\partial^2 T}{\partial z} \qquad (4\text{-}2)$$

Two dimensions:

$$\frac{\rho c_p}{\kappa} \frac{\partial T}{\partial t} = \frac{\partial^2 T}{\partial r^2} + \frac{1}{r} \frac{\partial T}{\partial r} + \frac{1}{r^2} \frac{\partial^2 T}{\partial \theta} \qquad (4\text{-}3)$$

and one dimension:

$$\frac{\rho c_p}{\kappa} \frac{\partial T}{\partial t} = \frac{1}{r} \frac{\partial}{\partial r}(r \frac{\partial T}{\partial r})$$ (4-4)

Where κ, ρ and c_p are constants and z is the length scale along the borehole length.

4.2   Equivalent Radius Model

The equivalent radius model is an approximation of the complex geometry in a u-pipe. The model uses an annular geometry with one centered pipe instead of two u-pipe legs. The equivalent radius model approximation is common in borehole heat exchanger simulations since the annular shaped geometry makes it possible to use a 2D axisymmetric model, which reduces the computer running time compared to a regular 2D and 3D model and because Nusselt relations for natural convection has been derived for vertical cylindrical annulus.
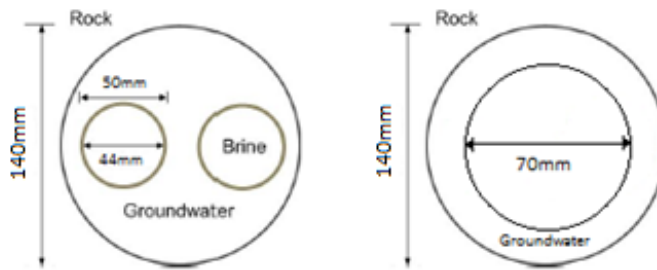
Figure 4-1 Equivalent radius model for constant temperature at the pipe wall

4.3   Groundwater effective thermal conductivity

Natural convection influences the borehole resistance as mentioned in 2.5.5. To implement natural convection to a model used to simulate temperature responses in BHEs an effective thermal conductivity can be implemented. This is a thermal conductivity based on Nusselt relations correlating convective heat transfer induced by density gradients in the fluid, and conductive heat transfer. An effective thermal conductivity is therefore a conductivity approximation to the convective heat transfer shown in equation (4-5)

$$\text{Nu} = \frac{\kappa_{\text{stagnant water}}}{\kappa_{\text{effective}}} \tag{4-5}$$

A cellular flow in a vertical cavity with different temperatures has been considered by many investigators. The fluid ascends along the hot wall and descends along the cold wall. An analogy between the vertical cavity and a borehole where the gap between the collector and the borehole wall is small can be drawn. For small Rayleigh numbers $\text{Ra}_l < 10^3$ the buoyancy driven force is small, and the heat transfer is primarily by conduction. The Rayleigh and the Grashof number for a flat plate is defined in Incropera and DeWitt (2002)

$$\text{Ra}_l = \frac{g\beta(T_1 - T_2)l^3}{\alpha\nu} = \text{Gr}_l \cdot \text{Pr} \tag{4-6}$$

where

$$\text{Pr} = \frac{\nu}{\alpha} \tag{4-7}$$

$$\text{Gr}_l = \frac{g\beta(T_1 - T_2)l^3}{\nu^2} \tag{4-8}$$

$$\beta = -\frac{1}{\rho}\left(\frac{\partial\rho}{\partial T}\right)_p \tag{4-9}$$

$$\alpha = \frac{\kappa}{\rho c_p} \tag{4-10}$$

T_1 is the temperature of the heated surface and T_2 is the temperature of the cooled surface. T_1 and T_2 can be referred to as the temperature at the borehole and the collector wall, respectively and l is the distance between the heated surfaces.

Incropera and DeWitt (2002) expressed the thermal expansion coefficient shown in (4-11) and the thermal expansion coefficient can be calculated with water property data from www.webbook.nist.gov. This is plotted in Figure 4-2 with temperature steps equal to 0.25K/step from state 1 to 2.

$$\beta = -\frac{1}{\rho}\left(\frac{\Delta\rho}{\Delta T}\right)_p = -\frac{1}{\rho_1}\frac{\rho_2-\rho_1}{T_2-T_1} \tag{4-11}$$
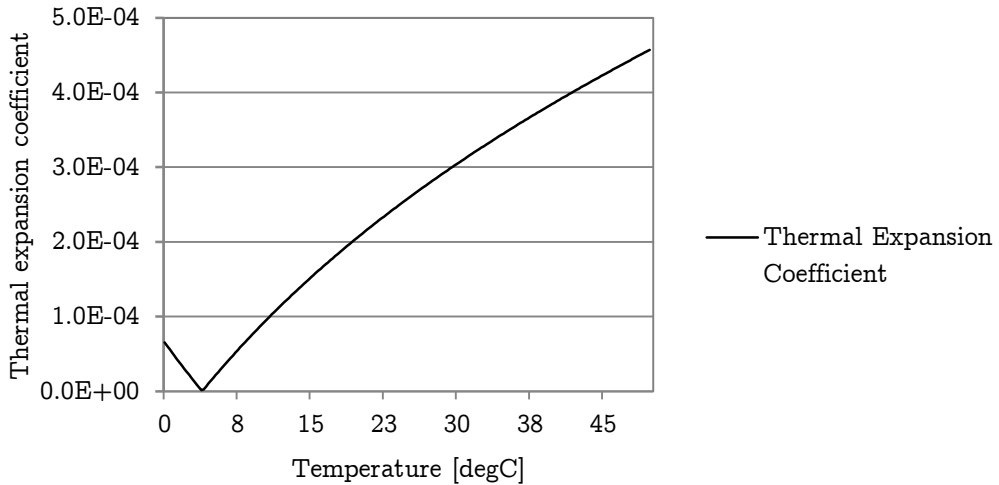
Figure 4-2 Thermal expansion coefficient at 1bar

The thermal expansion coefficient for 1 bar and 10 bar have been plotted with data from www.webbook.nist.gov and compared. The plots show that there is close to no differences in the thermal expansion coefficient for 1 and 10 bar, and the thermal expansion coefficient will therefore be treated independent of pressure. Since the thermal expansion coefficient is independent of pressure, also the Rayleigh number will be independent of pressure.

The heat transfer improves with increasing Rayleigh number, since the cellular flow intensifies next to the sidewalls. This results in a more effective heat transport than with pure conduction.

An expression for the Rayleigh number including the heat flux is presented as a modified Rayleigh number Ra*.

$$Ra^* = Pr \cdot Gr^* = \frac{g\beta\, l^4 q''}{\alpha\nu\kappa} \tag{4-12}$$

$$Gr^* = \frac{g\beta \, l^4 q''}{v^2 \kappa} \tag{4-13}$$

Where l is the distance between the heated surfaces and q'' has the dimension W/m^2.

The thermal effects of natural convection are highly dependent on the given geometry and orientation. A simplification of the borehole geometry is often used to make it possible to have a numerical solution. By approaching the u-pipe geometry to an equivalent radius, a numerical solution can be evaluated with Nusselt relations developed for a vertical cylindrical annulus with constant heat flux at the inner wall and a cooled outer wall, showed in Figure 4-3
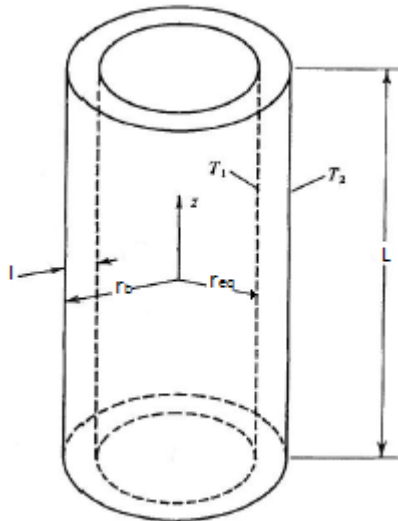
Figure 4-3 Schematic of the annular geometry, Choi and Korpela (1980)

Keyhani et al. (1983) presented the Nusselt relation for a vertical cylindrical annulus for constant heat flux.

$$Nu = 1.37 Ra^{*0.072}, \quad 2.6 * 10^3 < Ra^* < 1.8 * 10^4 \tag{4-14}$$

$$Nu = 0.253 Ra^{*0.244}, \quad 1.8 * 10^4 < Ra^* < 4.21 * 10^7 \tag{4-15}$$

4. MODEL DEVELOPMENT

The temperature that should be used to evaluate the properties needed for the Rayleigh and the Nusselt number are the average of the heated inner and outer wall temperatures.

For the Nusselt relation Keyhani et al. (1983) presented an assumption that the geometric parameters are independent of the boundary conditions and the effects of different boundary conditions will appear in the exponent of Rayleigh number and the constant of the correlation. This Nusselt number relation was given by (4-16) and (4-17), and with geometric parameter the relation was presented as

$$\mathrm{Nu} = 0.78\,\mathrm{Ra}^{*\,0.072}A^{-0.052}K^{0.505}, \qquad 2.6 * 10^3 < \mathrm{Ra}^* < 1.8 * 10^4 \qquad (4\text{-}16)$$

$$\mathrm{Nu} = 0.291\,\mathrm{Ra}^{*\,0.244}A^{-0.238}K^{0.442}, \qquad 1.8 * 10^4 < \mathrm{Ra}^* < 4.21 * 10^7 \qquad (4\text{-}17)$$

and

$$1 < A < 33$$

$$1 < K < 10$$

Where

$$A = {}^{L}\!/_{l}$$

$$l = r_b - r_{eq}$$

$$K = {}^{r_{outer}}\!/_{r_{inner}}$$

This is a good match for the modified Rayleigh number and radius ratio compared to a borehole filled with groundwater and the aspect ratio is discussed in 4.3.1.

Keyhani et al. (1983) Nusselt number dependence on temperature for a constant heat flux has been plotted in Figure 4-4. The plots have been made with constant radius ratio equal to 1.4 and aspect ratio of 33. Since 33 is the highest aspect ratio for the Nusselt number correlations in equation (4-16) and (4-17) an assumption that the different Nusselt number relations are transferable for larger aspect ratios is therefore necessary to make. This is reasonable to assume for a multicellular flow pattern. The height of the cell is unknown, and the best assumption is therefore to use the highest possible aspect ratio for the given Nusselt number correlation.
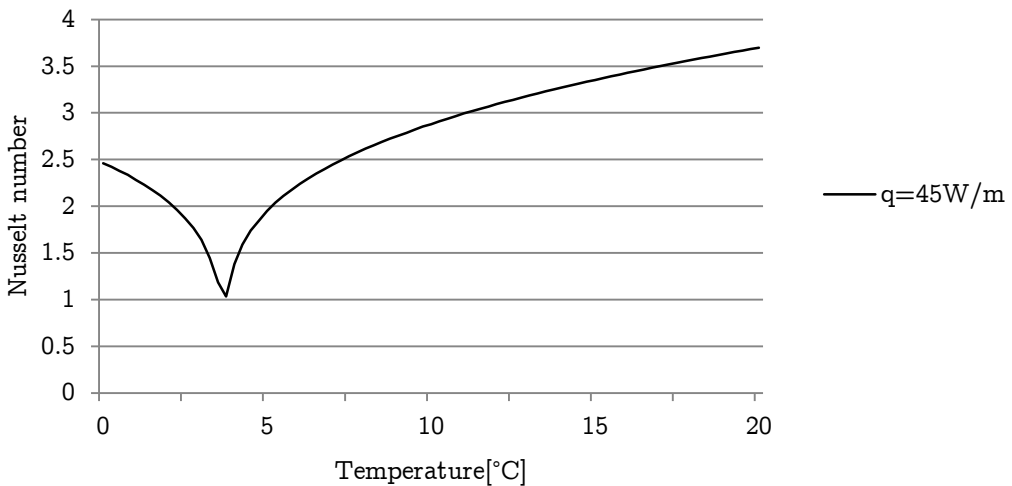
Figure 4-4 Nusselt number for K=1.4 H=33

Figure 4-4 shows the Nusselt number for a heat flux at the pipe wall equal to $q^{''}$=111 W/m^2 which corresponds to a heat rate of q=35 W/m for an equivalent radius model with r_{eq} = 0.05 meter. For temperatures near 4°C the heat transfer will mainly be controlled by conduction because water has its highest density near this temperature, and the Nusselt number relation should therefore be close to 1.

4.3.1   Multicellular flow

Two flow regimes are found for natural convective flow in a cavity, conduction regime and a multicellular flow. This motion is showed to be dependent on Rayleigh number, the Prandtl number, the aspect ratio A of the cavity and the distance between the heated surfaces.

For the conduction regime near the mid height of the enclosure, the flow is parallel to the walls and the core becomes nearly stagnant and heat is transferred across the core by pure conduction. The heat transferred by conduction increases with lower Rayleigh number because the cell height grows and reduces the total heat transfer.

An increase in temperature difference across the cavity filled with a low Prandtl number fluid, causes the conduction regime flow pattern to break up an undergo a transition to a multicellular flow pattern. This enhances the heat transfer. An illustration of the conduc-

tion regime and multicellular flow patter is shown in Figure 4-5 by increasing the Rayleigh number from the left to the right.
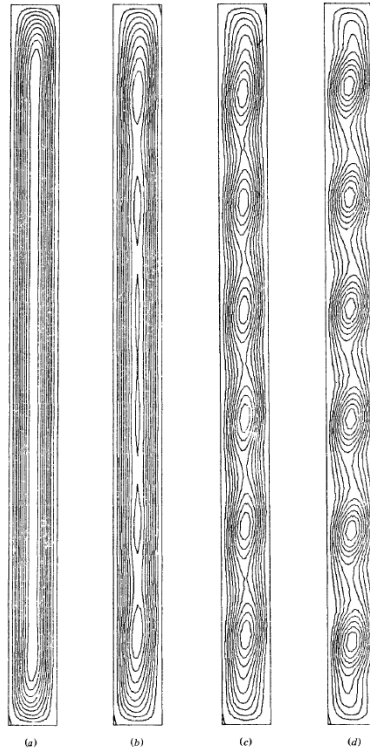
Figure 4-5 Streamlines of flow in a cavity with H=15 and increasing the Rayleigh number, Lee and Korpela (1983)

For large Rayleigh number a multicellular flow regime was observed. The local heat transfer coefficient on the inner wall was found to increase with radius ratio in the range of 1 to 4, but decrease with increasing aspect ratio.

With radius ratio varying from 1.2 to 10, Ho and Lin (1990) showed that with an aspect ratio higher than 8, a multicellular flow behavior of cold water may arise, and that for large aspect ratios the average Nusselt number clearly converges. Because of the cellular flow pattern develops at relative small aspect ratios compared to aspect ratios for BHEs, the natural convection effect can be assumed independent of the borehole depth as shown in Figure 4-6.
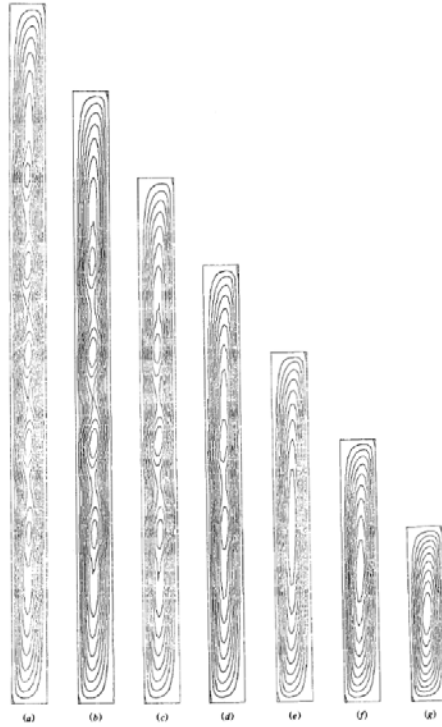
Figure 4-6 Example of a multicellular flow pattern for different aspect ratio with a constant Rayleigh number, Lee and Korpela (1983)

Figure 4-6 shows the natural convection induced flow pattern for different aspect ratios in a rectangular cavity with constant Rayleigh number.

The increase of radius ratio tends to enhance the average heat transfer coefficient. Because of the dependence on the difference in outer and inner radius, a larger radius ratio will contribute to a higher Rayleigh number and thereby a higher Nusselt number.

In general the axial temperature difference diminishes with higher radius ratios, and for radius ratio equal to 10 the inner wall is nearly isothermal. A drop in temperature along the inner wall of the annulus can be described by a higher convective heat transfer coefficient. This temperature drop at the inner wall is more pronounced for radius ratios between 1 and 3, but it is clearly dependent on the Rayleigh number. For a tall annulus a wavy temperature distribution along the inner wall forms because of a multicellular flow regime.

By assuming a stable multicellular flow pattern for the groundwater filling inside the borehole a Nusselt number relation can be obtained from equation (4-16) and (4-17) for an equivalent radius model representing the BHE geometry.

5 3D-Model

A three dimensional model is developed in Comsol Multiphysics with intentions of simulating the BHEs installed at Skoger elementary school, using the least possible assumptions. The computer software package Comsol Multiphysics is a finite element modeling software package that contains a number of predefined physics interfaces. The software is used to solve partial differential equations using the finite element method with different mathematical solvers.

An important feature of the 3D model is the simulation of fluid flow inside the collectors which makes it more realistic than other models that do not simulate fluid transport. The aims for the model is to evaluate a borehole resistance that can be used as an input for two dimensional model, where the thermal interaction between the five boreholes installed at Skoger elementary school will be studied. A Nusselt number relation for natural convection heat transfer derived in chapter 4.3 was implemented into the 3D model developed in Comsol Multiphysics.

A pipe flow module is used to represent fluid flow inside the u-pipe collector. This Comsol Multiphysics module is suitable for pipes which have length large enough so that the flow can be considered as fully developed and represented by a 1D approximation. By approximating the pipe with a 1D representation the geometry of the pipe in the solid is directly accounted for, and the heat transfer between the ground and the fluid occurs at the 1D line representation of the collector.

5.1 Geometry

Figure 5-1 shows the numerical simulation domain of the BHE with a pipe flow with a u-pipe collector representation. The simulation domain extends with a radius of 25 meter and a depth of 530 meter. Different domains are assigned to simulate different materials e.g. ground-water and the ground.
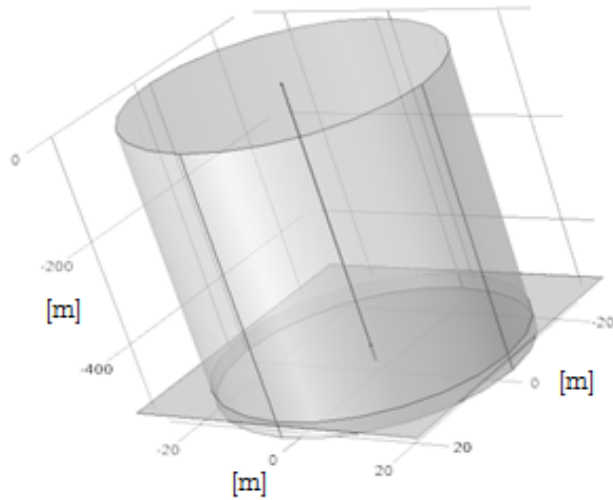
Figure 5-1 3D model with 1D pipe representation

The center of the collector pipe inlet and outlet are represented as dots from a horizontal 2D view. The center of the collector pipe inlet and outlet are located at a radius equal to 0.04 meter and the distance from center to center is 0.08 meter.
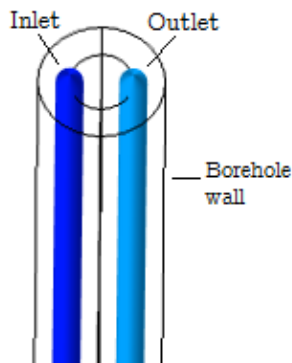
Figure 5-2 Inlet and outlet representation of the borehole

86

5.2 Boundary Conditions

Table 18 3D model input values

Description	Input variable	Units
3D u-pipe model		
Boundary condition		
Borehole		
Pipe (Polyethylene)		
Pipe wall thickness	3	mm
Thermal conductivity	0.42, Stene (2012)	[W/mK]
Inner diameter	44	mm
Pipe spacing, center to center	0.08	m
Pipe flow		
Boundary condition		
Inlet temperature	T_inlet	°C
Inlet velocity	Inlet_vel	m/s
Initial values		
Initial velocity	Init_vel	m/s
Initial temperature	Init_temp	°C
Fluid, Ethylene Glycol-water solution	Properties from chapter 3.1.2	
Friction model	Churchill	
Surface roughness, Thermoplastics	0.0015	mm
Groundwater		
Effective thermal conductivity	k_effective	[W/mK]
Ground		
Initial value	init_temp	°C
Undisturbed temperature	T_undisturbed	°C
Thermal conductivity	k_ground	[W/mK]
Temperature gradient	T_gradient	°C/100 meter

The thermophysical properties used in the 3D model for ground and groundwater are the predefined properties for granite and water, respectively, except for the properties defined in Table 18.

5.3   Mesh

A three dimensional mesh for the BHE was generated using Comsol's automatic mesh function. A 2D mesh was first generated with a fine mesh around the pipes and coarser mesh at the outer simulation domain. In this way more cells can be included in places where greater temperature gradients are expected and less cells far away from the borehole, where the temperature gradient is expected to be smaller. The 2D mesh was extruded along the borehole depth, using swept mesh generator in Comsol.
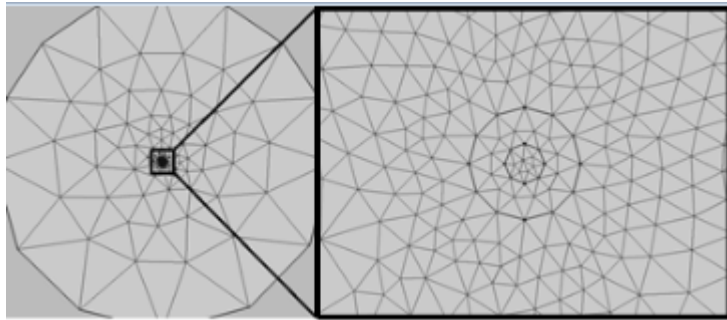
Figure 5-3 2D mesh overview

The 2D mesh is developed with a Free Triangular generator with custom element size parameters at the pipe wall, shown in Figure 5-3. The custom input of parameters makes sure that the maximum and minimum element sizes are small enough to be able to solve for. The swept mesh generator sweeps the 2D mesh along the borehole depth and divides the mesh into a number of layers, where the distance between each layer can vary. The properties of the mesh is shown in Table 19

Table 19 Mesh description, point

Model Mesh Description	Value
Element size	
Geometric entity level: Point	
General physics	
Maximum element size	0.05m
Minimum element size	0.04m
Maximum element growth rate	1.3
Resolution of curvature	0.2
Resolution of narrow regions	1
Swept mesh distribution	Each 10th meter

It is important to have the minimum element size as small so the smallest geometry can be solved. Since the collector pipe diameter is 0.044 meter a minimum element size was set to 0.04 meter. It is also important to keep the maximum element size small where the biggest temperature gradients are expected to be. The geometric entity level is specified to four points at the inner circle, (-0.04,0), (0.04,0), (0,0.04) and (0,-0.04) as a starting point for the mesh element size.

Because of the high depth to width ratio of the borehole and relatively low temperature gradients along the borehole depth, the mesh can be constructed with a relatively long distance between each layer in the z-direction shown in Figure 5-4.
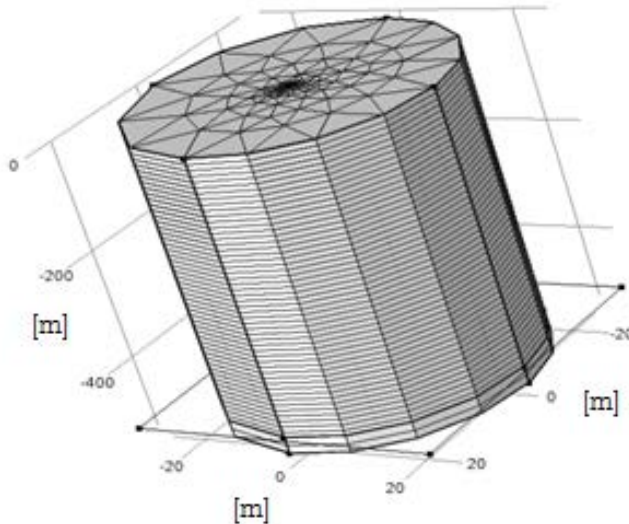
Figure 5-4 3D mesh overview

Unfortunately a swept mesh was not able to be built around the u-bend of the collector pipe, a physics controlled free tetrahedral mesh was therefore build with properties shown in Table 20. This mesh is built inside the outer circle showed in Figure 5-2 and at z-values of -499.85 and -500, which is the domain where the u-bend is built. This was done implementing two work planes at z-values of -499.85 and -500, and build the free tetrahedral mesh between the work planes. Because of computer capacity a physic controlled mesh for the whole 3D model was not possible to solve for.

Table 20 Mesh description, domain

Model Mesh Description	Value
Element size	
Geometric entity level: Domain	
General physics	
Maximum element size	16 meter
Minimum element size	0.04 meter
Maximum element growth rate	1.45
Resolution of curvature	0.5
Resolution of narrow regions	0.6

The mesh consists of 30297 domain elements. 4236 boundary elements, and 832 edge elements.

5.4 Simplification of the fluid

The fluid is set to follow two edges along the inner cylinder boundary with a radius of 0.05 meter, shown in Figure 5-2. This makes it possible to have a swept mesh along the borehole depth. The u-pipe bend was built using a work plane and a Bèzier Polygon with two quadratic segments shown in Figure 5-5 and connected to the edges along the inner circle.
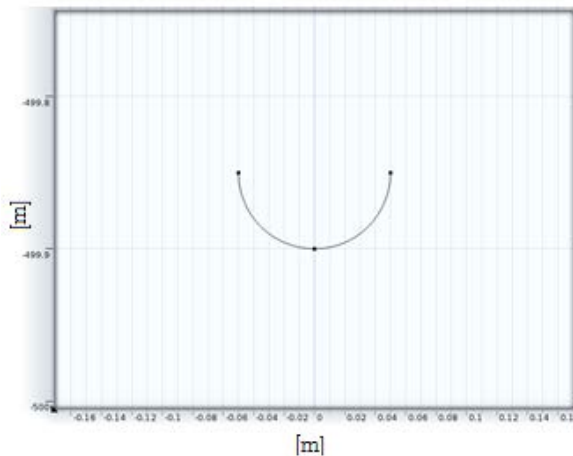
Figure 5-5 u-bend Bèzier Polygon

A wall heat transfer boundary from the non-isothermal pipe flow module is used to represent the collector pipe flow heat transfer. The wall heat transfer node has an internal film resistance and an external wall layer embedded. The internal film resistance is set to automatic, and for the wall layer the wall thickness and thermal conductivity is specified to 0.003 meter and 0.42 W/mK, respectively.

5.4.1   Borehole thermal resistance

Assuming the borehole is in steady state the amount of heat transfer rate per unit length between the ground and the heat carrier fluid can be expressed as

$$q = \frac{T_{bhw} - T_{f,mean}}{R_b} \qquad (5\text{-}1)$$

Where q [W/m] is the heat transfer rate between the fluid and the borehole wall and the borehole resistance, Rb [mK/W], includes the conductive resistance of the filling material, the conductive resistance of the pipes and the convective resistance between the fluid and the inner side of the collectorpipes. In development of analytical as well as some numerical BHE models the borehole resistance concept has been widely used, it is therefore an interesting parameter when comparing different BHE models, or evaluating BHE systems.

To keep the borehole resistance low, it is important to have a high thermal resistance between the down-and up going flows, and low thermal resistance between the either pipe and the borehole wall. It might be of interest to have a higher thermal resistance in one of the pipes to prevent heat being transferred between down-and up going flows. For a given heat extraction rate and borehole wall temperature the BHE geometry that gives the lowest R_b will be able to deliver the highest temperature to the heat pump, and have lower temperature driving forces between the fluid and the ground.

5.5   Model simplifications

A numerical model was developed in Comsol Multiphysics. Due to computer capacity restraints a model consisting of only one borehole including fluid flow was made. The model was therefore only used to evaluate the borehole resistance and temperature and wall heat transfer rate distributions along the borehole depth.

Since a TRT was not carried to predict the ground thermal conductivity out before installation of the BHEs at Skoger, ground conductivity values had to be based on ground conductivity values published by Geological Survey of Norway. The ground is considered homogeneous and is approximated to have a constant thermal conductivity along the borehole depth. Ground conductivity is based on values published by the Geological Survey of Norway, and information about groundwater flow was not available. Groundwater flow was therefore neglected in the model, but could easily be implemented in the Comsol 3D model by adding a porous medium module, but this will make the model more computational heavy.

Since the filling around the collector pipes is groundwater, a Nusselt number relation for natural convective heat transfer for water was implemented in the 3D model through an effective conductivity. No Nusselt number relation is available for u-pipe geometry and BHE applications, and the Nusselt number relation used is developed for an annular geometry. The borehole resistance calculated from the 3D model may therefore deviate from the real borehole resistance for the BHEs installed at Skoger. But this deviation is expected not to be an important factor for the long term performance of the BHE system.

5.6   Simulation result 3D model

A dynamic 3D finite element model for BHEs is developed and presented in chapter 5 providing a representation of the fluid transport in the collector pipes, the borehole geometry and the thermal mass of filling material. Because the 3D model is computationally heavy a two dimensional model was developed to represent the BHE system installed at Skoger elementary school in Drammen. The main purpose of the 2D representation of the BHE system is to evaluate the system performance including the thermal interaction between the boreholes. The 3D model will however provide input data for the 2D model.

5.7   Transient simulations

The thermal dynamic response of the BHE over short time scales can be of great interest in many applications. For example will the BHE response to a thermal response test or the response to variations in heat loads be important BHE design factors.

The 3D model is used to evaluate the borehole thermal resistance derived from equation (5-1).

$$R_b = \frac{T_{bhw} - T_{f,mean}}{q} \qquad (5\text{-}2)$$

5.7.1   TRT model

Literature recommendations of required response test duration vary from 48 to 70, and Gehlin (2002) recommends at least 50 hours. The 3D model was simulated for 50 hours to be sure of independence of initial fluid temperatures. A constant heat effect extracted or injected to the ground was made by making the inlet temperature dependent on the outlet temperature shown in equation (5-3) and (5-4), respectively.

$$T_{inlet} = T_{outlet-}\frac{Q}{\dot{V}\rho c_p} \qquad (5\text{-}3)$$

$$T_{inlet} = T_{outlet+}\frac{Q}{\dot{V}\rho c_p} \qquad (5\text{-}4)$$

Where the fluid properties ρ and c_p are temperature dependent and $\dot{V}$ [m^3/s] and Q [W] are constant. To make the 3D model less computational heavy a constant heat flux distribution along the borehole depth is assumed for the modified Grashof number shown in equation (4-13). Assumptions for the modified Grashof number used in the 3D model are done with the equivalent radius geometry showed in Figure 4-1 with a r_{eq}=0.05 meter and l=0.02 meter.

The influence of natural convection is implemented in the 3D model for the water surrounding the collector pipes through an effective thermal conductivity based on the Nusselt number relation in equation (4-16) and (4-17). The $\kappa_{effective}$ vary with the temperature dependent parameters in the Rayleigh number along the borehole depth, but restrictions in computer capacity and in Comsol Multiphysics made the model unable to implement the flux variations along the borehole depth into the Grashof number relation in equation (4-13). The Grashof number is therefore calculated assuming constant flux distribution along the borehole depth. Figure 5-6 shows $\kappa_{effective}$ for different heat rates used in the 3D model and the conductivity of stagnant water which excludes the thermal effects of natural convection. $\kappa_{effective}$ is only valid for temperatures over 0°C because the water freezes below 0°C and the thermal conductivity of frozen water is constant and

different from the water conductivity. It is therefore necessary to make sure that the groundwater around the collector pipe stays at temperatures over 0°C during the simulation.
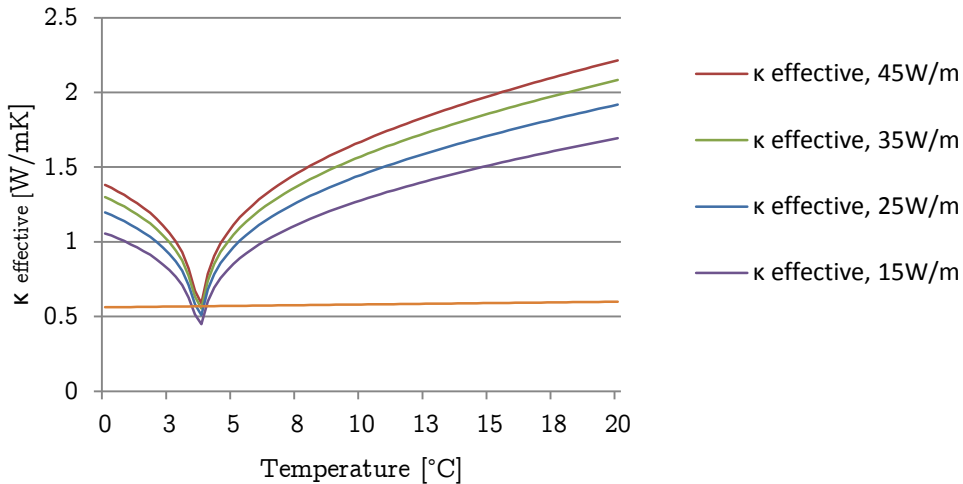
Figure 5-6 Groundwater effective thermal conductivity for different heat rates

5.7.2 Parametric study of the borehole resistance

An average of the borehole wall surface and a mean of the in-and outgoing fluid was evaluated to be able to calculate the average borehole resistance with boundary conditions presented in Table 21.

The 3D model developed was extremely sensitive to the initial temperature and to prevent temperature oscillations of the borehole wall temperature and fluid temperature, the maximum time step was set to 100 seconds, while the steps taken by the solver was set to intermediate. This made the simulations computational heavy, but the temperature oscillations was eliminated.

Table 21 3D model input

Description	Input variable	Value	Units
Pipe flow			
Boundary condition			
Inlet temperature	T_inlet	Equation (5-3)	°C
Inlet velocity	Inlet_vel	0.263	m/s
Initial values			
Pressure	Init_pressure		Pa
Tangential velocity	Init_vel	0.263	m/s
Temperature	Init_pipe_temp		°C
Wall layer			
Thermal conductivity	0.42		[W/mK]
Wall thickness	3		mm
Groundwater			
Effective thermal conductivity	k_effective	25W/m, 45W/m	[W/mK]
Ground			
Surface Temperature	T_surface	7.6	°C
Temperature gradient	T_gradient	1.96	°C/100 meter
Initial value	T_init	1.96	°C/100 meter
Undisturbed temperature	T_undisturbed	1.96	°C/100 meter
Thermal conductivity	k_ground	3.3	[W/mK]
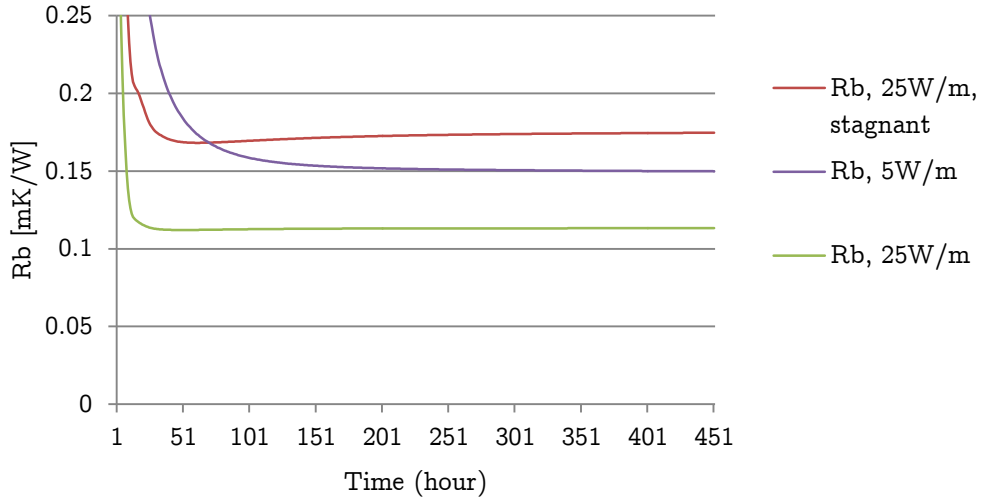
Figure 5-7 Borehole resistance with different heat extraction rates

Figure 5-7 shows an average borehole resistance for different heat extractions. 5 W/m equals to 5 W/m· 500 meter = 2500 W extracted from the borehole. The heat extraction [W] is held constant during the 50 hours, and a significantly lower thermal resistance is observed for heat extracted including $\kappa_{effective}$ compared to $\kappa_{stagnant}$ since the density gradient driven convective flow enhances the heat transfer. For 12,5 kW (25 W/m) extracted over 50 hours the borehole resistance including natural convection effects reduces the borehole resistance with 35% compared to the borehole resistance for the stagnant water case. Increasing the heat extracted from 5 W/m to 25 W/m decreases the borehole resistance shown in Figure 5-7, due to increased temperature gradients between the collector pipe and the borehole wall.

5.7.3 Heat extraction and injection influence on borehole resistance
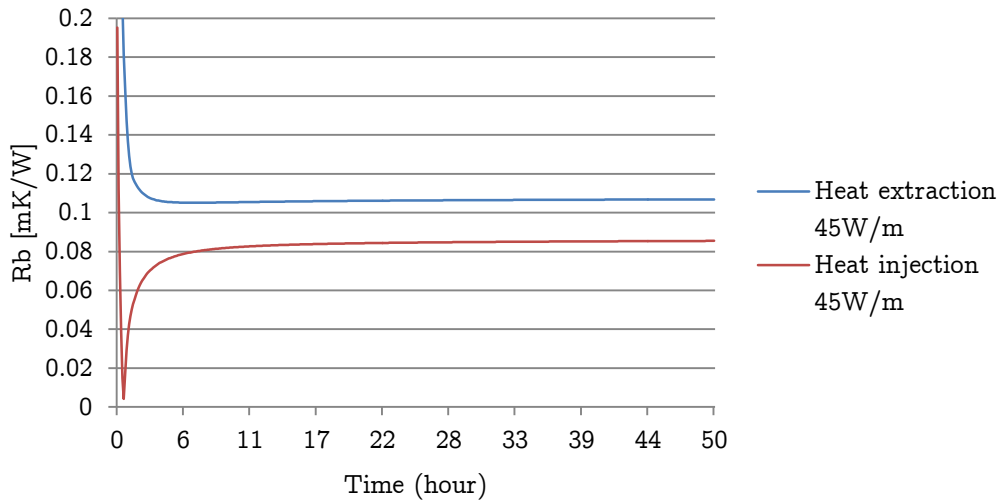
Figure 5-8 Heat injection and extraction borehole resistance dependence

The difference in borehole resistance is due to more effective heat transfer of the groundwater because the natural convection effects are bigger for higher temperatures. The difference in borehole resistance between heat injection and extraction is dependent on the magnitude of the injected and extracted heat effect as shown in Figure 5-8. Greater heat injection and extraction rates results in larger borehole resistance difference between heat injected and extracted because the temperature difference of the groundwater surrounding the collector pipes is higher for larger magnitudes of heat extraction and injection. This results in more effective heat transfer due to increased natural convection effects at higher temperatures.

5.7.4   Borehole diameter dependence
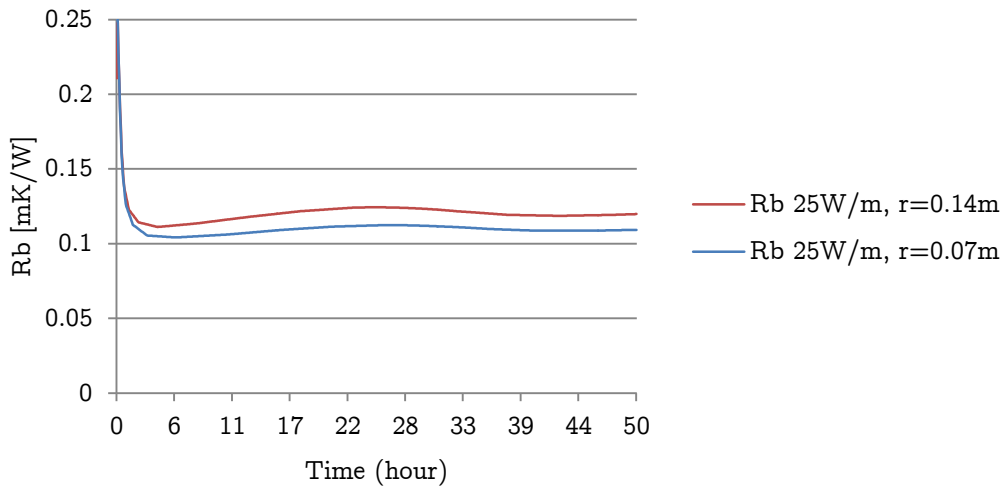
Figure 5-9 Borehole diameter influence on borehole resistance

The borehole at Skoger elementary school was drilled with a radius of 0.07 meter. Figure 5-9 shows that the borehole resistance is dependent of the borehole radius, and a smaller radius results in smaller borehole resistance. The borehole resistance influence on the $T_{f,mean}$ is discussed in chapter 6.4.2.1.

5.7.5 Ground thermal conductivity dependence
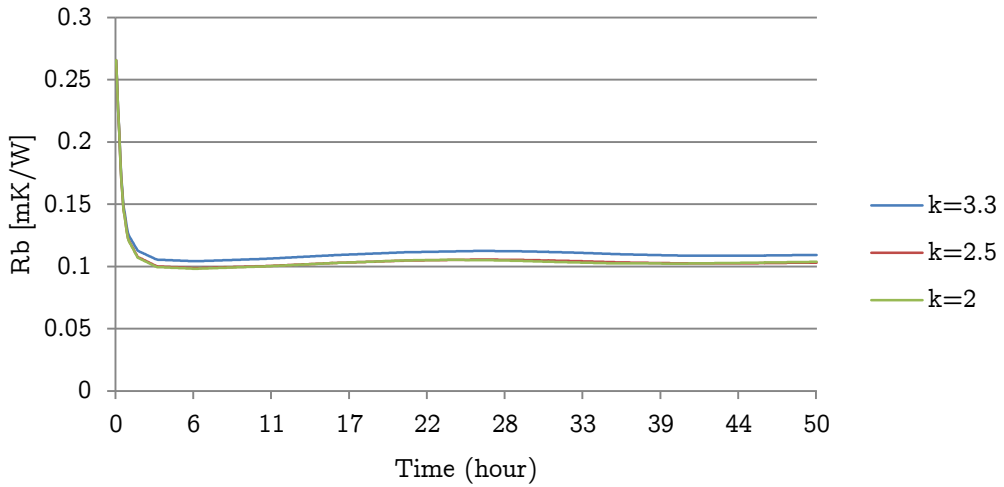
Figure 5-10 Borehole resistance and ground thermal conductivity for 25 W/m

For a constant heat extraction of 25 W/m the borehole resistance is dependent on the ground thermal conductivity, shown in Figure 5-10. This is because the ground has a larger thermal ground resistance with lower conductivity, and the borehole wall temperature used to calculate the borehole resistance will therefore be lower for lower ground thermal conductivities and results in lower borehole resistance for this case.

5.7.6 Ground temperature gradient dependence
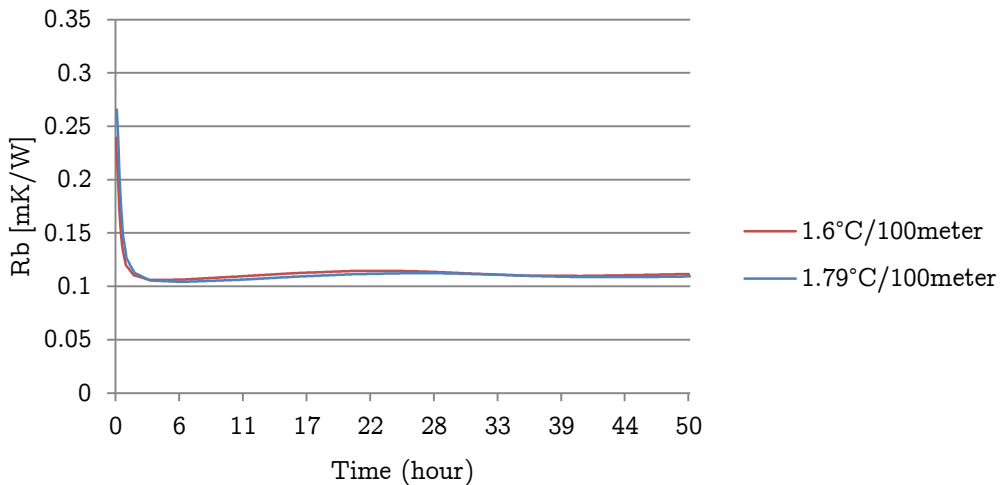
Figure 5-11 Borehole resistance for 25 W/m and different ground temperature gradient

The borehole resistance shown in Figure 5-11 is almost unaffected when lowering the temperature at the bottom at the borehole by 2°C, this is because the temperature decrease has a minimal influence on the average borehole wall temperature used to calculate the borehole resistance.

5.7.7 Mass flow effects

Table 22 Ethylene glycol -water solution flow

Condition	$\dot{V}$ [m³/s]	$\dot{m}$ [kg/m³]	V [liter/s]	v [m/s]
1	0.0008	0.84	0.8	0.263
2	0.0018	1.94	1.8	0.6
3	0.003	3.2	3	1

The convection heat transfer coefficient for turbulent pipe fluid flow is given from Incropera and DeWitt (2002) by equation (5-5).

$$h = \frac{0.023\ \text{Re}^{4/5}\text{Pr}^{n}\kappa}{D} \qquad (5\text{-}5)$$

Where n=0.4 for heating and 0.3 for cooling and D is the diameter of the pipe

$$\text{Re} = \frac{4\dot{m}}{\pi D \mu} \qquad (5\text{-}6)$$

Table 23 Ethylene glycol –water solution at 5°C for heating

Condition	1	2	3
Velocity[m/s]	0.263	0.6	1
$\dot{V}$ [m^3/s]	0.0008	0.00185	0.003
$\dot{m}$ [kg/m^3]	0.84	1.93	3.2
Reynolds number	6363	14620	23483
Convection Coefficient, h [W/m^{2}K]	1006	1958	2861

Table 22 shows three different operation conditions. The 3D model is used to compare the temperature profiles along the borehole depth, the collector pipe wall heat transfer rates and the borehole resistance for different mass flow rates with a constant heat extraction of 12500 W, or 25 W/m. The box in the right upper corner in figures in chapter 5.7.8 and 5.7.10 shows the time where the plots are evaluated at in hours. Plots in chapter 5.7.7 are taken directly from Comsol Multiphysics. The lowest velocity evaluated is 0.263 m/s, which is the BHE operating velocity at Skoger elementary school. Since a constant heat injection or extraction rate is used, low velocities results in larger temperature differences between the fluid inlet and outlet temperatures than Comsol Multiphysics are able to solve for because of thermal restraints. 0.263 m/s is therefore the lowest velocity studied in chapter 5.7.8 and 5.7.10.

In chapter 5.7.8 and 5.7.10 a negative wall heat transfer rates means that the fluid inside the collector transfer heat to the ground and positive wall heat transfer means that the ground transfer heat to the fluid inside the collector pipes.

The mass flow effects on the BHE performance is evaluated because this is a parameter that could easily be varied in real GSHP systems.

5.7.8   Heat extraction

Figure 5-12, Figure 5-14 and Figure 5-16 show the fluid temperature profiles along the borehole depth with fluid circulating at the velocities of 0.263 m/s, 0.6 m/s and 1 m/s, respectively. Velocities of the circulating fluid flow have been chosen to represent the full range of possible borehole heat exchanger fluid flow conditions. All of the simulations in this chapter have been done with a constant heat extraction of 12500W, or 25 W/m.

Condition 1
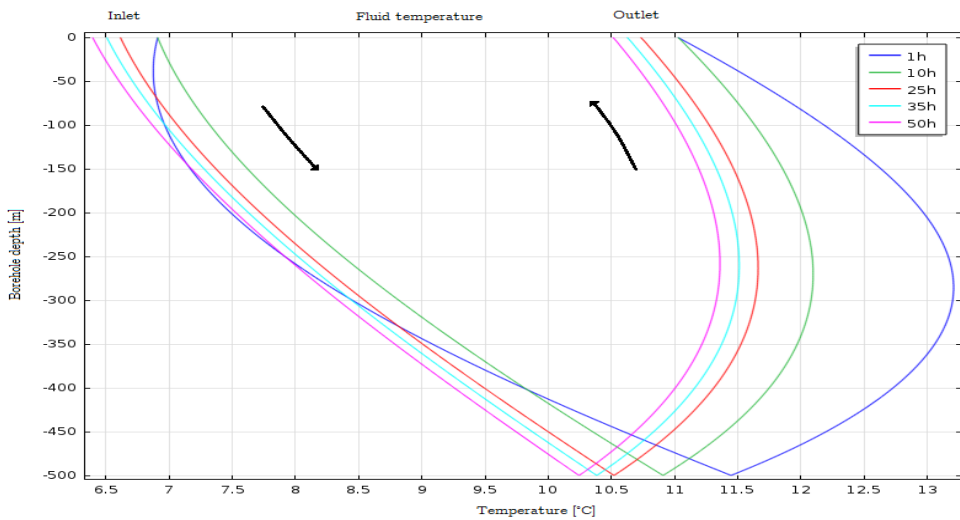
Figure 5-12 Temperature profiles for v=0.263 m/s

Figure 5-12 shows that the temperature profile changes with time. Bigger temperature difference is found for the downward fluid flow, than for the upward fluid flow. This is reflected in the wall heat transfer profile along the borehole depth in Figure 5-13, where the downward fluid flow has higher average wall heat transfer values than the upward fluid flow. At a depth of -250 meter the upward fluid flow reaches its maximum temperature, a decrease in temperature is therefore found at depth from -250 meter to the surface. This temperature decrease is reflected in Figure 5-13 where a negative wall heat rate is shown for the upward fluid flow at depth above -250 meter.
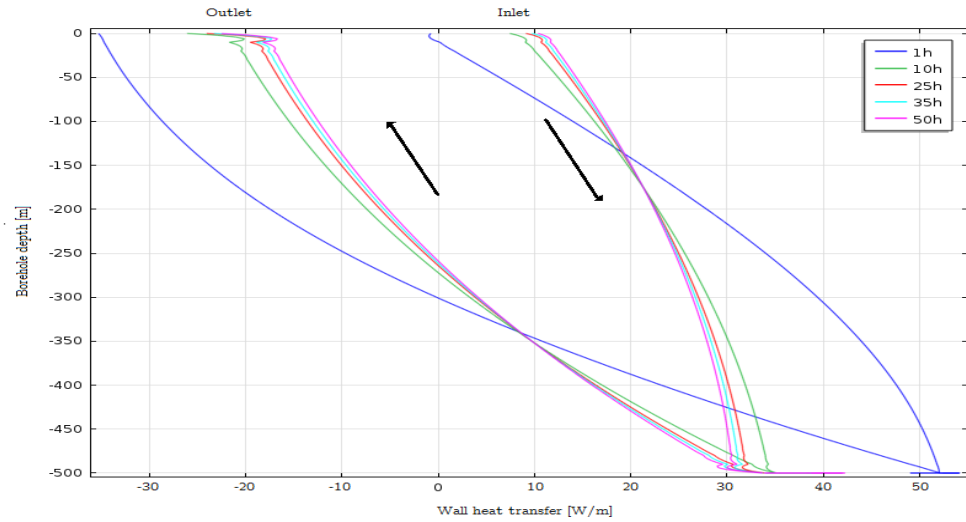
Figure 5-13 Heat transfer rate profiles v=0.263 m/s

Figure 5-13 shows that the wall heat transfer rates changes with borehole depth. An increase of heat transfer rate along the borehole depth, and the largest part of the total heat transfer from the ground is located at depths lower than -250 meter for heat extraction cases. A negative wall heat transfer is observed for the upward fluid flow direction for borehole depth above -250 meter due to thermal short circuiting effects between the upward and downward fluid flow and heat transfer from the fluid to the ground. This reduces the thermal efficiency of the borehole and only 750 meter of the total 1000 meters are used to heat the fluid inside the collectors. The fluid temperature decrease for upward fluid flow above borehole depths at -250 meter shown in Figure 5-12 is reflected in the negative borehole wall heat transfer for upward fluid flow above -250 meter in Figure 5-13.

Condition 2
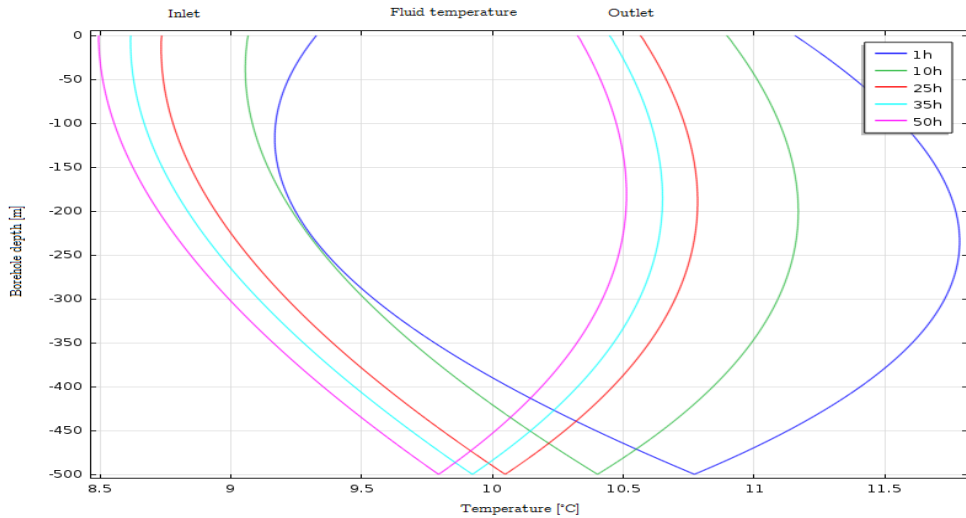
Figure 5-14 Temperature profiles for v=0.6 m/s

Figure 5-14 shows that for higher velocities a smaller temperature difference for the upward fluid flow from -250 meter and the surface is found, than for lower velocities shown in Figure 5-12. A more even temperature difference between the downward and upward fluid flow is observed in Figure 5-14 than for Figure 5-12, due to reduced thermal short-circuiting between the upward and downward fluid flow. A more similar wall heat transfer between the upward and downward fluid flow will therefore enhance the thermal efficiency of the BHE.
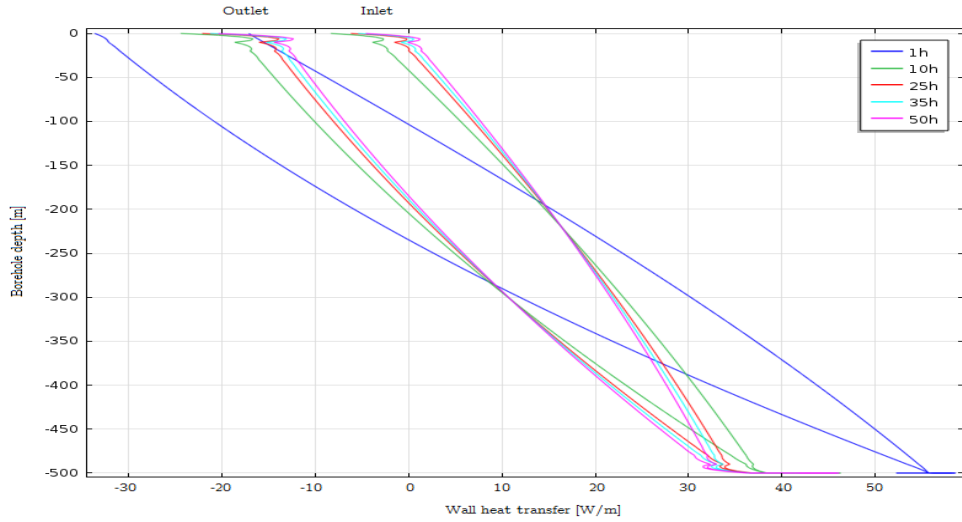
Figure 5-15 Heat transfer rate profiles v=0.6 m/s

A smaller negative wall heat transfer for the upward fluid flow is shown in Figure 5-15 with fluid velocities of 0.6 m/s than for fluid velocities of 0.263 m/s shown in Figure 5-13. This means that the thermal short circuit and the heat transport from the fluid inside the collector to the ground is reduced due to smaller temperature differences between the downward and upward fluid flow. This results in a more effective BHE.

Condition 3
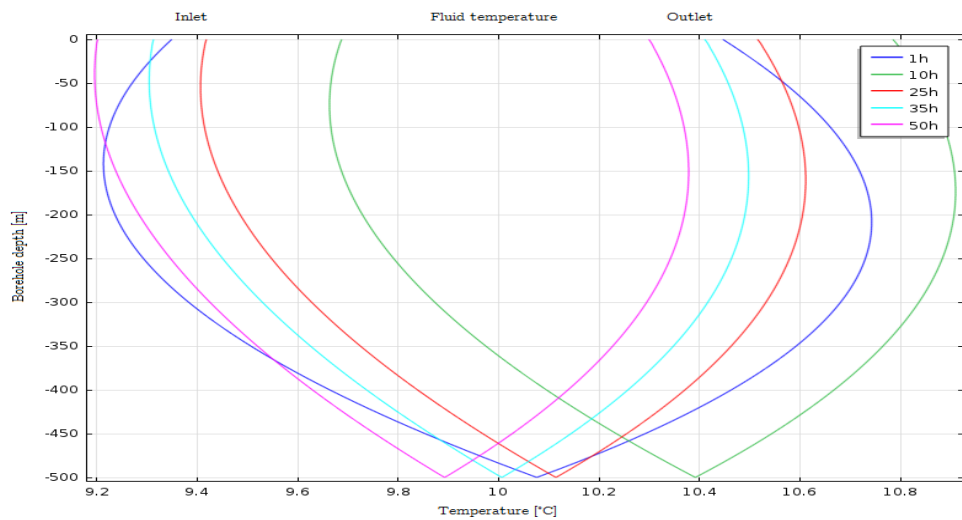
Figure 5-16 Temperature profiles for v=1 m/s

Temperature profiles in Figure 5-16 are more linear than temperature profiles in Figure 5-14. Further increase in velocity will therefore reduce the thermal short circuiting between the upward and downward fluid flow and the heat transport from the fluid inside the collector to the ground. A linear temperature profile will therefore increase the performance of the BHE.
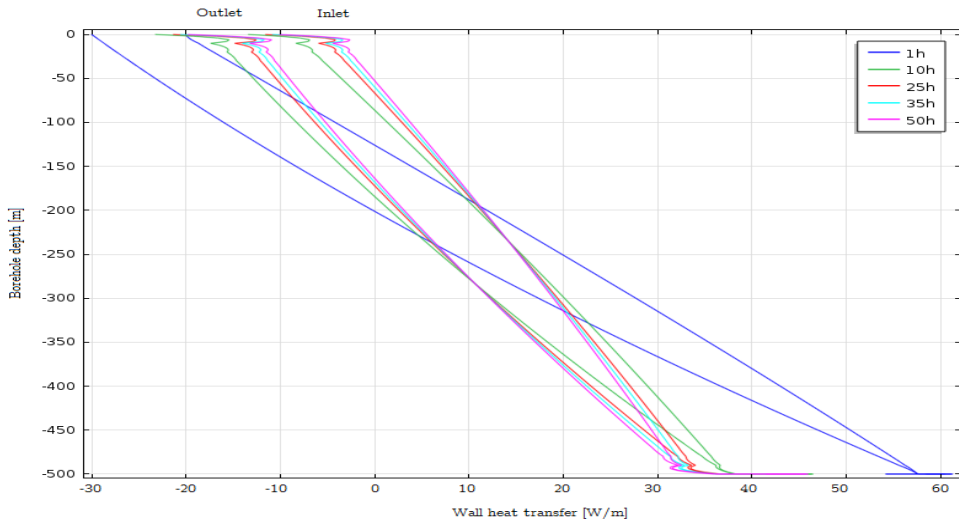
Figure 5-17 Heat transfer rate profiles v=1 m/s

A linear wall heat transfer distribution for upward and downward fluid flow is shown in Figure 5-17 and reflects the linear temperature profiles for both upward and downward fluid flow shown in Figure 5-16.

The fluid temperature profiles differ for fluid circulating at different velocities. For high fluid velocities the temperature distribution is more linear than the temperature profiles for low velocities. Higher fluid velocities will results in higher thermal efficiency of the BHE because of smaller short-circuiting effects between the upward and the downward flowing fluid. A negative wall heat transfer reduces the active length of the BHE where heat is transferred from the ground to the fluid. This influences the BHE performance in a negative manner, and an optimized BHE should have an active BHE length equal to the length of the collector.

The thermal short circuiting between the upward and downward fluid flow is expected to be larger for deeper boreholes, since the temperature difference between the adjacent pipes inside the borehole is higher than shorter boreholes. High fluid velocities is shown to reduce the short circuiting effects between upward and downward fluid flows because

of smaller temperature difference between the adjacent pipes inside the borehole, and further studies should be done to optimize deep BHEs with respect to the fluid circulating velocities and the depth of the BHE.

The convection heat transfer of the circulating fluid is also increased with higher fluid velocities, but the internal thermal resistance of the collector is already low because of a turbulent flow pattern even for low fluid velocities. The thermal effect of increased convection heat transfer is therefore rather small compared to the effects of a more linear temperature profile along the borehole depth.

Higher velocity results in a more linear temperature profile and a higher convective heat transfer of the circulating fluid, and smaller temperature differences of the in-and outgoing fluid temperatures for a certain amount of extracted heat.

5.7.8.1   Stagnant groundwater case, excluding thermal effects of natural convection

Condition 1
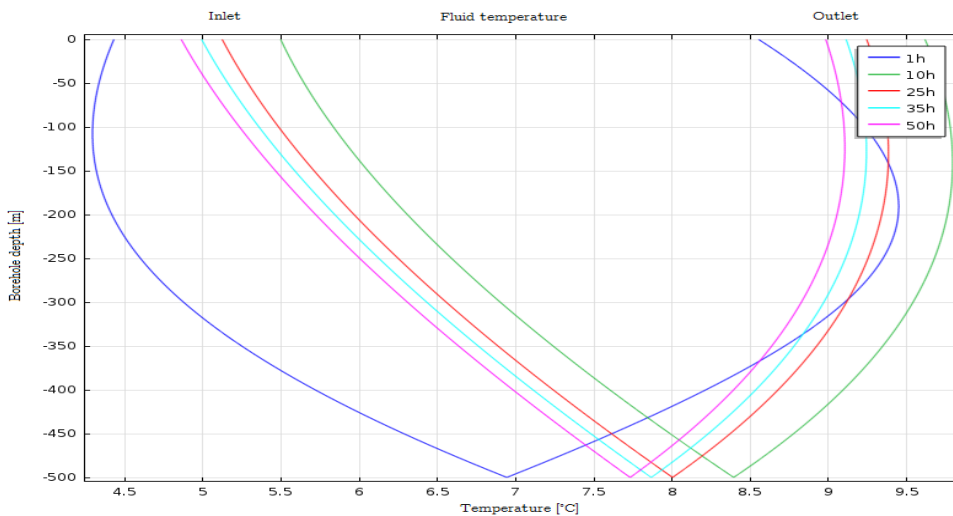
Figure 5-18 Temperature profiles for v=0.263 m/s without natural convection heat transfer effects

Figure 5-18 shows the temperature profile where the natural convective heat transfer effects are excluded. This will in practice reduce the thermal conductivity of the groundwater surrounding the collectors. This will lead to a reduction of the thermal short-

circuiting effect due to larger thermal resistance of the groundwater between the collector pipes. The outlet and inlet temperatures are lower for the stagnant groundwater case than for the case including natural convection effects. By excluding the heat transfer effects from convective flow induced by density difference of water in BHE simulation models for groundwater filled BHEs, the temperature response will differ and the output of the model will not represent the real temperature response of the BHE in an adequate way. After 50 hours the outlet temperature is 1.5°C lower for the stagnant water case than for the model including natural convection effects. A simulation model excluding the natural convection effect implemented into building energy simulation software for groundwater filled boreholes, will therefore not give a precise output to the building energy software. This may lead to a less efficient system and higher building energy consumption. It is therefore important for BHE simulation programs used for evaluation of groundwater filled BHEs, to include the thermal effects of density change in the groundwater to calculate a correct short time thermal response of the BHE.
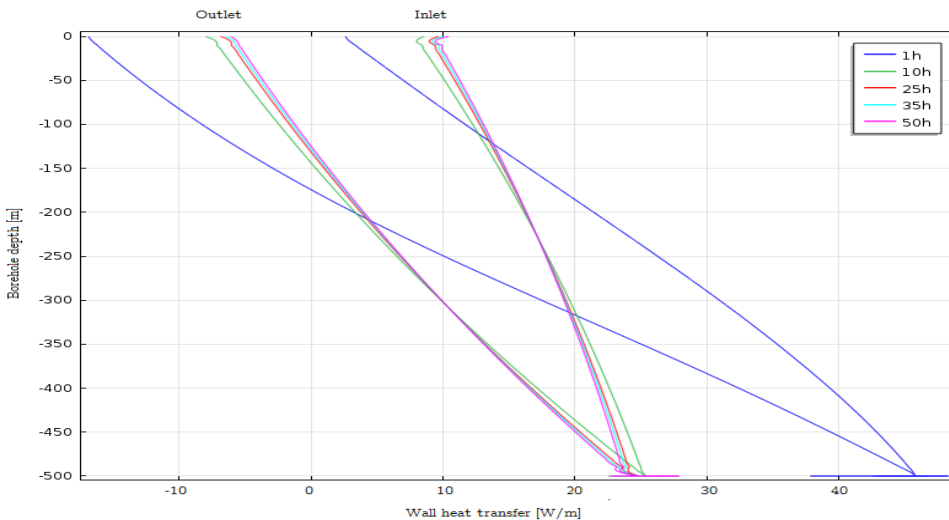
Figure 5-19 Heat transfer rate profiles v=0.263 m/s without natural convection heat transfer effects

Figure 5-18 shows that the temperature response for the case excluding the thermal effects of natural convection, differs from the case include this effect

A lower borehole resistance results in a lower outlet temperature for constant inlet temperature, which reduces the thermal performance of the GSHP system. To get a precise output from models implied into building energy simulation software, the BHE model should account for the thermal mass of the filling, the collector pipe and the circulating fluid, together with heat transfer effects of natural convection of the groundwater.

5.7.9   Mass flow rate influence on borehole resistance
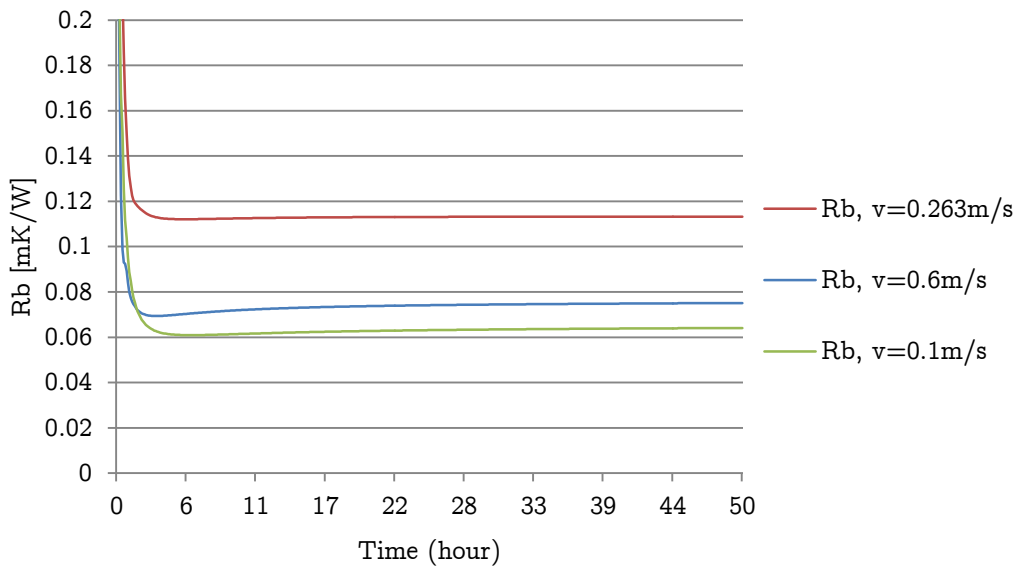
Figure 5-20 Borehole resistance for different mass flow rates

A marked drop in borehole resistance for fluid velocities from 0.263 m/s to 1 m/s is caused by a steeper temperature profile along the borehole depth and higher convective heat transfer inside the collectors for higher fluid velocities. This is because the fluid temperature difference between the in-and outlet for a given amount of energy extracted is lower for higher velocities. A reduction in the borehole resistance with higher fluid velocities is caused by higher average temperature between the downward and upward fluid flow and higher convective heat transfer inside the collector for a constant heat extraction of 12500 W (25 W/m) for 50 hours.

A more linear temperature profile results in a larger thermal effect because of a larger temperature difference between the fluid inside the collectors and the borehole wall and reduced thermal borehole resistance.

Higher fluid velocities results in more effective heat transfer from the ground to the fluid, and it reduces the short circuiting because the temperature differences between the adjacent pipes inside the borehole is smaller. The drawback with higher fluid velocities is higher pumping power requirements.

An increase in fluid velocity is favorable from a thermodynamic point of view, and by increasing the velocity from 0.263 m/s to 0.6 m/s and from 0.263 m/s to 1m/s a decrease in borehole resistance of 32% and 43%, respectively, and an increased BHE performance can be achieved. The restrictions for increasing the fluid velocity are the capacity of the heat exchanger inside the heat pump and the pumping power increase.

5.7.10 Heat injection

A solution was only possible to achieve for the 3D model for velocities of 0.263 m/s, 0.6 m/s and 1 m/s for a constant heat injection of 22500 W (45 W/m). This effect is therefore used for evaluation of borehole resistance with heat injection.

Figure 5-21, Figure 5-23 and Figure 5-25 show the fluid temperature profiles along the borehole depth for 45 W/m heat injection with fluid circulating at the velocities of 0.263 m/s, 0.6 m/s and 1 m/s, respectively.

The initial temperature of the fluid results in lower temperature profile and wall heat transfer evaluated at 1 and 10 hours.

Condition 1
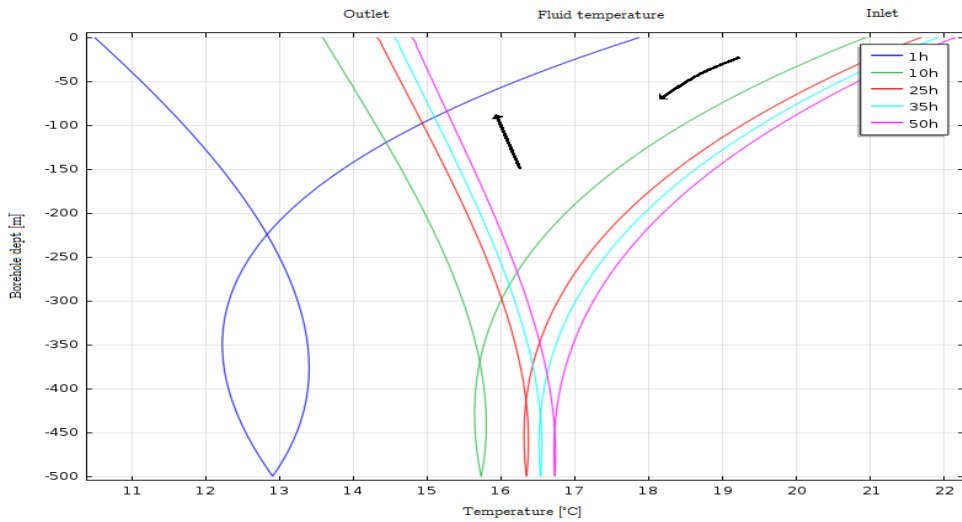
Figure 5-21 Temperature profiles for v=0.263 m/s

For heat injection at fluid velocity of 0.263 m/s Figure 5-21 shows that the temperature of the downward fluid flow has a larger temperature difference between the surface and bottom of the BHE than the upward fluid flow. Unlike the temperature profiles for heat extraction, the steepest temperature profile is found at the top of the borehole. This is because the largest temperature difference between the fluid and the ground is located near the surface. At depth lower than approximately -425 meter the temperature remains constant, and from Figure 5-22 the heat rate is almost zero at depth lower than -400 meter. A thermal short circuit effect between the upward and downward is responsible for the constant temperature profile from -425 meter to -500 meter. An active borehole length can be used to evaluate the effects of fluid velocity change. The active borehole length is the total length of the collector pipes where heat is extracted from the ground to the fluid inside the collectors for BHE heat extraction operation, and heat is extracted from the fluid inside the collector pipes to the ground for BHE heat injection operation.

A heat transfer from the fluid to the ground occurs only for the first 425 meters for velocities at 0.26 m/s and 50 hours, resulting in a reduced active borehole length of $2 \cdot 500$ meter $- 2 \cdot 425$ meter $= 150$ meter. The active borehole length should be considered in the design process for buildings with high cooling demand.
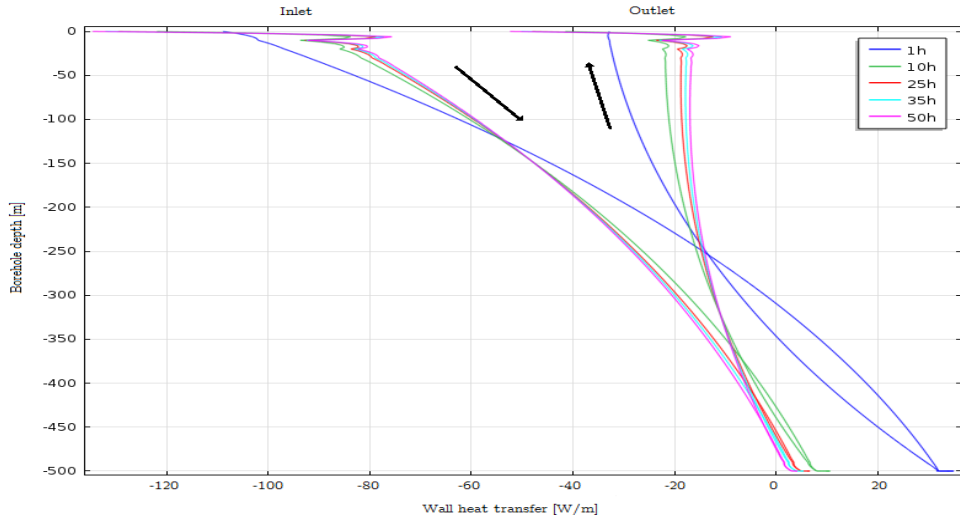
Figure 5-22 Heat transfer rate profiles v=0.263 m/s

Figure 5-22 shows that the downward fluid flow injects more heat to the ground than the upward fluid flow. This is because the upward fluid flow has a lower temperature than the downward fluid flow, which results in smaller temperature driving forces for the heat transfer. The wall heat transfer for the downward and upward are almost zero near the bottom of the borehole, and the largest wall heat transfer for both downward and upward fluid flow will be located near the surface due to larger temperature gradients between the fluid and the ground.

Condition 2
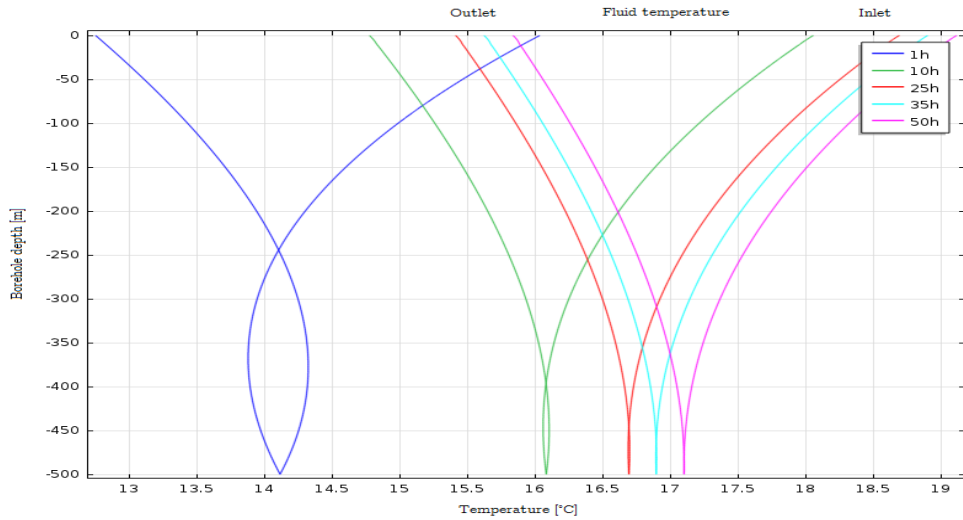
Figure 5-23 Temperature profiles for v=0.6 m/s

Comparing Figure 5-21 to Figure 5-23, a more even temperature profile for fluid velocity is shown for 0.6 m/s than for 0.263 m/s between the downward and upward fluid flow. The active borehole length is increased compared to the active borehole length for fluid velocity equal to 0.263 m/s, due to reduced thermal short circuiting effect. Increasing the active borehole length results in higher thermal efficiency and higher outlet temperatures for a given inlet temperature. The temperature between the downward and upward fluid flow is constant at borehole depth below -450 meter, and an active borehole length of approximately 50 meter is therefore gained by increasing the fluid velocity from 0.263 m/s to 0.6 m/s.
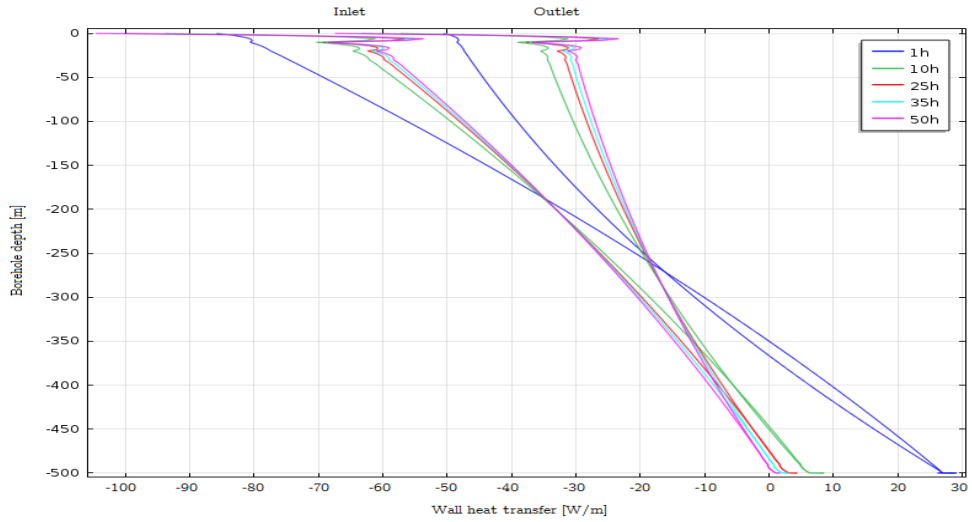
Figure 5-24 Heat transfer rate profiles v=0.6 m/s

Figure 5-22 shows that the wall heat transfer is more even for the downward and upward fluid flow for fluid velocities of 0.6 m/s than for 0.263 m/s. This is because the upward fluid flow temperature is higher for a velocity equal to 0.6 m/s than for 0.263 m/s.

Condition 3
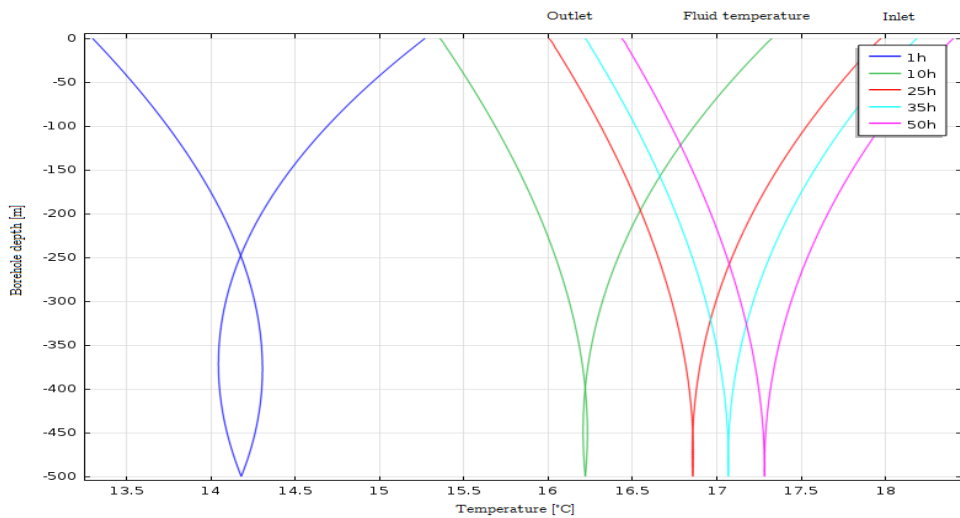
Figure 5-25 Temperature profiles for v=1 m/s

An even temperature profile for the up-and downward fluid flow is shown for fluid veloci-ties equal to 1 m/s. This results in an almost equal thermal performance of the upward

and the downward fluid flow. The active length is not increased compared to fluid velocities of 0.6 m/s which show that the thermal short-circuiting effect is not further reduced.
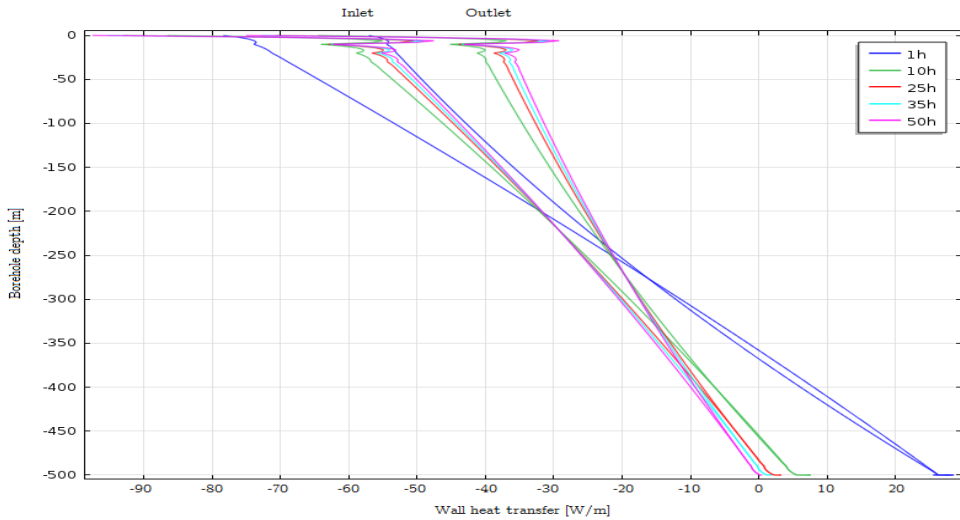
Figure 5-26 Heat transfer rate profiles v=1 m/s

A more even wall heat transfer between the downward and upward fluid flow for velocities of 1 m/s and 0.26 m/s is shown in Figure 5-22 and Figure 5-26, reflecting the similarity of the temperature profiles shown in Figure 5-25.

High inlet temperature is important to be able to extract an average of 45 W/m at low temperatures. To secure high heat injection load for a given inlet temperature, the fluid velocity should be increased. Since the inlet temperature is limited because of the dependence to the medium that is heat exchanged with the ethylene glycol-water solution, high fluid velocities will therefore secure a high heat transfer rate from the fluid to the ground. Increasing the fluid velocity from 0.263 m/s to 0.6 m/s will increase the thermal efficiency for heat injection operation of a 500 meter deep BHE.

5.7.11 Mass flow rate influence on borehole resistance
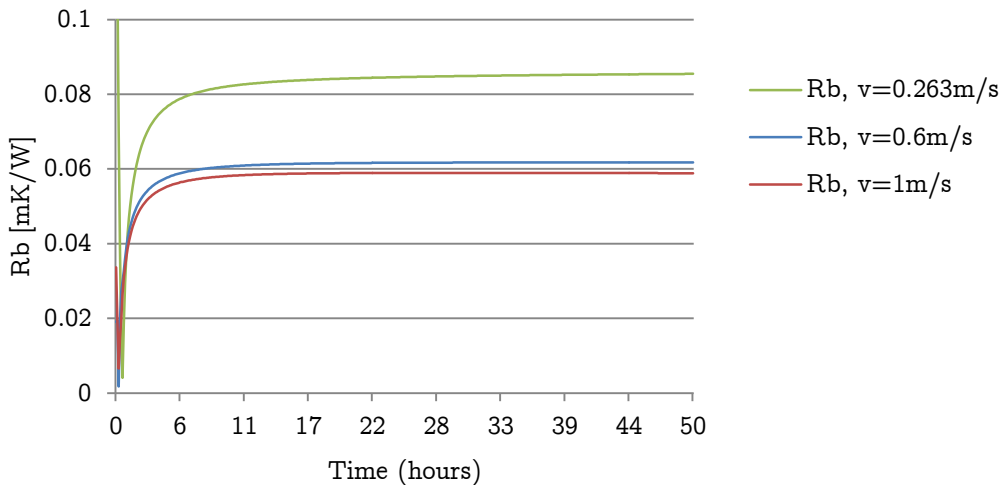
Figure 5-27 Borehole resistance for different mass flow rates

A for the energy extraction case, the borehole resistance is reduced significantly with increased fluid velocity. A larger amount of heat can therefore be extracted for lower inlet temperatures, as shown in Figure 5-28. Heat injected to the borehole during the summer will therefore have a higher thermal efficiency, and the ground will be able to absorb more energy at lower inlet temperatures.

A small borehole resistance difference for a fluid circulating with a velocity of 0.6 m/s and 1 m/s is shown in Figure 5-27. The difference is caused by increased convective heat transfer inside the collector, and will not have a large influence on the long term BHE performance.
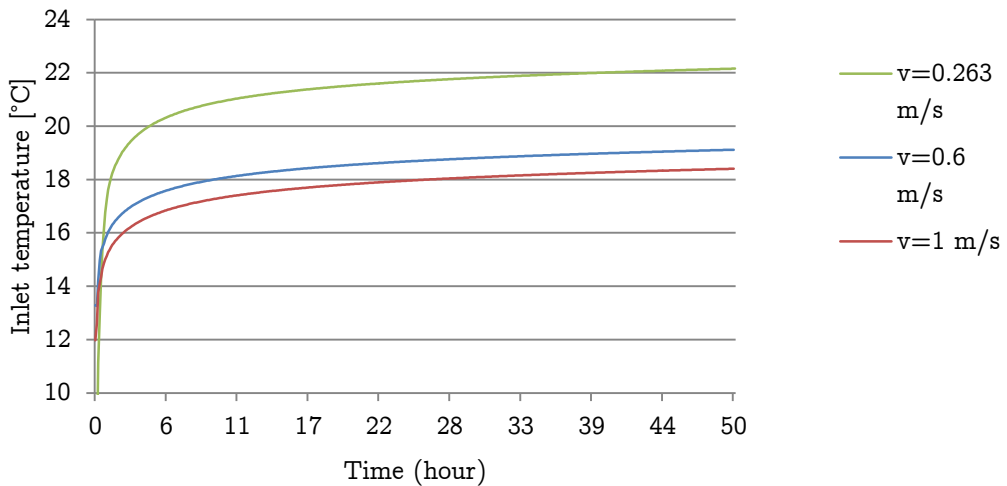
Figure 5-28 BHE inlet temperature for injection of 45W/m

Figure 5-28 shows the BHE inlet temperature for a constant heat injection of 22500 W (45W/m) for a period of 50 hours with varying fluid velocity.

5.7.11.1   Increased velocities and influence on pressure drop

Table 24 Velocity and pressure drop

Velocity [m/s]	$\dot{V}$ [m³/s]	Pressure drop [Pa]	Required power [W]
0.263	0.0008	$3.49 \cdot 10^4$	27.9
0.6	0.00185	$1.42 \cdot 10^5$	262.7
1	0.003	$3.42 \cdot 10^5$	1039

Table 24 shows the pressure drop, calculated from Comsol Multiphysics, and the power delivered to the fluid calculated from equation (5-7) and (5-9) given from White (2008).

$$P_{EG} = \rho \cdot g \cdot \dot{V} \cdot H \qquad (5\text{-}7)$$

Where H is the net H is the pump head supplied minus the pump head losses.

$$H = \frac{\Delta p}{\rho \cdot g} \qquad (5\text{-}8)$$

Since the pressure drop was calculated with Comsol Multiphysics, the power required to drive the pump assuming an efficiency of 1 is given in equation (5-9).

$$P_{EG} = \dot{V} \cdot \Delta p \qquad (5\text{-}9)$$

By increasing the fluid velocity a higher thermal performance of the BHE is achieved, but at a cost of higher pumping power. The pumping power increases exponentially with the velocity increase, and an optimization between thermal performance and pumping power cost is therefore necessary to make, especially for deeper boreholes than 500 meter because of little experience with the thermal performance of deep BHE.

The borehole resistance is significantly reduced when the fluid velocity is increased from 0.263 m/s to 0.6 m/s, for both extraction and injection of energy from and to the energy wells. The pumping power increase is approximately 10 times higher for fluid velocity increase from 0.263 m/s to 0.6 m/s, and about 40 times for a velocity increase from 0.263 m/s to 1m/s. The pumping power cost increases with the same ratio, but the increased cost is relatively small compared to power input to the heat pump.

Because of the restrictions of the 3D model, a long term performance of fluid velocity influence on the long term performance of the BHE could not be performed.

5.8   3D model discussion

A numerical model was developed in Comsol Multiphysics. Due to computer capacity restraints a model consisting of only one borehole including fluid flow was made. The model was therefore used to study the borehole resistance and the effects of changing the fluid velocity. The borehole resistance calculated in the 3D model was implemented in a 2D model also developed using Comsol Multiphysics. A constant effect was extracted or injected from the ground to study the thermal response of a 3-dimensional BHE. Ground data was collected from the Geological Survey of Norway and Norwegian Meteorological Institute, and implemented in the model.

In Norway BHEs are most cases groundwater filled BHEs. The heat transfer from the ground to the fluid inside the collector pipe is therefore dependent on the heat transfer coefficient of the groundwater. The thermal effects of natural convection are temperature dependent and improves the heat transfer compared to the stagnant water case, and should therefore be accounted for in models used for design of groundwater filled BHE. The 3D model developed in Comsol Multiphysics implements a natural convection heat transfer relation through an effective thermal conductivity developed for an annular geometry.

A borehole resistance reduction of 35% between the model with and without heat transfer effects of natural convection is shown. This emphasizes the importance of including the natural convection heat transfer effect in models used for BHE design purposes.

Through the winter heat is extracted from the ground and works as a heat source for the heat pump, and in the summer the ground is recharges by excess energy from heating batteries. The borehole resistance is dependent on whether heat is extracted or injected to the ground, because the temperature differences between the ground and the fluid inside the collector pipes influences the thermal effects of the natural convection. Higher temperatures results in better heat transfer due to increased natural convection effects.

Simulation done with the 3D model shows that the average thermal borehole resistance changes is small for moderate reduction of ground temperature gradient and for constant heat extraction a low ground thermal conductivity results in lower borehole resistance.

Large reduction in borehole resistance is found with fluid velocity increase. This improves the thermal performance of the BHE, but increases the pumping power demand. A reduction of the borehole resistance of 33% and 30% is found for an increase of the fluid velocity from 0.263 m/s to 0.6 m/s for heat extraction of 12500 W and heat injection of 22500 W, respectively. Both heat injection and extraction case increased the active length of the borehole when the velocity was increased. Together with a reduction in borehole resistance the increase of the active length of the borehole will lead to a significant increase in the BHE efficiency can be achieved by increasing the fluid velocity.

Since the efficiency of the heat pump installed in the GSHP system at Skoger elementary school is very sensitive to evaporation temperature, an increase of the fluid velocity may therefore improve the BHE efficiency and increase the heat pump inlet temperature. This will increase the COP and reduce the heat pump power input. By reducing the heat

pump power input more than the increase of pumping power input, a more effective system will be achieved.

It is impossible to make a cost analysis of the GSHP installed at Skoger for different fluid velocities, because of lack in recorded operation data from the BHEs installed at Skoger. A test period where the BHE and the heat pump performance for a velocity of 0.263 m/s and 0.6 m/s were analyzed could be an interesting proposal for further work. The following data should be logged for the test:

1. Heat pump power input and output
2. Inlet and outlet temperatures from the energy wells
3. Power input for circulating the ethylene glycol –water solution
4. Mass flow rate of ethylene glycol -water solution
5. In and outgoing temperatures from the heat recovery batteries

This will prove enough information to optimize the velocity of the ethylene glycol –water solution for the GSHP system installed at Skoger elementary school.

The borehole resistance is calculated with the 3D model that is developed using least possible assumptions compared to the system at Skoger elementary school. Because the ground conditions at Skoger are difficult to predict without doing a TRT, and the borehole resistance varies with heat extraction and injection rates, the borehole resistance found in the 3D model for a heat extraction rate of 25 W/m and heat injection rate of 45W/m are used in the 2D model to simulate the long term performance of the BHE system installed at Skoger elementary school.

6   2D-Model

The model is built with an ellipse representing the ground with a=120 meter and b=80 meter shown in Figure 6-1. This gives a sufficient large domain to keep the temperatures at the outer boundary undisturbed.
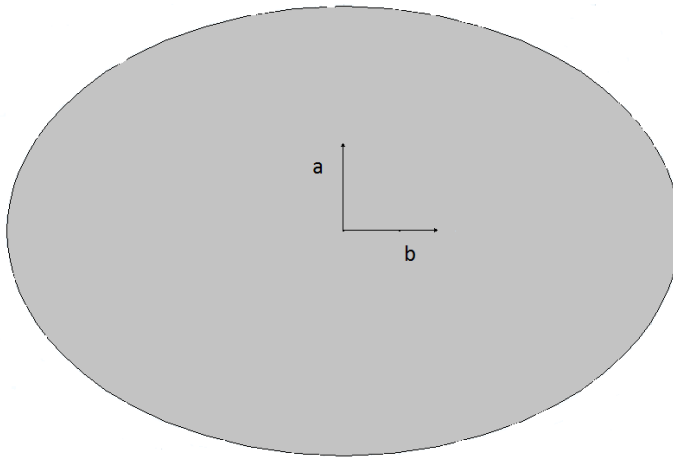
Figure 6-1 Elliptic domain representing the ground surrounding the boreholes

6.1   2D resistance model

The 2D resistance model represents the $T_{f,mean}$ by a given borehole resistance, a heat rate at the borehole wall for a borehole radius equal to 0.07 meter and a borehole wall temperature. A borehole resistance is calculated from the 3D model in chapter 5.7. In this way an average borehole resistance for a 3D model can be implemented in a 2D model to evaluate the $T_{f,mean}$ over several decades, which has a direct influence of the performance of the heat pump.

The boreholes are designed with a heat flux at the borehole wall for a radius equal to 0.07 meter shown in Figure 6-2.

6.1.1   Model simplifications

A two dimensional model is not able to consider the variation in fluid temperature with borehole depth, and an average borehole resistance from the 3D model is therefore used in the 2D model to calculate the $T_{f,mean}$.

6. 2D-MODEL

The 2D model is based on average values of the ground temperature distribution and the thermal ground conductivity found in chapter 3.4 and 3.5.
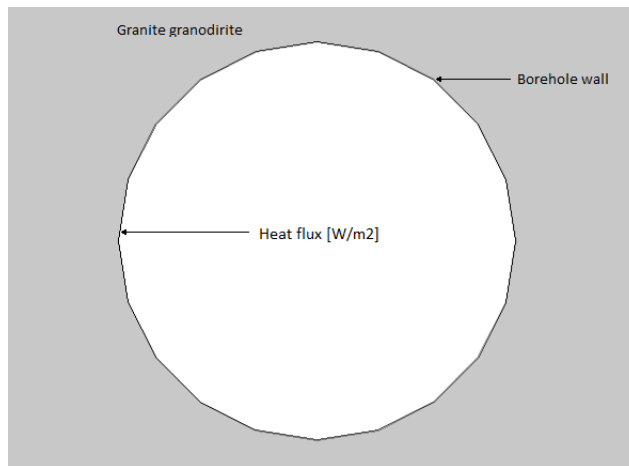
Figure 6-2 Model of the resistance model

6.1.2   Boundary Conditions

Table 25 Constant values 2D model

Model Description	Value	Units
Borehole		
Borehole wall radius	0.07	m
Distance between boreholes	20	m

Table 26 2D input data

Description	Input variable	Units
2D resistance model		
Boundary condition		
Borehole		
Initial value	init_temp	°C
Heat rate at the outer boundary	heat_flux	[W/m^2]
Ground		
Initial value	init_temp	°C
Undisturbed temperature	T_undisturbed	°C
Thermal conductivity	k_ground	[W/mK]

6.2   Mesh

Two dimensional mesh for the BHE was generated using Comsol's automatic mesh function. A 2D mesh was generated with a fine mesh around the pipes and coarser mesh at the outer simulation domain. In this way more cells can be included in places where greater temperature gradients are expected and less cells far away from the borehole, where the temperature gradient is expected to be smaller.
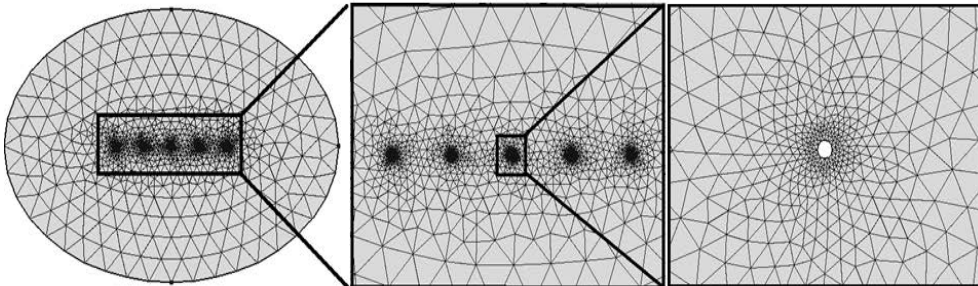
Figure 6-3 2D model mesh

The 2D mesh is developed with a Free Triangular generator with custom element size parameters at the borehole wall, shown in Figure 6-3. The custom input of parameters makes sure that the maximum and minimum element sizes are small enough to be able to solve for. The properties of the mesh are shown in Table 27.

Table 27 2D model mesh description, point

Model Mesh Description	Value
Element size	
Geometric entity level: Point	
General physics	
Maximum element size	0.05m
Minimum element size	0.04m
Maximum element growth rate	1.1
Resolution of curvature	0.2
Resolution of narrow regions	1

Complete mesh consists of 6010 domain elements and 100 boundary elements.

6.3   Simulation result 2D model

The 2D resistance model was used to evaluate $T_{f,mean}$. The main purpose was to study the long term performance of the system and thermal interaction between the boreholes and the influence of the $T_{f,mean}$.

6.3.1   Parametric study of the borehole field installed at Skoger elementary school

The 2D model was simulated by extrapolating energy loads for 30 years with energy recharge shown in Figure 6-4 and without recharge energy, shown in Figure 6-5.
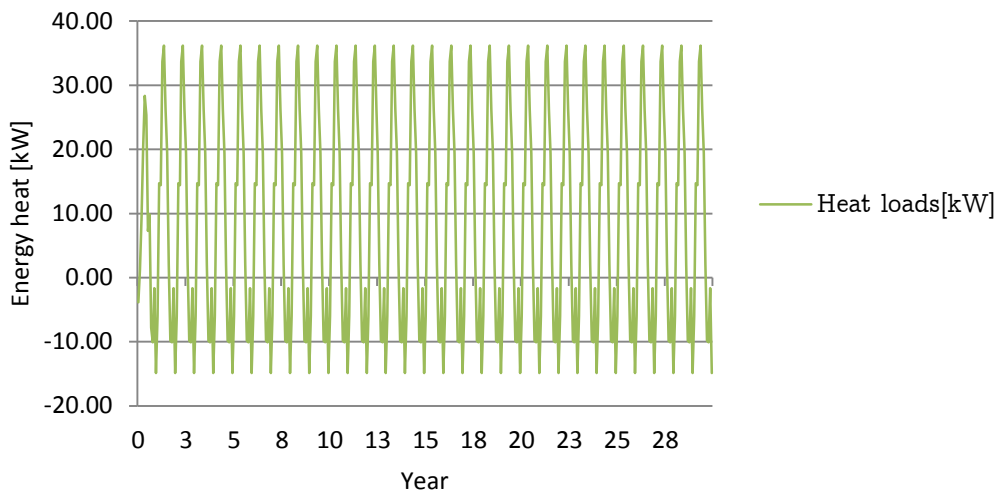
Figure 6-4 Heat effects from energy wells with recharge from heat recovery batteries for extrapolation period of 30 years
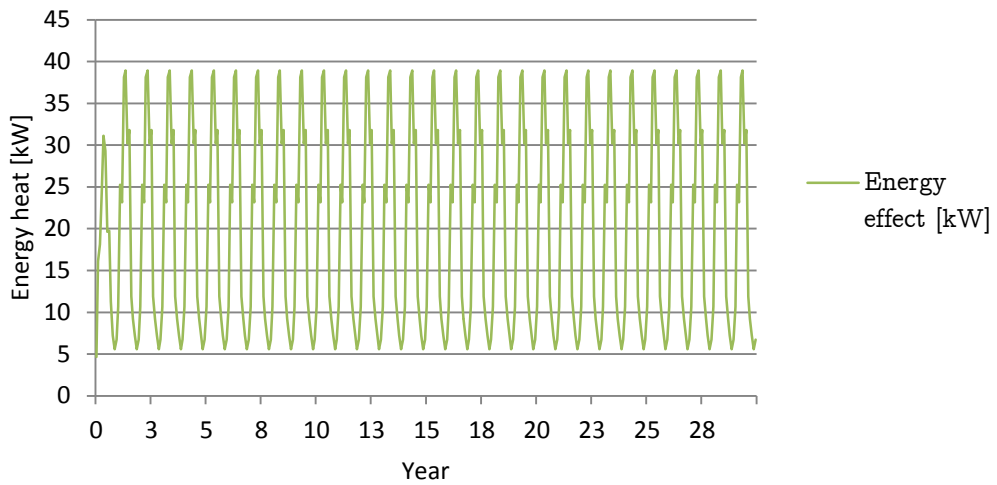
Figure 6-5 Heat effects from energy wells without recharge from heat recovery batteries for extrapolation period of 30 years

The heat extracted and injected to the wells are based on the COP described in chapter 3.3.1 and is used in the simulations done in this chapter.

Table 28 COP1

Average COP, April-October	Average COP, November-March
2.7	2.1

The heat loads are based on monthly values, and do not take the intermitted heat pump operation into account because this effect is assumed to be rather small for long time periods. Ground and borehole initial and boundary conditions are shown in Table 29.

Table 29 2D model input variables

Description	Input variable		Units
2D resistance model			
Boundary condition			
Borehole			
Heat flux at the inner boundary	heat_flux	Function with varying heat flux	[W/m^2]
Ground			
Initial value	init_temp	12.5	°C
Undisturbed temperature	T_undisturbed	12.5	°C
Thermal conductivity	k_ground	3.3	[W/mK]
Thermal borehole resistance, extraction		0.11	[mK/W]
Thermal borehole resistance, injection		0.09	[mK/W]

An initial and undisturbed value for the ground of 12.5°C is used because this temperature represents the average ground temperature between the surface and the bottom of the BHE.

Since the borehole resistance depends on whether heat is extracted or injected from the energy wells, two different boreholes resistances was used for the summer and winter month when $T_{f,mean}$ was calculated from the 2D model. A borehole resistance of 0.11 mK/W is used from October to April and 0.09 mK/W is used in the 2D model from May to September. The borehole resistance was calculated from the 3D model with borehole resistance evaluated for a heat extraction of 25 W/m and a heat injection rate of 45 W/m.

$T_{f,mean}$ and minimum $T_{f,mean}$ are plotted in Figure 6-6
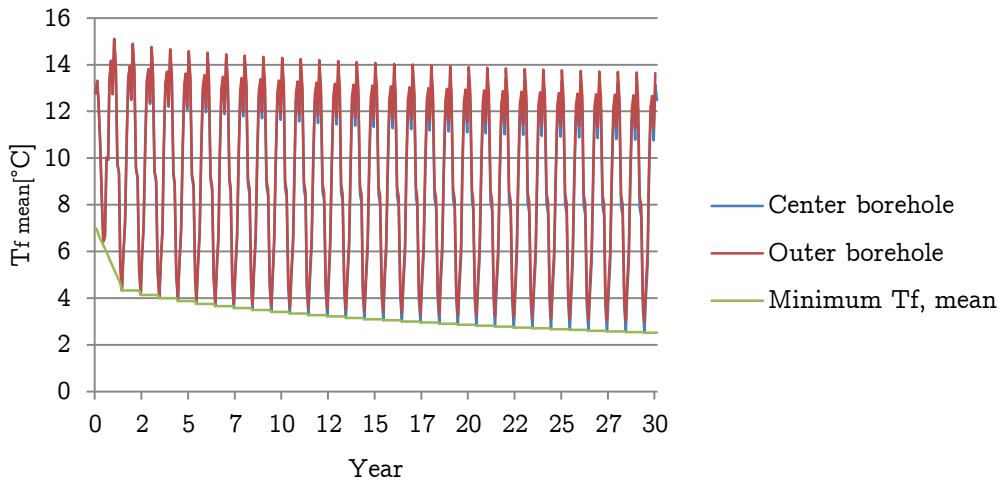
Figure 6-6 Heat injection and extraction with 5 boreholes

Figure 6-6 shows that for operational time of 30 years the borehole in middle and the borehole with only one neighboring borehole has almost the same $T_{f,mean}$, meaning that the thermal interaction between the boreholes are minimal. This is because the average heat load demand at Skoger elementary school is quite small and the distance between the boreholes is sufficient to keep the boreholes thermally independent of each other. A slight decrease in $T_{f,mean}$ is observed in Figure 6-6, to stabilize the temperature in the borehole field and the $T_{f,mean}$, a higher heat injection by the recovery batteries is needed. Since $T_{f,mean}$ shown in Figure 6-6 is based on a monthly average value, a smaller $T_{f,mean}$ is likely to presume when the schools energy demand is at its highest for the real case at Skoger. A monthly average peak of 35 kW gives a heat extraction rate of 14 W/m for each borehole. In reality the heat pump operates with intermitted sequences, on and off operation, where the maximum heat pump heating capacity is shown in Figure 3-17. Since the highest heat demand for Skoger elementary school will be highest during the winter months, the maximum heat delivered from the heat pump will most likely occur during these months. Assuming an evaporation temperature and condensation temperature equal to 0°C and 60°C, respectively, maximum heat pump heat capacity is 200 kW, which equals to a heat extraction rate of 38 W/m assuming a COP equal to 2.1.
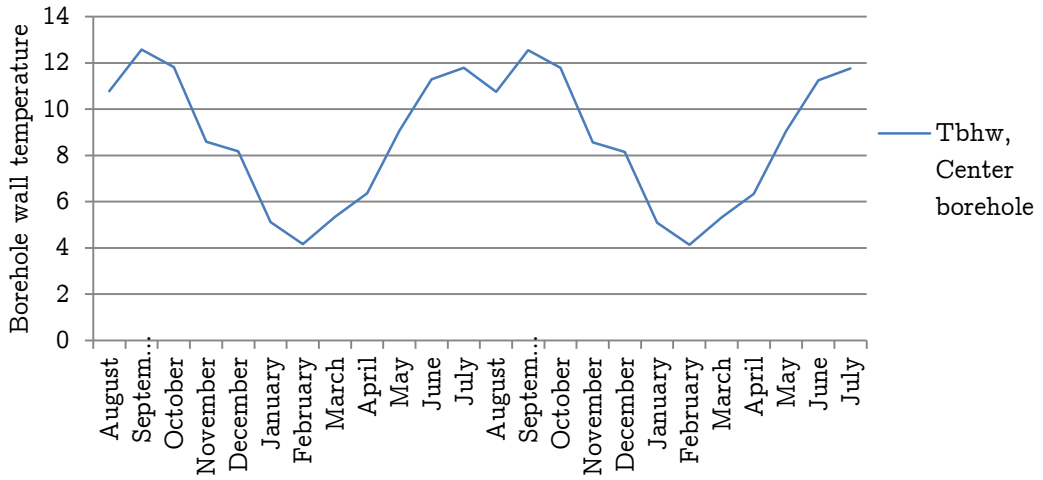
Figure 6-7 Center borehole wall temperature after 28 years of operation for heat injection and extraction with 5 boreholes

Figure 6-7 shows how the borehole temperature varies with the season. The borehole temperature peaks in around the end of September due to high injection rates during the summer. The lowest temperature is found in February where the schools heat demand and the heat extraction rate from boreholes are at its highest.
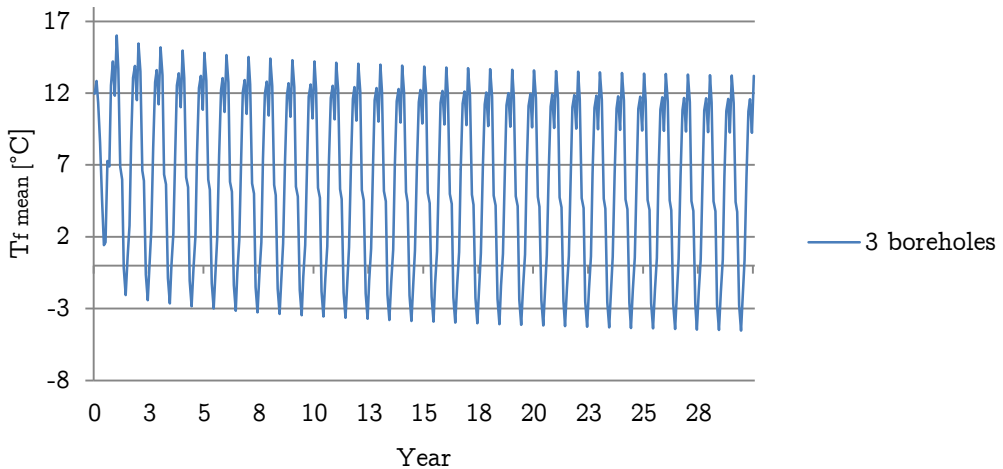
Figure 6-8 $T_{f,mean}$ for 3 boreholes with the same total heat load as in Figure 6-10

Figure 6-8 is plotted assuming the borehole field only consists of three boreholes, but the same total heat is extracted as in Figure 6-6. A larger fluctuation of $T_{f,mean}$ is observed in Figure 6-8 compared to Figure 6-6. This is because the average heat rate extracted and injected is higher per borehole. A high minimum $T_{f,mean}$ results in a higher evaporation temperature, which influences the heat pump COP in a positive manner.

In Figure 6-8 the minimum $T_{f,mean}$ falls below 0°C during the first year of operation, while the minimum $T_{f,mean}$ remains above 0°C even after 30 years of operation. It is therefore much higher possibilities for problems with borehole freezing if the boreholes are designed for high heat demands. Under sized BHE systems might therefore have reduced system performance and less effective ground heat transfer conditions. Well instrumented operational data logger should therefore be installed at all BHE installations, so that warnings signals, as e.g. rapid decrease of $T_{f,mean}$, can help to prevent reduced system performance at an early stage in of the operation time.

Even though the heat extracted and injected per borehole is higher in Figure 6-6, compared to the amount of heat extracted and injected per borehole in Figure 6-6, the minimum $T_{f,mean}$ do not decrease more rapidly with three than five boreholes during 30 years of operation because the average $T_{f,mean}$ remains constant. This means that a descending rate of minimum $T_{f,mean}$ is only dependent on the heat extraction and injection ratio, and not on the number of boreholes.

6.3.1.1   Borehole resistance effects
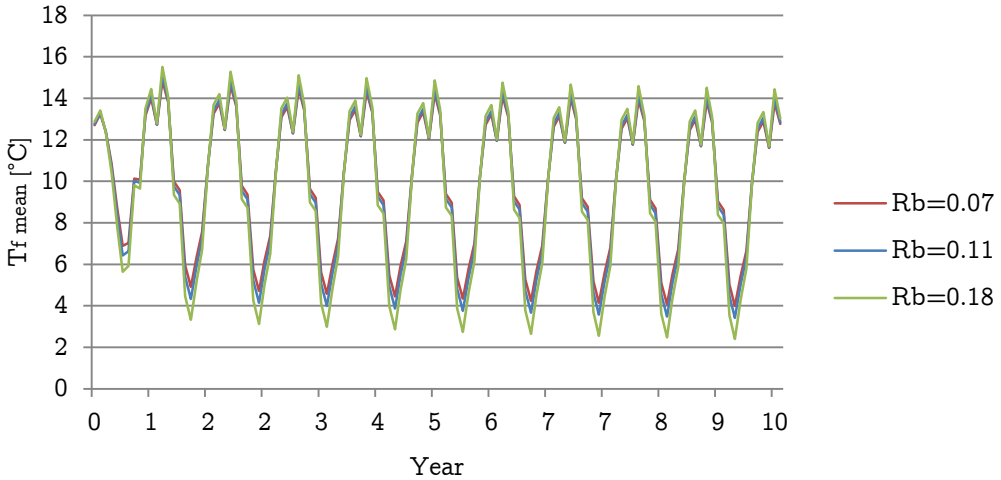
Figure 6-9 $T_{f,mean}$ for Rb=0.18, 0.11 and 0.07

Figure 6-9 shows that the borehole resistance influences the $T_{f,mean}$. The borehole resistance of 0.18, 0.11 and 0.7 mK/W represents the borehole resistance for the stagnant water case with a velocity of 0.263 m/s, velocity of 0.263 m/s and a velocity of 0.6 m/s including natural convection effects, respectively.

By increasing the fluid velocity from 0.263 to 0.6 m/s a reduction in borehole resistance from 0.11 mK/W to 0.07 mK/W is found. Figure 6-9 shows that this velocity increase will increase the minimum $T_{f,mean}$ by approximately 1°C, when the heat extraction is at its highest.

Lower borehole resistance gives lower fluctuations in $T_{f,mean}$, and a higher minimum $T_{f,mean}$ is achieved during the heat extraction period. This result in better operating conditions for the heat pump, since a higher evaporation temperature is achieved. A development of a collector geometry that reduces the borehole resistance at low velocities compared to the u-pipe geometry, will improve the GSHP system performance. Since a u-pipe collector is installed at Skoger, different collector types are not studied in this thesis.

6.3.1.2   Heat recovery batteries effects
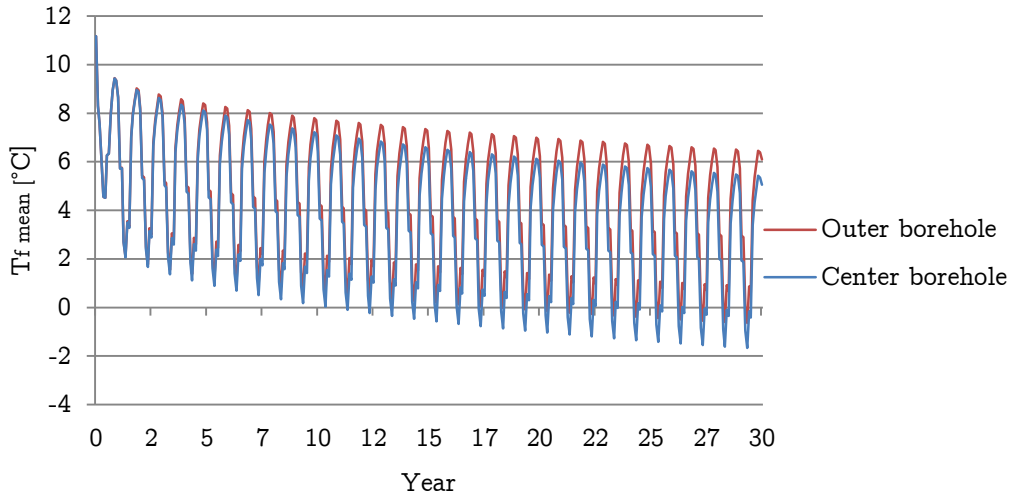
Figure 6-10 $T_{f,mean}$ without heat recovery batteries, 5 boreholes Rb=0.11

Heat recovery batteries are installed at the system at Skoger elementary school, to re-charge the energy wells with excessive heat from the air ventilation system. Figure 6-10 is plotted with the same ground and heat extraction properties as Figure 6-6, but energy recharge is excluded. Figure 6-10 shows a rapid decrease of the minimum $T_{f,mean}$ because more heat is extracted from the ground faster than the ground is able to transport heat to the borehole field. To secure an effective long term operation of the GSHP system which implies a non-decreasing minimum $T_{f,mean}$, energy recharge is indispensable. With-out energy recharge a greater difference in $T_{f,mean}$ between the outer and center borehole is observed in Figure 6-10, meaning that the thermal interaction between boreholes in the borehole field becomes larger as time goes for systems without energy recharge compared to systems with energy recharge. A greater distance between the adjacent boreholes is therefore necessary to preserve the efficiency of the boreholes with, in this case, two adja-cent boreholes.
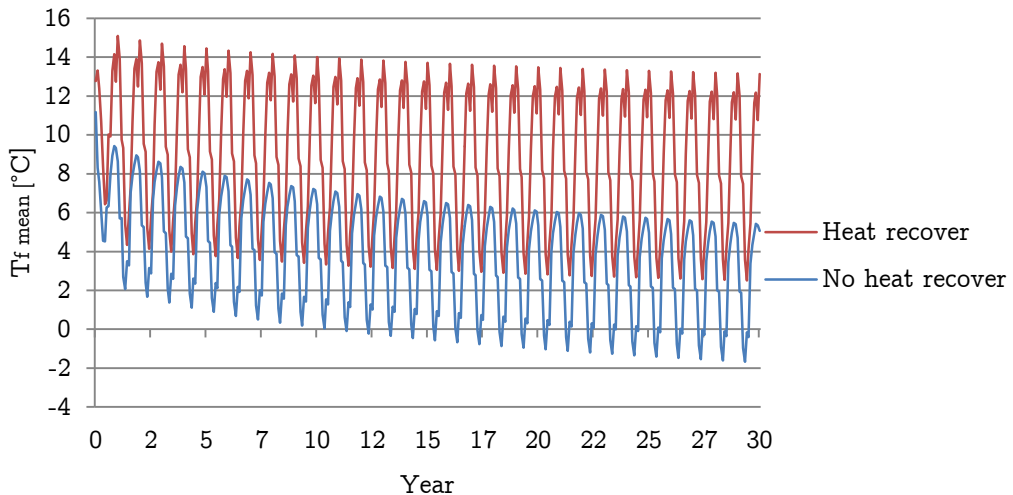
Figure 6-11 With and without heat recovery batteries

The difference in heat extracted and heat injected is the vital factor to keep a high performance of a GSHP system. A decrease in the minimum $T_{f,mean}$ will occur if the difference in heat extracted and injected exceeds a certain amount, and as shown in Figure 6-11 no recharge will lead to a decrease in system performance, even for low heat extraction rates. The energy difference is specific for each GSHP system, and a comprehensive evaluation of factors that influences the long term performance of the borehole should be done when designing a GSHP system.

For the installation at Skoger, the heat delivered from the heat recovery batteries are indispensable, because the COP will decrease drastically when the evaporation temperature drops. Figure 6-11 shows that after 30 years of operation without heat recovery batteries, the $T_{f,mean}$ will be approximately 4°C lower with heat recovery batteries than without heat recovery batteries. Since the heat pump installed at Skoger is very sensitive to changes in the evaporation temperature, a drop between 10-25% in COP can be expected if the heat recovery batteries are not used. Since the compressors at Skoger already operates outside their design evaporation and condensation temperature, a stable $T_{f,mean}$ is important to reduce the risk further decrease in heat pump performance.
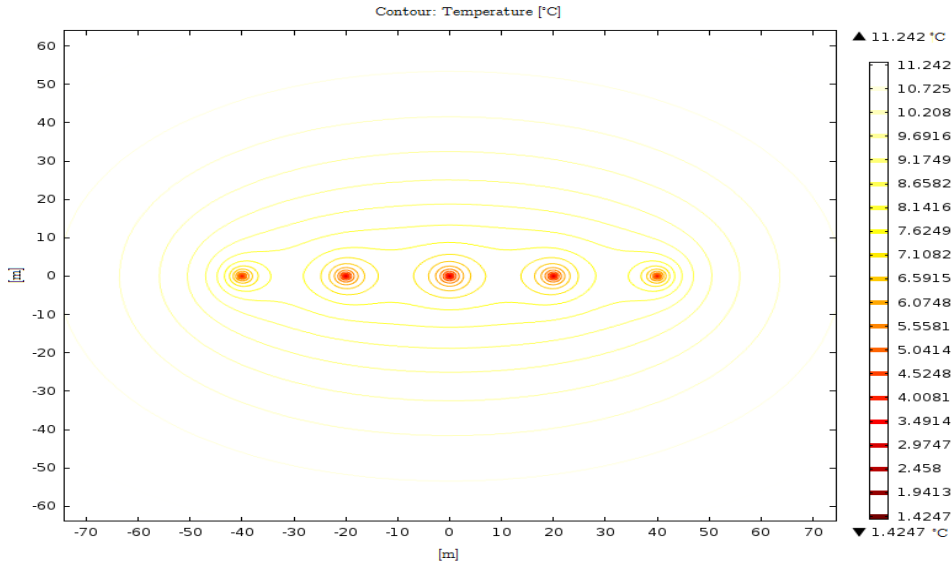
Figure 6-12 Isothermal contours without heat recovery, January year 30
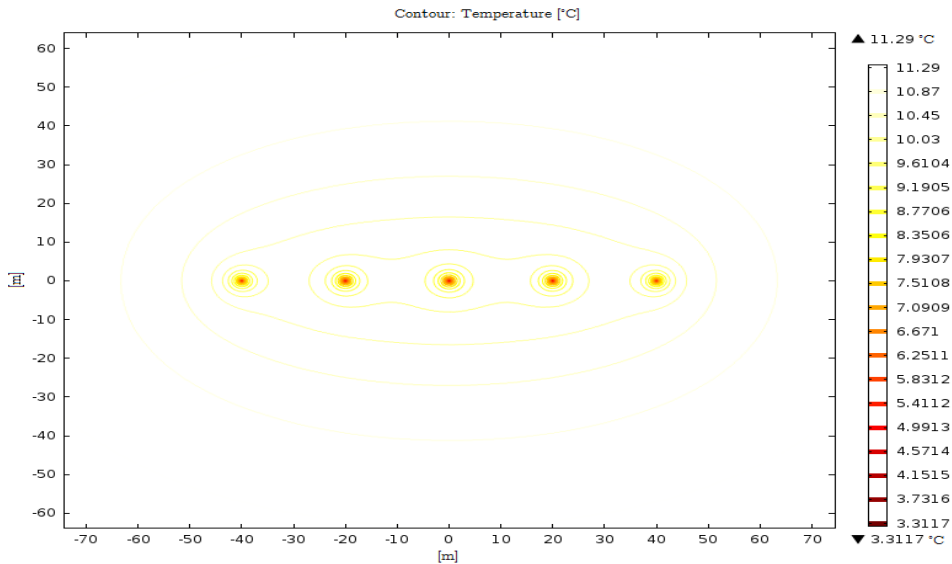
Figure 6-13 Isothermal contours with heat recovery, January year 30

Figure 6-12 and Figure 6-13 shows isothermal contours of the ground in January after 30 years of operation. This is the time of the year where the heat extraction is at its highest, and the thermal interaction between the adjacent boreholes is expected to be largest. Figure 6-13 shows that the isothermal contours around each borehole do not spread out, and the thermal interaction between the boreholes is therefore kept low for a borehole

distance of 20 meter. Without the heat injection in the summer months a larger radius of the isothermal contours around each borehole than in Figure 6-13 is observed. Figure 6-10 shows that the $T_{f,mean}$ is lower for the center borehole than the outer borehole after 30 years of operation because of larger thermal interaction between the boreholes shown in Figure 6-12 for cases without heat injection, than for cases with heat injection during the summer.

6.3.1.3   Borehole distance effects

The system at Skoger elementary school has 20 meter distance between two adjacent boreholes, which is shown to be a sufficient distance to have a high long term performance of the center borehole. Reducing the borehole distance from 20 meter to 10 meter a larger thermal interaction between the boreholes is expected, especially for the case of no heat recovery. All simulations in this chapter have been done with five boreholes.
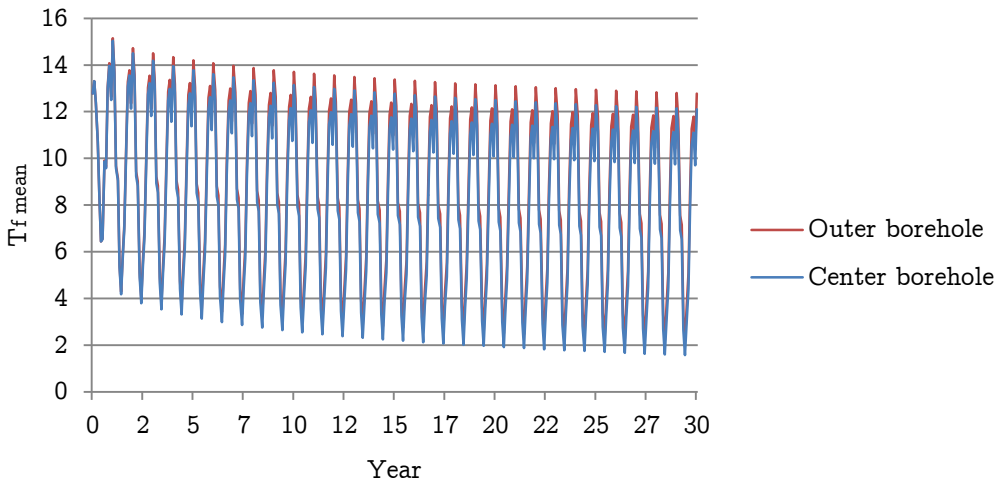
Figure 6-14 Heat extraction and injection with 10 meter distance between adjacent boreholes

A slight decrease in $T_{f,mean}$ is observed when the distance between the boreholes is 10 meter. Compared to Figure 6-6 a larger difference in $T_{f,mean}$ between the center and the outer borehole is found. This is expected because the thermal interaction becomes greater with reduced distance between the boreholes. The lowest $T_{f,mean}$ in Figure 6-14 is only

1°C lower than the lowest $T_{f,mean}$ found in Figure 6-6, which means that the BHE would have operated efficiently with distances of 10 meter between the adjacent boreholes.
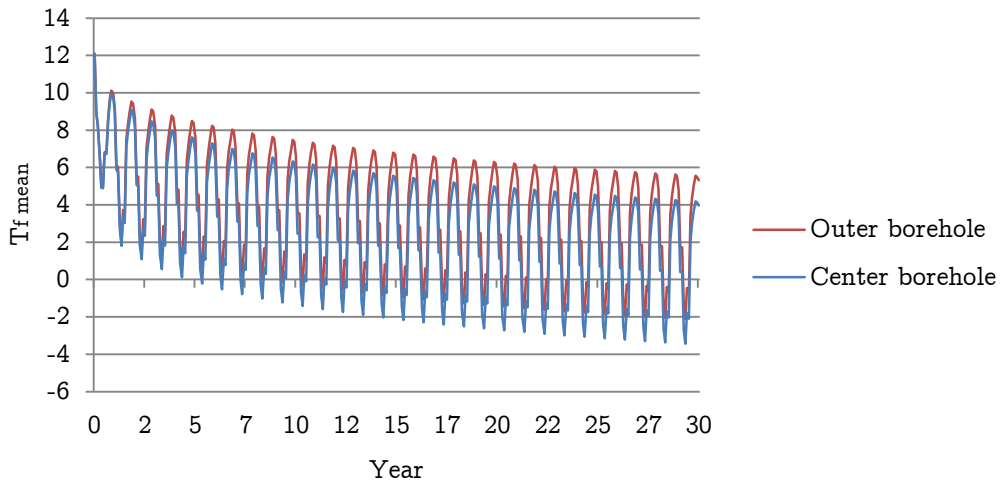
Figure 6-15 Heat injection with 10 meter distance between adjacent boreholes

Without heat injected to the ground from the heat recovery batteries, the distance between the adjacent boreholes becomes important, and a reduced thermal performance of the center borehole compared to the outer borehole due to lower $T_{f,mean}$ is shown in Figure 6-15.
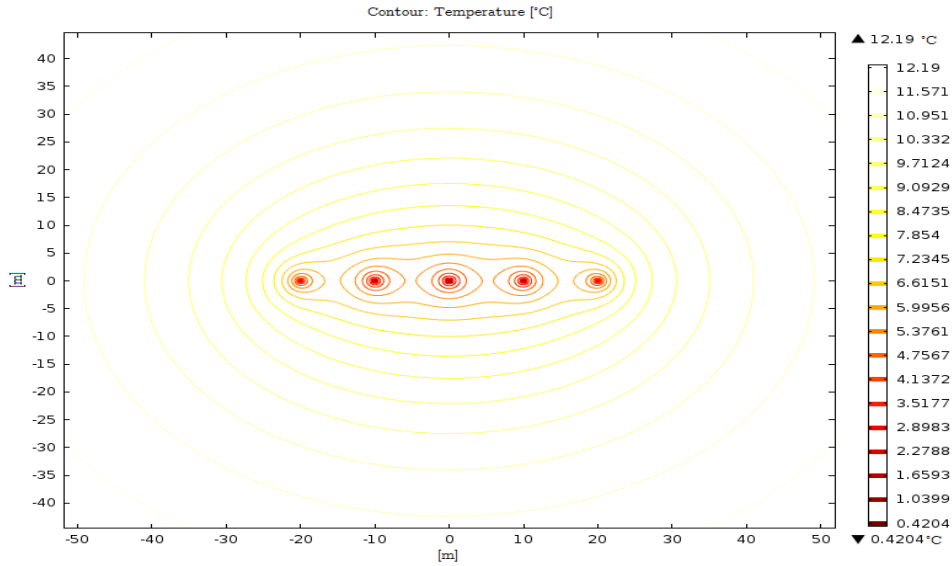
Figure 6-16 Isothermal contour without heat recovery and 10 meter distance between boreholes, January year 30
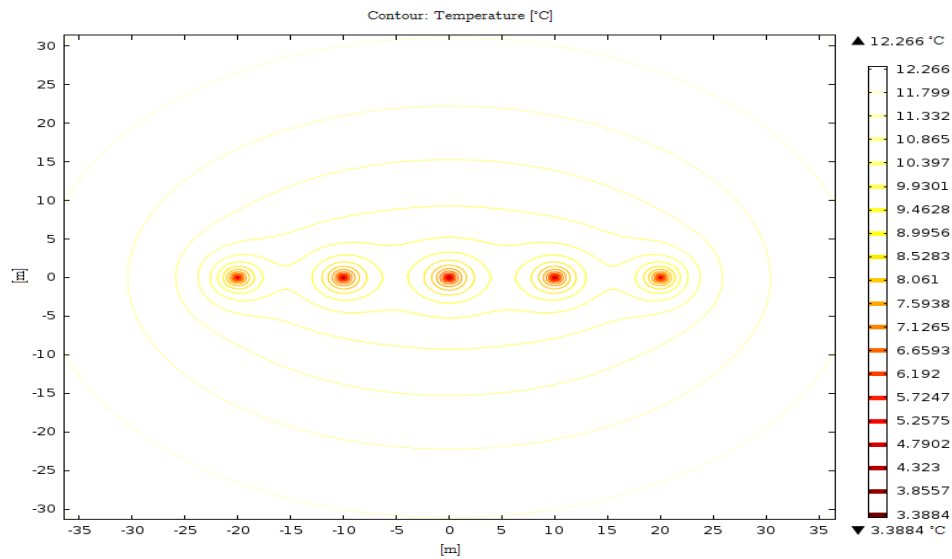
Figure 6-17 Isothermal contour with heat recovery and 10 meter distance between boreholes, January year 30

Figure 6-16 and Figure 6-17 shows the ground isothermal contours for heat injection and extraction case and only extraction case, respectively. For only heat extraction, a larger

136

thermal interaction between the three boreholes in the middle of the BHE line array for only heat extraction than for heat extraction and injection is shown in Figure 6-16 and Figure 6-17 because the isothermal contours around the boreholes are larger for the heat injection case than for the heat injection and extraction case.
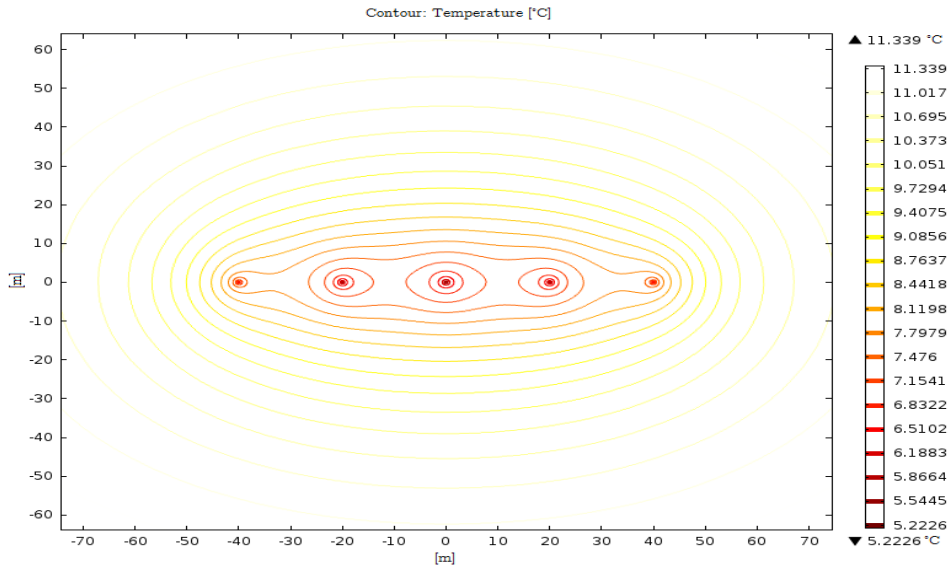
Figure 6-18 Isothermal contours without heat recovery and 20 meter distance between boreholes, June year 30

For heat extraction form the ground, a large distance between the boreholes results in better BHE performance because the thermal interaction between the boreholes is reduced. On the other hand, smaller distance between the boreholes localizes the heat injected and improves the heat injection efficiency. This should be considered in design processes for larger BHE systems, and regulate the heat injection to only the center boreholes to make sure of a stable temperature in the borehole field.

6.3.1.4   Effects of ground thermal coefficient
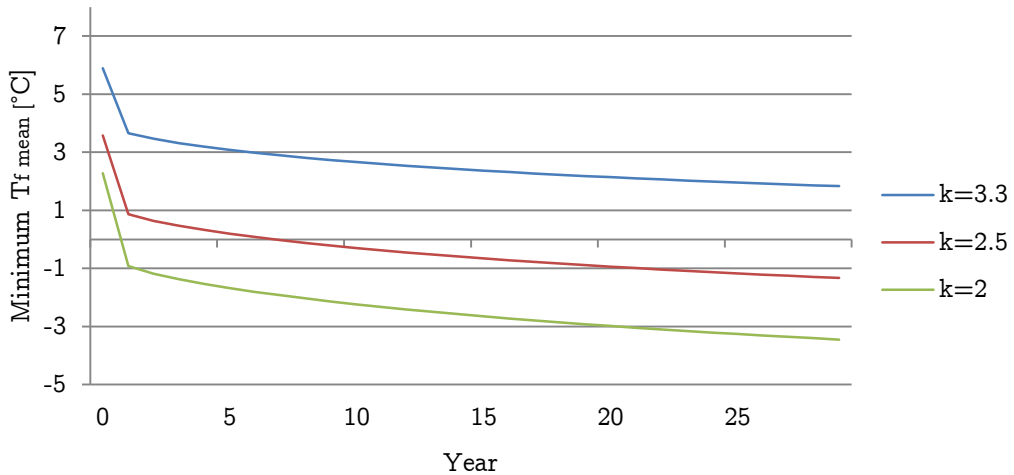
Figure 6-19 Injection and extraction with change in ground thermal conductivity

From Figure 6-19 a weak descending of the minimum $T_{f,mean}$ can be seen for a GSHP operating time of 30 years is more distinct for lower ground conductivity. To predict a correct ground thermal conductivity is of great relevance when designing a GSHP system, because it has a direct influence on the $T_{f,mean}$ amplitude and the minimum $T_{f,mean}$. A higher ground thermal conductivity results a higher minimum $T_{f,mean}$, which is improves the heat pump working conditions because a higher evaporation temperature can be achieved.

6.3.1.5   Ground temperature gradient effects

Temperature logs for deep boreholes done in Fredrikstad by the Geological Survey of Norway, gave a temperature gradient of 1.79°C /100meter, and at 500 meter the temperature was measured to 15,5°C. Data from Figure 3-21 shows that a higher temperature gradient was expected in Fredrikstad, and the uncertainties around the temperature gradient should be considered when designing BHEs.

With an average surface temperature of 7.58°C found in chapter 3.5 and a temperature of 15,5°C at 500 meter depth, the temperature gradient is 1.6°C/100meter. Average temperature of the ground is therefore 11.5°C.
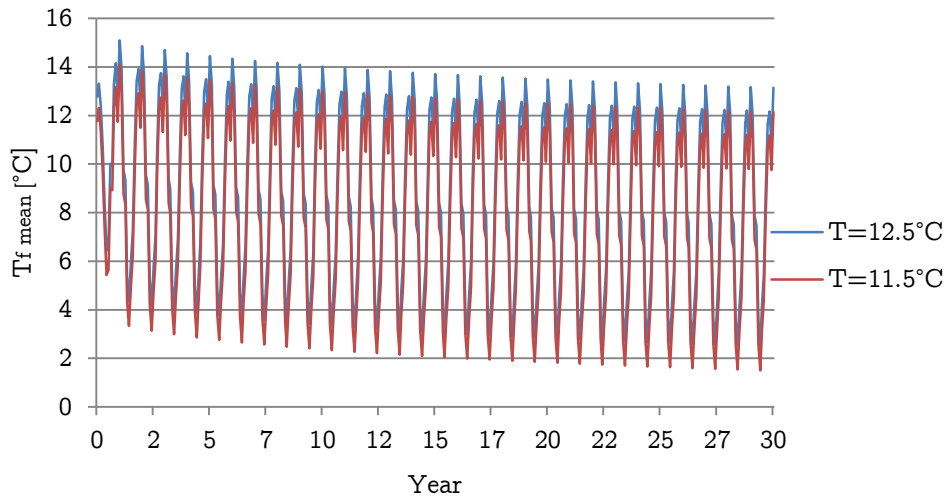
Figure 6-20 Change in temperature gradient

A lower temperature gradient does not affect the $T_{f,mean}$ to a steeper decrease during the operation time, but it lowers the minimum $T_{f,mean}$ which reduces the heat pump COP. A difference of approximately 1°C of the minimum $T_{f,mean}$ after 30 years of operation is shown in Figure 6-20. This may lead to a reduction in COP by 1-3%, Stene (2012).

6.4 2D model discussion

Results from the 2D models is based on boundary and geometry conditions with least possible assumptions compared to data collected from the system at Skoger elementary school. The results give an indication of the BHEs installed at Skoger long term performance, and the ground and operation conditions that has the largest influence on the BHE long time performance. Because the lack of operational data a comparison between the results from the 2D model and the borehole field at Skoger is impossible.

A 2D model was developed to investigate the long term performance of the BHE system installed at Skoger elementary school and to highlight change in ground and operating conditions. The model was made with the same line array as the BHEs installed at Skoger consisting of five boreholes with an internal distance of 20 meter between the boreholes. A time dependent heat flux based on monthly average operational system data from 2012 at Skoger elementary school was used as a boundary condition for the 2D model at the borehole wall to evaluate the temperature response of the ground and the borehole field. The borehole wall temperatures calculated from the 2D model, the time dependent heat load inserted at the borehole wall and the borehole resistances calculated from the 3D model in chapter 5 were used to evaluate $T_{f,mean}$ of the system. $T_{f,mean}$ has a direct influence on the system performance and the heat pump COP, and is therefore suitable for BHE and system evaluation. A stable $T_{f,mean}$ secures a high long term BHE performance. For long term performance evaluation of the BHE system at Skoger, monthly average heat flux values collected from operational data was used as a boundary condition at the borehole wall in the 2D model. Only a small decrease in $T_{f,mean}$ with 2012 average heat loads was shown for the BHEs installed at Skoger. A stable BHE performance can therefore be assumed when extrapolating the heat loads in 2012 for a period of 30 years. To have stable long time BHE performance at Skoger, the BHEs are highly dependent on the heat recovery batteries. Without heat injected back to the boreholes an instant decrease in $T_{f,mean}$ is shown. This will reduce the system performance drastically, and since the compressors installed at Skoger already operates near the maximum operation pressure ratio, the compressors might be unable to operate if the evaporation temperature is significantly reduced and the set point is kept at 55.8°C. Since the evaporation temperature has a great influence of the compressors efficiency it is essential to keep a stable minimum $T_{f,mean}$ during a long operation time.

Because the ground area available was not a limiting factor, the boreholes at Skoger were installed with a distance of 20 meter. A larger distance between adjacent boreholes results in less thermal interaction and higher performance of the boreholes with two or more neighboring boreholes. For the BHE case at Skoger elementary school no or little differences in $T_{f,mean}$ between the center borehole and the outer borehole was shown. The boreholes will therefore have an insignificant thermal influence on each other, and the thermal performance of the boreholes will be practically equal. Excluding the heat injected to the boreholes during the summer months, the thermal interaction is much larger than for the heat extraction and injection case, resulting in a lower minimum $T_{f,mean}$ and reduced BHE performance of the center borehole compared to the outer borehole.

It should be noticed that since the COP data for the GSHP system installed at Skoger was unavailable, the heat extraction amount from the energy wells is based on a COP calculated from heat the pump software Ecat2 and Coolselector.

Larger fluctuations in $T_{f,mean}$ is observed if the borehole field installed at Skoger only existed of three instead of five BHEs with the same heat load as for five boreholes. This results in lower evaporation temperatures during the winter months when heat is extracted, which results in reduced heating capacity and COP. Fewer boreholes reduces the installation cost, but increases the heat extracted per borehole during the winter months.

The minimum $T_{f,mean}$is directly related to the ground thermal conductivity and is therefore an important BHE design parameter. The thermal ground conductivity do not influence the steepness of the $T_{f,mean}$ decrease, but lower ground conductivity results in a significantly reduced minimum $T_{f,mean}$. A TRT should therefore be done for large BHE systems to secure a correct local ground conductivity value which reduces the risk of under sizing the BHE system in the design process.

The influence of a reduction of the temperature gradient from 1.79°C /100meter to 1.6°C /100meter is shown to have a low influence of the long term performance of the BHE system at Skoger elementary school, and will therefore not be a crucial BHE design factor.

Low borehole resistance results in a more effective heat transfer from the borehole wall to the fluid inside the collector, and gives lower amplitude of $T_{f,mean}$ and better working conditions for the heat pump.

Development of collector geometries that reduces the borehole resistance together with reduced short-circuiting between downward and upward fluid flow will improve the BHE

performance. Since the collector used at Skoger is a u-pipe, evaluation of different collector pipe geometries has not been discussed in this thesis.

The design parameters that influence the BHE performance the most are the difference between the yearly energy extracted and injected to the energy wells and the ground thermal conductivity. Since the ground conductivity describes the ability of the ground to conduct heat an underestimation of the thermal ground conductivity in the design process results in overestimation of the BHE array size and depth which gives higher initial cost. Overestimation of the conductivity of the ground results in under sizing of the whole system and might be crucial for the BHE performance and might lead to system failure. The difference in the yearly energy amount extracted and injected to the ground is shown to be a crucial factor to secure long term performance of the BHE system. Heat recovery batteries installation is essential for buildings with small cooling demand, to make sure that borehole field temperature remains stable. Buildings with cooling and heat demand is perfectly fitted to use the ground as an energy source and sink, since the ground can be used as an energy sink for free cooling of the building. This recharges the energy wells with energy from cooling the building, using only energy to pump the fluid through the collectors. A precise estimation of the buildings heating demand is crucial for the design of BHE depth and array size, and a BHE simulation software should be used to check the long term performance of the BHE with the estimated building heating and cooling demand. A rapid decrease in $T_{f,mean}$ over a couple of years could be expected if the building heating and cooling demand is not well balanced and an extra energy source such as a gas boiler might be installed to cover peak loads for buildings with large heating demand, and as an energy source back-up if the BHE system is shown to be undersized.

To be able to analyze the system and BHE performance, the heat pump input and output power, the outgoing temperatures and the power input of the heat recovery batteries, in- and outgoing temperatures from the energy wells, volumetric flow rate inside the BHE collectors and in- and outgoing temperatures from the hot side of the heat pump should be recorded as a standard for new system installations. This makes it possible to evaluate and optimize the GSHP system, to prevent a decrease in system performance at an early stage and to regulate the heat extracted or injected to the BHE to secure a stable long term performance.

The collection of operational data for this thesis was very time-consuming, and entrepreneurs involved in renovating the school and installation of BHEs did not have for example system description and data available. As a customer, Drammen municipality does not have the capacity to control check the installation specifications of every new building and must therefore rely on the work of the entrepreneurs. The heat pump installed at Skoger elementary school has compressors working outside their design pressure ratio for low evaporation temperatures, which results in large thermodynamic losses in the compressors and low COP of the heat pump. Two possible solutions to increase the COP are to lower the evaporation temperature, or change the compressors with compressors designed for higher pressure ratios. When lowering the evaporation temperature a significantly higher COP is achieved which result in reduction of heat pump power input and yearly operation cost.

Summary

The primary work was to develop a model to predict the performance of the BHE system installed at Skoger elementary school in Drammen. A 3D and a 2D model were developed in Comsol Multiphysics to simulate the BHE based on operation data collected from the system at Skoger and local ground condition data published by the Geological Survey of Norway. Due to limiting operational data available from the BHE system at Skoger, verification of the numerical models developed in Comsol Multiphysics was not possible.

3D model

Due to computer capacity restraints a model consisting of only one borehole including fluid flow was made. The model was therefore used to evaluate the borehole resistance, which was used as an input data for the 2D model.

A thermal resistance between the borehole wall and the circulating fluid inside the collectors, referred to as the borehole resistance, was calculated from the 3D model simulating a single BHE using least possible assumptions compared to the BHEs installed at Skoger. Both ground and operation conditions were varied to evaluate their influence on the borehole resistance with a constant heat extraction and injection to the ground

Lower borehole resistance gives smaller seasonal fluctuations of the average temperature between the in- and outgoing BHE fluid temperature which results in better heat pump working conditions by raising the evaporation temperature.

A Nusselt number correlation for natural convective heat transfer is implemented in the 3D model through an effective conductivity. The natural convection flow effects are caused by the water density gradient at different temperatures, where larger density gradient results in larger convective flow. Excluding the natural convection effects for a constant heat extraction of 12500 W (25W/m) the borehole resistance was increased by 50%. This increase in the borehole resistance was shown to affect the temperature response and the temperature profile along the borehole depth for a heat extraction case of 25 W/m. It is therefore important to implement the thermal effects of natural convection for simulations of groundwater filled boreholes.

The borehole resistance is shown to be dependent on whether heat is extracted or injected because the heat transfer of the water surrounding the collector pipes increases the

heat transfer coefficient with increased temperature, due to higher density differences at high temperatures of the water surrounding the collectors. Heat injected gives therefore lower borehole resistance than heat extraction operation. The fluid velocity is shown to have the largest influence of the borehole resistance. Increasing the fluid velocity from 0.26 m/s to 1 m/s a borehole resistance reduction of 43% and 30% is shown with constant heat extraction of 12500W (25 W/m) and injection of 22500 W (45 W/m) over 50 hours, respectively. The drawback with increased fluid velocity is increased pumping power.

Operational data restrictions

The only operational data available after the completion of the GSHP system at Skoger elementary school were heat delivered from the heat pump and the heat recovery batteries. To use this information in BHE evaluation, a COP has to be predicted. Since the COP of the Carrier 30RW-300 heat pump installed at Skoger is shown to be highly dependent on the evaporation temperature, an average COP for the winter months and an average COP for the summer month was used to predict the heat amount extracted from the energy wells. With the recording equipment installed in the GSHP system at Skoger elementary school, the engineers at Drammen municipally were unable to evaluate the system or the BHE performance. A flow sheet print screen from 16.01.2013, shown in Figure 3-1, and conversation with a supplier of Carrier heat pumps showed that the heat pump installed at Skoger was working outside its operation limits during the winter months which resulted in a low COP. A significantly higher COP can be achieved with reducing the heat pump condensation temperature and the yearly heat pump power input cost could be reduced by approximately 25% if the evaporation temperature is reduced from 60°C to 50°C.

Designers of GSHP systems should be careful to make sure that important data for evaluation and optimization of the GSHP performance are able to be logged. A minimum data that should be logged at new installations are:

1. In-and outgoing temperatures from the energy wells
2. Volumetric flow rate of the circulating fluid inside the collectors
3. Outgoing temperatures from the heat recovery batteries
4. In-and outgoing temperatures at the hot side of the heat pump
5. Heat pump power input and output
6. Recovery batteries thermal power output

In and outlet temperatures from the energy wells, temperatures on hot side of the heat pump should be recorded to see the COP change with change in in-and outlet temperatures. This makes it possible to optimize the system as time goes on when better insight of the building heat demand and energy well temperature responses has been recorded. Inlet and outlet temperature, and the volume flow rate from the energy wells should be recorded to be able to perceive warning signals like rapidly descending minimum $T_{f,mean}$ over the years, to avoid problems with freezing around the boreholes and system failure.

2D model

Because the 3D model developed was computationally heavy, a 2D model had to be developed using the borehole resistance calculated from the 3D model as an input to evaluate the average temperature of the fluid inlet and outlet, referred to as $T_{f,mean}$. The model was made to predict the long term performance of the BHE system at Skoger and has been used to study the influence of the long term BHE performance when ground and operating conditions was varied. The energy wells heat loads was based on heat delivered from the heat pump for 2012 with a winter COP of 2.1 and a summer COP of 2.7. This heat load was used and extrapolated for a period of 30 years to predict the long term performance of BHEs installed at Skoger. Only a slight decrease in $T_{f,mean}$ was shown for the BHE system for an operation time of 30 years. The same long time simulation was done without heat recharge of the energy wells. This resulted in a marked decrease in $T_{f,mean}$. Heat injection is therefore indispensable to secure a stable long time BHE performance.

Together with the difference between energy extracted and injected, the ground thermal conductivity is shown to be critical design factors for the BHE long time performance and the heat pump working conditions. Underestimation of the ground thermal conductivity will result in overestimation of the BHE array size and lead to higher installation cost. Ground conductivity overestimation in the design process may result in under sizing the BHE system and may lead to reduced system performance, and worst case system failure. The thermal performance of a given BHE system is therefore to a large extent dependent on pre-determined factors as the site ground conductivity. It is therefore necessary to know the local geological conditions before large BHE systems are constructed.

Conclusion

Based on the literature review of different methods for simulation of a Borehole Heat Exchanger (BHE), a 3D model and a 2D model was developed in Comsol Multiphysics using least possible assumptions to evaluate the BHE system installed at Skoger elementary school in Drammen. The 2D model was developed to predict the long term performance since extensive computational time was needed for the 3D model.

i) Lack of temperature and power input recording equipment installed for the Ground Source Heat Pump (GSHP) system at Skoger elementary school located in Drammen, made it impossible to validate the simulation models developed to the system operational data. Only heat delivered from the heat pump and the recovery batteries were recorded. The engineers at Drammen municipality were therefore unable to evaluate the performance of the heat pump or the BHEs. After an evaluation of the installation, an ineffective operation of the heat pump was discovered, due to operation outside the heat pump design conditions. The need of system control and system condition overview is essential, and a minimum of data that should be logged at new GSHP systems to provide data for evaluation and optimization of the installed BHEs are:

 1. In-and outgoing temperatures from the energy wells
 2. Volumetric flow rate of the circulating fluid inside the collectors
 3. Outgoing temperatures from the heat recovery batteries
 4. In-and outgoing temperatures at the hot side of the heat pump
 5. Heat pump power input
 6. Recovery batteries thermal power output

ii) A reduction of thermal resistance between the borehole wall and the fluid inside the collector, borehole resistance, with increased heat effect extraction and injection is found. Excluding the heat transfer effects of natural convection flow resulted in an increase of the borehole resistance of 50% for a constant average heat extraction rate of 12500W (25 W/m). Including heat transfer effects of natural convection in BHE simulation models is therefore of great importance for short as well as long time simulation for groundwater filled boreholes. A difference in the borehole resistance between heat injected and extracted is found because larger density gradients of the groundwater at high temperatures results in increased heat transport.

iii) If the volumetric flow rate is increased while keeping a constant heat injection or extraction, a more even temperature profile between the up-and downward fluid flow is found. This, together with increased heat transfer coefficient and lower short-circuiting effects between the up-and downward fluid flow, are shown to reduce the borehole resistance and raise the thermal performance of the BHE for a constant heat extraction and injection case.

iv) The long term performance of a GSHP system relies on a stable average fluid temperature, $T_{f,mean}$, between in-and outlet of the BHE. Important design parameters for sizing a BHE system are the local ground conductivity and the building heating and cooling demands. BHE systems with unbalanced heat- extraction and injection from the energy wells may have significantly reduced performance due to a steep decline in $T_{f,mean}$ during the operation time. Estimation of a precise local ground thermal conductivity is therefore important to reduce the risk of under sizing the of a BHE system, which may lead to reduced heat pump working conditions, and in worst case system failure.

v) With data from the BHE system installed at Skoger, the 2D model, with input data from the 3D model, showed that the heat balance between the heat injected and extracted to the energy wells will secure a constant long term performance of BHEs installed at Skoger.

.

Further work

Areas that need further work are specified below, together with a brief explanation of each area.

i) Validation

Validate the 2D and 3D model to data logged from March 2013 collected from the GSHP system installed at Skoger elementary school

ii) Improvement of 3D model

Improve the 3D model to account for the BHE heat flux distribution along the borehole depth when calculating the Nusselt number correlation for natural convection.

iii) Simulation of intermitted heat pump operation

Implement a step change in effect extracted or injected into the 3D model input values to simulate the thermal response of intermitted sequence heat pump operation.

iv) Improve the HVAC system at Skoger

Suggest changes that can be made to improve the efficiency of the heat pump installed at Skoger elementary school.

v) System response to increased fluid velocity

Evaluate the real system performance of the GSHP system at Skoger with change in fluid velocity.

vi) Compare 3D model with analytical models used for TRT evaluation

Compare analytical models used for TRT evaluation with the 3D model developed, to evaluate the thermal ground conductivity estimation error for deep boreholes because of simplifications assumptions used in the analytical models.

Bibliography

Acuña, J. (2013). "Distributed thermal respone tests - New insights on U-pipe and Coaxial heat exchangers in groundwater-filled boreholes." (KTH School of Industrial Engineering and Management).

Zijdemans, D. (2012). "Vannbaserte oppvarmings- og kjølesystemer (in norwegian)." (Skarland Press).

Zarrella, A., M. Scarpa and M. D. Carli (2011). "Short time step analysis of vertical ground-coupled heat exchangers The approach of CaRM." (Renewable Energy).

Yavuzturk, C. (1999). "Modeling of Vertical Ground Loop Heat Exchangers for Ground Source Heat Pump Systems." (Oklahoma State University).

White, F. M. (2008). "Fluid Mechanics." **Sixth Edition**(McGraw-Hill).

Stene, J. (2012). "Presentation in the course TEP16: Ground-Source Heat Pumps, Bedrock or Groundwater as Heat Source."

Signorelli, S., S. Bassetti, D. Pahud and T. Kohl (2006). "Numerical evaluation of thermal response tests."

Reddy, J. N. (1993). "An Introduction to the Finite Element Method." **2. Edition**.

Ramstad, R. K., H. Tiarks and K. Midttømme (2008). "Ground source energy – Thermal conductivity map in the Oslo region."

Ramstad, R. K. (2012). "Test lecture notes, Power point presentation - Ground source based heat pump systems."

Pascal, C., H. Elvebakk and O. Olesen (2010). "An Assessment of Deep Geothermal Resources in Norway." NGU.

Midttømme, K., B. O. Hilmo, H. Skarphagen and A. Nissen (2000). "Kartlegging av energipotensialet i berggrunnen på kartblad Bekkestua, Bærum kommune: Varmeledningsevnen til bergarter.(In norwegian)."

Lee, Y. and S. A. Korpela (1983). "Multicellular natural convection in a vertical slot."

Lazzari, S., A. Priarone and E. Zanchini (2010). "Long-term performance of BHE (borehole heat exchanger) fields with negligible groundwater movement." (Elsevier).

Kreyszig, E. (2006). "Advanced Engineering Mathematics." **9.edition**.

Kjellsson, E. (2009). "Solar Collectors Combined with Ground-Source Heat Pumps in Dwellings." (Lund University).

Keyhani, M., F. A. Kulacki and R. N. Christensen (1983). "Free Convection in a Vertical Annulus With Constant Heat Flux on the Inner Wall."

Ingersoll, L. R., O. J. Zobel and A. C. Ingersoll (1954). "Heat Conduction with Engineering, Geological and Other Applications." New York, McGraw-Hill.

Ingersoll, L. R. and H. J. Plass (1948). "Theory of the Ground Pipe Heat Source for the Heat Pump." (ASHVE Transactions).

Incropera, F. P. and D. P. DeWitt (2002). "Fundamentals of Heat and Mass Transfer." **5. Edition**.

Ho, C. J. and Y. H. Lin (1990). "Natural Convection of Cold Water in a Vertical Annulus With Constant Heat FLux in the Inner Wall."

He, M. (2012). "Numerical Modelling of Geothermal Borehole Heat Exchanger Systems."

Gustafsson, A.-M. and L. Westerlund (2011). "Heat extraction thermal response test in groundwater-filled borehole heat exchanger e Investigation of the borehole thermal resistance." (Elsevier).

Gustafsson, A.-M. and L. Westerlund (2009). "Multi-injection rate thermal response test in groundwater filled borehole heat exchanger." (Elsevier).

Gehlin, S. and G. Hellström (2003). "Influence on thermal response test by groundwater flow in vertical fractures in hard rock." (Elsevier).

Gehlin, S. (2002). "Thermal Response Test - Method Development and Evaluation."

Eskilson, P. (1987). "Thermal Analysis of Heat Extraction Boreholes." (University of Lund).

Diersch, H.-J. G., D. Bauer, W. Heidemann, W. Rühaak and P. Schätz (2010). "Finite element modeling of borehole heat exchanger systems Part 1.Fundamentals." (Elsevier).

Diersch, H.-J. G., D. Bauer, W. Heidemann, W. Rühaak and P. Schätzl (2010). "Finite element modeling of borehole heat exchanger systems Part 2.Numerical simulation." (Elsevier).

Choi, J. C., J.Park and S. R. Lee (2012). "Numerical evaluation of the effects of groundwater flow on borehole heat exchanger arrays."

Choi and S. A. Korpela (1980). "Stability of the Conduction Regime of Natural Convection in a Tall Vertical Radius."

Carlslaw, H. S. and J. C. Jaeger (1947). "Conduction of Heat in Solids." (Claremore Press, Oxford).

Carli, M. D., M. Tonon, A.Zarrella and R. Zecchin (2009). "A computational capacity resistance model (CaRM) for vertical ground couple heat exchangers." (Renewable Energy).

Bauer, D., W. Heidemanna and H.-J. G. Diersch (2011). "Transient 3D analysis of borehole heat exchanger modeling." (Elsevier).

Al-Khoury, R., P. G. Bonnier and R. B. J. Brinkgreve (2005). "Efficient finite element formulation for geothermal heating systems. Part I: Steady state." (Wiley InterScience).

Al-Khoury, R. and P. G. Bonnier (2006). "Efficient finite element formulation for geothermal heating systems. Part II: Transient." (Wiley InterScience).